A NEW APPROACH TO THE MODELING AND ANALYSIS OF FRACTURE THROUGH AN EXTENSION OF CONTINUUM MECHANICS TO THE NANOSCALE

A Dissertation

by

TSVETANKA BOZHIDAROVA SENDOVA

Submitted to the Office of Graduate Studies of
Texas A&M University
in partial fulfillment of the requirements for the degree of

DOCTOR OF PHILOSOPHY

December 2008

Major Subject: Mathematics

A NEW APPROACH TO THE MODELING AND ANALYSIS OF FRACTURE THROUGH AN EXTENSION OF CONTINUUM MECHANICS TO THE NANOSCALE

A Dissertation

by

TSVETANKA BOZHIDAROVA SENDOVA

Submitted to the Office of Graduate Studies of
Texas A&M University
in partial fulfillment of the requirements for the degree of

DOCTOR OF PHILOSOPHY

Approved by:

Chair of Committee,	Jay R. Walton
Committee Members,	Peter Kuchment
	Raytcho Lazarov
	John C. Slattery
Head of Department,	Albert Boggess

December 2008

Major Subject: Mathematics

ABSTRACT

A New Approach to the Modeling and Analysis of Fracture Through an Extension of Continuum Mechanics to the Nanoscale. (December 2008)

Tsvetanka Bozhidarova Sendova, B.S., Sofia University St. Kliment Ohridski

Chair of Advisory Committee: Dr. Jay R. Walton

The dissertation focuses on the analysis, through combined analytical and numerical techniques, of the partial differential equations arising from a new approach to modeling brittle fracture, based on extension of continuum mechanics to the nanoscale. The main part of this work deals with the analysis of several fracture models. Integral transform methods are used to reduce the problem to a Cauchy singular, linear integro-differential equation. It is shown that ascribing constant surface tension to the fracture surfaces and using the appropriate crack surface boundary condition, given by the jump momentum balance, leads to a sharp crack opening profile at the crack tip, in contrast to the classical theory of brittle fracture. However, such a model still predicts singular crack tip stress. For this reason a modified model is studied, where the surface excess property is responsive to the curvature of the fracture surfaces. It is shown that curvature-dependent surface tension, together with boundary conditions in the form of the jump momentum balance, leads to bounded stresses and a cusp-like opening profile at the crack tip. Further, an alternative approach, based on asymptotic analysis, which is suitable to apply in cases when the model includes a mutual body force correction term, is considered. The nonlinear nonlocal problem, resulting from the proposed model, is simplified which allows us to approximate the crack opening profile and derive asymptotic forms for the cleavage stress in a neighborhood of the crack tip. Finally, two possible fracture criteria, in the context of

the new theory, are discussed. The first one is an energy based fracture criterion. Classically the energy release rate arises due to singular fields, whereas in the case of the modeling approach adopted here, a notion analogous to the energy release rate arises through a different mechanism, associated to the rate of working of the surface excess properties at the crack tip. Due to the fact that the proposed modeling approach allows us to fully resolve the stress in a neighborhood of the crack tip, without the customary singularity, a second fracture criterion, based on crack tip stress, is possible.

To my parents, Евгения и Божидар Сендови

ACKNOWLEDGMENTS

First and foremost I would like to express my deepest gratitude to my advisor Prof. Jay Walton not only for his invaluable support and help in my research but also for his unfailing enthusiasm and optimism throughout the numerous ups and downs we went through working on this project. I feel privileged to be his student and I am thankful to him for his guidance, advice and encouragement. With his expertise in the areas of mathematical modeling, continuum mechanics and material science he has taught me so much, but also from his positive outlook on life I learned to see "the glass as half full" (at least in most cases).

I am grateful to Prof. Peter Kuchment and Prof. Raytcho Lazarov for serving on my committee and most importantly for being my teachers. Dr. Kuchment's lectures in Partial Differential Equations are one of the most memorable courses I have taken. I can only hope to be able to convey complicated mathematical ideas the way he does and to have his enthusiasm and love for mathematics and teaching.

I would like to express my particular appreciation to Prof. John Slattery and Dr. Kaibin Fu for the numerous discussions which helped me obtain a deeper understanding of the problem.

I wish to thank the Department of Mathematics at Texas A&M University and its faculty and staff for providing such a wonderful and friendly environment for studies and research. I am especially thankful to Ms. Monique Stewart for the uncountable timely reminders, for making the administration run smoothly and seamlessly and for all her help. I am very appreciative of the financial support provided by the Department of Mathematics and the Air Force Office of Scientific Research through Grant FA9550-06-0242.

I would like to thank Prof. Stefka Dimova and Prof. Raytcho Lazarov for sug-

gesting the graduate program at Texas A&M University to me.

I am thankful to my family for all their support and for always being there for me, despite being on a different continent. Special thanks to all my friends who made my stay away from home so much easier and enjoyable. It is difficult for me to put into words my love and appreciation for Dimitar who steadfastly supported and believed in me.

I am so lucky to have met you all.

TABLE OF CONTENTS

Page

CHAPTER Page

CHAPTER Page

LIST OF TABLES

LIST OF FIGURES

CHAPTER I

INTRODUCTION

1.1. Fracture Mechanics: Continuum to Atomistic Approaches

Fracture of brittle materials has been modeled over a broad range of approaches - from classical continuum theories like linear elastic fracture mechanics (LEFM) to particulate theories such as molecular dynamics.

Various attempts have been made to supplement the classical continuum approaches in an attempt to circumvent the internal inconsistencies in the LEFM theory. Cohesive and process zone models are among the most widely studied generalizations of the classical crack tip model. These types of models require the specification of constitutive properties of the cohesive or crack tip process zone, which are very difficult to determine experimentally. Thus, the models used are either based on ad hoc choices for the constitutive behavior of the cohesive/process zone or on simplified views of the fracture process.

The primary motivation for studying fracture through atomistic scales, in addition to the fact that they take into account the nanoscale interfacial physics, which plays a crucial role in a neighborhood of the fracture edge, is that the classical continuum models do not contain the necessary physics to predict fracture. In this sense, molecular dynamics offers an appealing approach to studying the initiation and propagation of fracture, which explains the growing literature devoted to this technique ([2, 3, 4, 13, 29, 31, 48, 49]). On the other hand, it requires an accurate description of the long-range and short-range intermolecular forces in the bulk material, which is a difficult task in the case of liquids and solids ([29]).

This dissertation follows the style of the SIAM Journal on Numerical Analysis.

Various multiscale models (so called *atom-to-continuum modeling*) have also recently gained considerable attention. One of the most extensively studied methods of this type, in the context of finite element method (FEM) approximations to continuum models, is the quasi-continuum method introduced by Tadmor et al in 1996 ([50]). Based on an atomistic view of material behavior, its continuum aspect comes from the fact that the FEM is based on energy minimization. A different type of atom-to-continuum modeling is a recently proposed approach by Xiao and Belytschko in [55] which involves the introduction of *bridging domains* between regions modeled using bulk (continuum) descriptions of material behavior and regions modeled using atomistic descriptions of material behavior. Both of these approaches involve adjustable parameters that one needs to fit for every particular application.

Other attempts to incorporate microscale processes into fracture modeling include models based on configurational forces, as considered by Gurtin and Podio-Guidugli ([25, 26]), Gurtin and Shvartsman ([27]), Sivaloganathan and Spector ([45]), Maugin and Trimarco ([33]), Fomethe and Maugin ([15]) and others. Also gaining attention is the peridynamic paradigm for modeling fracture ([44]).

In contrast to the latter theories, which introduce either an entirely new additional force system (configurational forces) or an entirely new continuum modeling paradigm (peridynamics), the theory proposed herein uses conventional ideas of continuum mechanics through the introduction of a dividing surface endowed with excess properties together with a mutual force. Our approach builds upon a hybrid theory introduced by Oh et al ([39]). Unlike a start-from-scratch atom-to-continuum approach, this theory is based on a continuum theory of material behavior that takes into account effects due to long-range intermolecular forces from adjoining phases in the vicinity of the fracture surfaces. This correction of bulk continuum behavior makes use of a scalar point-to-point potential constructed using molecular dynamics

simulations. No adjustable parameters are needed and, as demonstrated in Chapter III, the theory using curvature-dependent surface tension predicts a finite crack tip stress amplification of the applied loading, in contrast to the crack tip stress singularity exhibited by models in classical elastic fracture mechanics. This allows us to formulate a fracture criterion based upon the notion of a *Critical Crack Tip Stress* (CCTS) defined to be the minimum crack tip stress level required to propagate the crack in addition to an energy based criterion similar to the classical notion of a critical Energy Release Rate (ERR) defined in the setting of singular crack tip stresses and strains.

1.2. Current vs. Reference Configuration

Classical fracture theories are customarily formulated in a reference configuration. However, aspects of the theory discussed here are more easily described in the current or deformed configuration. Consequently, we present the theory in both the spatial (Eulerian) and material (Lagrangian) frames. We assume that there exists a surface (Cauchy) stress tensor $\mathbf{T}^{(\sigma)}$ which gives contact forces on a curve in the fracture surface Σ. For example, one of the advantages of working in the spatial frame is that for purposes of approximating the crack opening profile, it is exceedingly useful to take an approach which uses perturbation theory in the deformed configuration. Furthermore, the correction potential which determines the mutual body force term and, depending on the model, the crack surface excess properties is set up only when chemical bonds have been broken and depends on the crack opening profile.

On the other hand, formulating a fracture theory in the current configuration presents certain complications. First, it is not entirely clear how one should mathematically define a fracture in the deformed configuration, where the crack is opened,

as traditionally a crack is defined as a surface in the reference configuration across which the displacement, velocity, stress fields, etc. could sustain a discontinuity. Also, the notions of crack length and crack velocity in the current configuration are ambiguous, since one needs to separate *crack tip motion due to crack growth* from *motion due to deformation*. Furthermore, to prove that the proposed modeling approach leads to bounded stresses and strains, we employ the method of integral transforms which is most easily applied when using the undeformed configuration as reference. Thus, it is useful to formulate the fracture problem in both the reference and current configurations.

CHAPTER II

PRELIMINARIES

2.1. Extension of Continuum Mechanics to the Nanoscale

The physics of interfaces is a very large subject in material science, but in essence there are two basic models. The modeling of a material interface can be approached from a fully discrete perspective, using a particulate (molecular) model, or from a continuum perspective.

In what follows, we apply a theory of fracture, based upon an extension of continuum mechanics to the nanoscale similar to the one proposed by Oh et al ([39]). The theory assumes that the standard constitutive equation describing both the short- and long-range intermolecular forces predicts well the bulk material behavior outside the interfacial region. However, for material points within a nanoscale neighborhood of an interface, one needs to take into account that they are subjected to intermolecular forces from distinct phases.

In a classical approach to modeling an interface between two different material phases that dates back to Gibbs ([18]), the entire interfacial region is collapsed to a two dimensional dividing surface. This view, in the context of the present discussion, assumes that all the effects of long-range intermolecular forces are taken into account through the introduction of excess properties (such as surface energy γ) to the dividing surface.

As described in [39], we model herein the phase interface as a two dimensional dividing surface. The effect of long-range intermolecular forces is only partially accounted for by assigning excess properties $\tilde{\gamma}$ to the dividing surface. The rest of this effect is captured through the introduction of a body force correction term

$\mathbf{b}^{(corr)} = -\text{grad}\Phi$. Both $\tilde{\gamma}$ and Φ are based on a scalar potential describing the point-to-point interaction forces between material points in the interfacial region.

Note that unlike in the classical view which assumes that all the effects of long-range intermolecular forces from the adjacent phase are incorporated into the surface energy γ, in the approach taken herein this effect is accounted for partly through the excess property $\tilde{\gamma}$ and partly through a body force correction term.

Modeling the interfacial region through the introduction of both excess properties on a two dimensional dividing surface and mutual body force term allows us to construct a more realistic approximation to the true stress field in a neighborhood of a fracture.

2.2. Use of Hooke's Law in the Current Configuration

Consider a map $\mathbf{f} : \mathcal{B}_\kappa \to \mathcal{B}$ which takes a point $\mathbf{X}$ in the reference configuration $\mathcal{B}_\kappa$ into a point

$$\mathbf{x} = \mathbf{f}(\mathbf{X}) \in \mathcal{B}$$

in the current configuration. We assume that $J = \det \nabla \mathbf{f} > 0$ and denote by $\mathbf{F}$ the deformation gradient

$$\mathbf{F}(\mathbf{X}) = \nabla \mathbf{f}(\mathbf{X}).$$

Also, let the vector

$$\mathbf{u}(\mathbf{X}) = \mathbf{f}(\mathbf{X}) - \mathbf{X}$$

denote the displacement of $\mathbf{X}$. Let $\mathbf{I}$ denote the identity tensor, $\mathbf{H}$ be the displacement gradient, i.e., $\mathbf{H} = \nabla \mathbf{u} = \mathbf{F} - \mathbf{I}$, and let

$$\mathbf{E} = \frac{1}{2}(\mathbf{H} + \mathbf{H}^T) \tag{2.1}$$

be the linearized strain tensor. Let $\mathbf{T}$ denote the Cauchy stress tensor and $\mathbf{T}_\kappa$ be the first Piola-Kirchhoff stress. Assume that the elastic constitutive equation is given by

$$\mathbf{T} = \hat{\mathbf{T}}(\mathbf{F}),$$

or alternatively, in terms of the Piola-Kirchhoff stress, by

$$\mathbf{T}_\kappa = \hat{\mathbf{T}}_\kappa(\mathbf{F}).$$

Recall that

$$\mathbf{T}_\kappa = J\mathbf{T}_m\mathbf{F}^{-T}, \tag{2.2}$$

where $\mathbf{T}_m$ is the material description of $\mathbf{T}$. For $\mathbf{F}$ near $\mathbf{I}$ we have

$$\hat{\mathbf{T}}_\kappa(\mathbf{F}) = \hat{\mathbf{T}}_\kappa(\mathbf{I}) + \mathrm{C}[\mathbf{E}] + o(\mathbf{H}),$$

where $\mathrm{C} = D\hat{\mathbf{T}}_\kappa(\mathbf{I})$ is the elasticity tensor. One easily shows ([22]) that if the material is isotropic at $\mathbf{X}$, there exist scalars $\mu(\mathbf{X})$ and $\lambda(\mathbf{X})$ such that

$$\mathrm{C}[\mathbf{E}] = 2\mu\mathbf{E} + \lambda(\operatorname{tr}\mathbf{E})\mathbf{I}.$$

λ and μ are called *Lamé moduli*. If the residual stress vanishes ($\hat{\mathbf{T}}_\kappa(\mathbf{I}) = \hat{\mathbf{T}}(\mathbf{I}) = \mathbf{0}$), (2.2) yields

$$\mathbf{T} = \frac{1}{J}\mathbf{T}_\kappa\mathbf{F}^T = (1 - \operatorname{tr}(\mathbf{H}) + o(\mathbf{H}))\,\mathrm{C}[\mathbf{E}]\left(\mathbf{I} + \mathbf{H}^T\right) = \mathrm{C}[\mathbf{E}] + o(\mathbf{H}).$$

Now, let $\tilde{\mathbf{u}}(\mathbf{x})$ be the Eulerian description of the displacement vector, where

$$\mathbf{u}(\mathbf{X}) = \tilde{\mathbf{u}}(\mathbf{f}(\mathbf{X}))$$

and let[1] $\mathbf{e} = \frac{1}{2}\big(\text{grad}\tilde{\mathbf{u}} + (\text{grad}\tilde{\mathbf{u}})^T\big)$. Then

$$\mathbf{H} = \nabla\mathbf{u} = (\text{grad}\tilde{\mathbf{u}})\mathbf{F}.$$

Consequently, $\text{grad}\tilde{\mathbf{u}} = \mathbf{H}\mathbf{F}^{-1} = \mathbf{H} + o(\mathbf{H})$, hence

$$\mathbf{e} = \mathbf{E} + o(\mathbf{H}).$$

Thus, provided strains remain small and if there is no residual stress, one can use Hooke's law with the current configuration taken as reference to model the Cauchy stress, i.e., we can assume a constitutive equation of the form

$$\mathbf{T} = 2\mu\mathbf{e} + \lambda(\text{tr}\mathbf{e})\mathbf{I}. \tag{2.3}$$

As we are going to see in Chapter III, in contrast to LEFM which predicts infinite stresses and strains in neighborhood of the crack tip, the results of the theory proposed herein are consistent with the above assumptions.

2.3. Problem Description

We consider a classical Griffith crack, meaning a static, mode I crack of finite length $2a$ in an infinite linear elastic body, subjected to far field tensile loading σ. Later on, in Chapter V, dynamic crack propagation will be studied. The analysis presented herein for a classical Griffith crack can be easily extended to the case of an edge crack.

It is assumed that the stress away from the crack surfaces can be modeled using Hooke's law (2.3).

Another essential feature in our model, apart from the constitutive equation modeling the bulk material behavior, is the way we account for the long-range in-

[1]The gradient and divergence operators are denoted by grad and div in the spatial frame, and by ∇ and Div in the material frame.

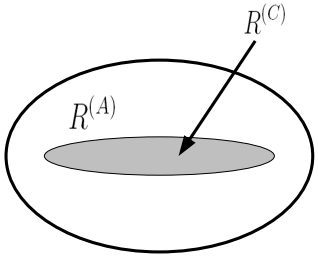

Fig. 2.1. A two-phase body.

termolecular (dispersion) forces between material points in the interfacial region. To correct for the use of bulk material behavior in the interfacial region, we introduce a point-to-point intermolecular force potential $\phi^{(A,C)}$ between a point in the region $R^{(A)}$ and a point in $R^{(C)}$ (Fig. 2.1). Since the intermediate phase is vacuum (or possibly a gas), we only need $\phi^{(A,A)}$.

The point-to-point potential $\phi^{(A,A)} = \phi_n^{(A,A)} + \phi_f^{(A,A)}$ is split into two parts - the first one, $\phi_n^{(A,A)}$, going into an excess property $\tilde{\gamma}$ ascribed to the dividing surface Σ. One could perceive that this is done by collapsing a small neighborhood around the interfacial region to Σ and ascribing the part of the potential active in this neighborhood as an excess property of the dividing surface. We assume that the upper/lower crack surface $\Sigma^{\pm}$ is parameterized by $\Sigma^{\pm} = \{\mathbf{x} \,|\, \mathbf{x} = \langle x_1, \pm h(x_1)\rangle\}$. The excess property $\tilde{\gamma}$ is modeled as a functional of the crack opening profile $h(x_1)$, defined by

$$\tilde{\gamma}(x_1) = \int_{\Gamma\{h(x_1)\}} \Phi^{(n)} ds, \tag{2.4}$$

where

$$\Phi^{(n)}(x_1, x_2) = \int_{R^{(C)}} {n^{(A)}}^2 \phi_n^{(A,A)} d\mathbf{r} \tag{2.5}$$

and $\Gamma\{h(x_1)\}$ is the ray emanating from the point $(x_1, h(x_1))$, extending into the

body along the vector normal to the crack surface. Here $n^{(A)}$ is the number density in phase A (the number of molecules or atoms per unit volume in $R^{(A)}$).

The rest of $\phi^{(A,A)}$, denoted by $\phi_f^{(A,A)}$, goes into a body force correction term which, by analogy with [39], is defined by

$$\mathbf{b}^{(corr)} = \text{grad} \int_{R^{(C)}} {n^{(A)}}^2 \phi_f^{(A,A)} d\mathbf{r} = -\text{grad}\Phi. \tag{2.6}$$

In practice the potential is obtained through fitting a given empirical form to *ab initio* calculations. Depending on the chosen empirical form, the potential could either be an analytic function of the intermolecular distance (e.g. Morse-type potentials) or could have a singularity (e.g. Lennard-Jones-type potentials). In the case of singular potentials we apply hard-sphere approximation through the use of a cut-off function.

The following nondimensionalization of the parameters is used in the subsequent analysis of the governing equations

$$\begin{array}{lll} x_i^\star = \dfrac{x_i}{a} & \mathbf{u}^\star = \dfrac{\mathbf{u}}{a} & h^\star(x_1^\star) = \dfrac{h(x_1)}{a} \\ \tilde{\gamma}^\star = \dfrac{\tilde{\gamma}}{Ea} & \mu^\star = \dfrac{\mu}{E} & \sigma^\star = \dfrac{\sigma}{E} \\ \Phi^\star = \dfrac{\Phi}{E} & \mathbf{T}^\star = \dfrac{\mathbf{T}}{E} & \end{array} \tag{2.7}$$

where $E = \mu \dfrac{3\lambda + 2\mu}{\lambda + \mu}$ is Young's modulus.

2.4. Balance of Linear Momentum

Let $\mathcal{P}$ be a part of the body intersecting the dividing surface Σ. Let $\mathcal{P}^+$ denote the domain occupied by the first phase and $\mathcal{P}^-$ be the one occupied by the second. Then $\mathcal{P} = \mathcal{P}^+ \cup (\Sigma \cap \mathcal{P}) \cup \mathcal{P}^-$. By $\partial\mathcal{P}^+$ and $\partial\mathcal{P}^-$ we denote the outer boundaries of $\mathcal{P}^+$ and $\mathcal{P}^-$ respectively, i.e., not including the dividing surface Σ (Fig. 2.2). Let the limit of

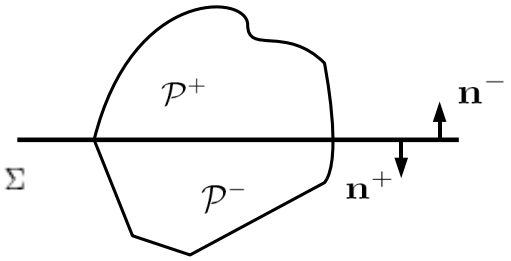

Fig. 2.2. Part $\mathcal{P}$ of a body, intersecting the dividing surface Σ.

a generic bulk field $\phi(\mathbf{x})$ in $\mathcal{P} \setminus \Sigma$ be defined by

$$\phi^{\pm}(\mathbf{x}) = \lim_{s \to 0^+} \phi(\mathbf{x} - s\mathbf{n}^{\pm}) \qquad \forall \mathbf{x} \in \Sigma$$

where $\mathbf{n}^{\pm}$ is the outward (for $\mathcal{P}^{\pm}$) unit normal vector to the dividing surface Σ. Given a field $\phi(\mathbf{x})$ we define the jump of ϕ across Σ by

$$[\![\phi]\!] = \phi^+ - \phi^-.$$

Then by the Divergence Theorem

$$\begin{aligned} \int_{\mathcal{P}} \mathrm{grad}\Phi \, dv &= \int_{\mathcal{P}^+} \mathrm{grad}\Phi \, dv + \int_{\mathcal{P}^-} \mathrm{grad}\Phi \, dv \\ &= \int_{\partial\mathcal{P}^+} \Phi\mathbf{n} \, da + \int_{\Sigma\cap\mathcal{P}} \Phi^+\mathbf{n}^+ da + \int_{\partial\mathcal{P}^-} \Phi\mathbf{n} \, da + \int_{\Sigma\cap\mathcal{P}} \Phi^-\mathbf{n}^- da \qquad (2.8) \\ &= \int_{\partial\mathcal{P}} \Phi\mathbf{n} \, da + \int_{\Sigma\cap\mathcal{P}} [\![\Phi]\!]\mathbf{n}^+ da. \end{aligned}$$

In a similar way,

$$\int_{\partial\mathcal{P}} (\mathbf{T}^{(bulk)} - \Phi\mathbf{I})\mathbf{n} \, da = \int_{\mathcal{P}} \mathrm{div}(\mathbf{T}^{(bulk)} - \Phi\mathbf{I}) \, dv - \int_{\Sigma\cap\mathcal{P}} [\![\mathbf{T}^{(bulk)} - \Phi\mathbf{I}]\!]\mathbf{n}^+ da, \qquad (2.9)$$

where $\mathbf{T}^{(bulk)}$ is the stress in the bulk material, given by (2.3). We also have

$$\int_{\partial\mathcal{P}} \mathbf{T}^{(bulk)}\mathbf{n}\, da = \int_{\mathcal{P}} \mathrm{div}(\mathbf{T}^{(bulk)})\, dv - \int_{\Sigma\cap\mathcal{P}} [\![\mathbf{T}^{(bulk)}]\!]\mathbf{n}^{+} da. \tag{2.10}$$

Let $\mathbf{f}(\mathcal{P})$ be the body forces acting on $\mathcal{P}$. Since the force system is not additive unless the stress tensor is continuous across the dividing surface, we have to define the forces acting on $\mathcal{P}$ as a whole, in contrast to defining the forces which act on $\mathcal{P}^{+}$, $\mathcal{P}^{-}$ and Σ. Theoretically we have two choices for what we declare to be the tensor used to compute the surface tractions. We can either choose this to be the bulk stress $\mathbf{T}^{(bulk)}$ or the corrected stress $\mathbf{T}^{(bulk)} - \Phi\mathbf{I}$.

- Case 1: surface tractions are computed using $\mathbf{T}^{(bulk)}$. Ignoring gravitational effects, the force acting on $\mathcal{P}$ in this case is

$$\mathbf{f}(\mathcal{P}) = \int_{\partial\mathcal{P}} \mathbf{T}^{(bulk)}\mathbf{n}\, da - \int_{\mathcal{P}} \mathrm{grad}\Phi\, dv + \int_{\partial(\Sigma\cap\mathcal{P})} \mathbf{T}^{(\sigma)}\boldsymbol{\nu} ds, \tag{2.11}$$

  where $\mathbf{T}^{(\sigma)}$ is the surface stress in the dividing surface Σ, $\partial(\Sigma\cap\mathcal{P})$ is the boundary of $\Sigma\cap\mathcal{P}$ (a curve in three dimensional space) and $\boldsymbol{\nu}$ is a unit conormal vector to $\partial(\Sigma\cap\mathcal{P})$, i.e., tangent to Σ and normal to $\partial(\Sigma\cap\mathcal{P})$. By the surface divergence theorem ([47], p. 670)

$$\int_{\partial(\Sigma\cap\mathcal{P})} \mathbf{T}^{(\sigma)}\boldsymbol{\nu}\, ds = \int_{\Sigma\cap\mathcal{P}} \mathrm{div}_{(\sigma)}\mathbf{T}^{(\sigma)} da. \tag{2.12}$$

  Substituting (2.10) in (2.11) and then applying (2.12), one obtains

$$\begin{aligned}\mathbf{f}(\mathcal{P}) &= \int_{\mathcal{P}} \mathrm{div}(\mathbf{T}^{(bulk)})dv - \int_{\Sigma\cap\mathcal{P}} [\![\mathbf{T}^{(bulk)}]\!]\mathbf{n}^{+} da \\ &\quad - \int_{\mathcal{P}} \mathrm{grad}\Phi\, dv + \int_{\partial(\Sigma\cap\mathcal{P})} \mathbf{T}^{(\sigma)}\boldsymbol{\nu}\, ds \\ &= \int_{\mathcal{P}} (\mathrm{div}(\mathbf{T}^{(bulk)}) - \mathrm{grad}\Phi)dv + \int_{\Sigma\cap\mathcal{P}} (\mathrm{div}_{(\sigma)}\mathbf{T}^{(\sigma)} - [\![\mathbf{T}^{(bulk)}]\!]\mathbf{n}^{+})da.\end{aligned} \tag{2.13}$$

By the Localization Theorem, the differential momentum balance is

$$\mathrm{div}(\mathbf{T}^{(bulk)}) = \mathrm{grad}\Phi \tag{2.14}$$

and the jump momentum balance is

$$\mathrm{div}_{(\sigma)}\mathbf{T}^{(\sigma)} - [\![\mathbf{T}^{(bulk)}]\!]\mathbf{n}^{+} = \mathbf{0}. \tag{2.15}$$

- Case 2: Surface tractions are computed using the corrected stress $\mathbf{T}^{(bulk)} - \Phi\mathbf{I}$. In this case there is no body force term. Then

$$\mathbf{f}(\mathcal{P}) = \int_{\partial\mathcal{P}} (\mathbf{T}^{(bulk)} - \Phi\mathbf{I})\mathbf{n}\, da + \int_{\partial(\Sigma\cap\mathcal{P})} \mathbf{T}^{(\sigma)}\boldsymbol{\nu} ds. \tag{2.16}$$

In a similar way, we substitute (2.9) into (2.16) and use (2.12):

$$\begin{aligned}\mathbf{f}(\mathcal{P}) &= \int_{\mathcal{P}} \mathrm{div}(\mathbf{T}^{(bulk)} - \Phi\mathbf{I}) dv - \int_{\Sigma\cap\mathcal{P}} [\![\mathbf{T}^{(bulk)} - \Phi\mathbf{I}]\!]\mathbf{n}^{+} da + \int_{\partial(\Sigma\cap\mathcal{P})} \mathbf{T}^{(\sigma)}\boldsymbol{\nu} ds \\ &= \int_{\mathcal{P}} (\mathrm{div}(\mathbf{T}^{(bulk)}) - \mathrm{grad}\Phi)\, dv \\ &\quad + \int_{\Sigma\cap\mathcal{P}} (\mathrm{div}_{(\sigma)}\mathbf{T}^{(\sigma)} - [\![\mathbf{T}^{(bulk)} - \Phi\mathbf{I}]\!]\mathbf{n}^{+})\, da.\end{aligned} \tag{2.17}$$

We obtain the same differential momentum balance equation as in the first case, but the jump momentum balance is

$$\mathrm{div}_{(\sigma)}\mathbf{T}^{(\sigma)} - [\![\mathbf{T}^{(bulk)} - \Phi\mathbf{I}]\!]\mathbf{n}^{+} = \mathbf{0}, \tag{2.18}$$

which is exactly the view taken in [39] and view (iv) in [47].

Remark 1. *From here on, we adopt the view taken in Case 1, i.e., we use the bulk stress to compute surface tractions at the crack surfaces. The reason for this choice being that the approach in Case 2 gives no stress amplification in a neighborhood of the crack tip. To simplify the notation, we leave out the superscript (bulk) from* $\mathbf{T}^{(bulk)}$*,*

which should not be confused with the notation $\mathbf{T}$ *used for the corrected stress in [39].*

2.5. Surface Gradient and Surface Divergence

Let $\phi(\mathbf{x})$ be a scalar field defined in a neighborhood of the dividing surface Σ, $\mathbf{n}$ be a unit vector normal to Σ and let $\mathbf{P}$ denote the projection tensor onto the tangent space to Σ - a second-order tensor field that transforms every tangential vector field into itself, i.e.,

$$\mathbf{P} = \mathbf{I} - \mathbf{n} \otimes \mathbf{n}. \tag{2.19}$$

Then the surface gradient of $\phi(\mathbf{x})$ is given by ([47], p. 632)

$$\mathrm{grad}_{(\sigma)}\phi = \mathbf{P}\mathrm{grad}\phi. \tag{2.20}$$

In a similar way, the surface gradient of a vector field $\mathbf{v}(\mathbf{x})$ may be expressed in the following form ([47], p. 648)

$$\mathrm{grad}_{(\sigma)}\mathbf{v} = (\mathrm{grad}\mathbf{v})\,\mathbf{P} \tag{2.21}$$

and consequently for the surface divergence of $\mathbf{v}$ one obtains

$$\mathrm{div}_{(\sigma)}\mathbf{v} = \mathrm{tr}((\mathrm{grad}\mathbf{v})\,\mathbf{P}). \tag{2.22}$$

As for the surface divergence of a second order tensor field $\mathbf{A}(\mathbf{x})$, it can be easily shown ([47], p. 661) that it satisfies

$$\mathbf{c} \cdot \mathrm{div}_{(\sigma)}\mathbf{A} = \mathrm{div}_{(\sigma)}(\mathbf{A}^T\mathbf{c}) \tag{2.23}$$

for any constant vector $\mathbf{c}$. Equation (2.23) can be used as a definition of $\mathrm{div}_{(\sigma)}\mathbf{A}$. The surface divergence and surface gradient satisfy product rules analogous to the standard ones (for div and grad).

Lemma 1. *Let ϕ, $\mathbf{v}$, $\mathbf{w}$, and $\mathbf{A}$ be smooth fields with ϕ - scalar valued, $\mathbf{v}$ and $\mathbf{w}$ - vector valued, and $\mathbf{A}$ - tensor valued. Then*

$$div_{(\sigma)}(\phi\mathbf{A}) = \mathbf{A}grad_{(\sigma)}\phi + \phi div_{(\sigma)}\mathbf{A}, \tag{2.24}$$

$$div_{(\sigma)}(\mathbf{v}\otimes\mathbf{w}) = \mathbf{v}div_{(\sigma)}\mathbf{w} + (grad_{(\sigma)}\mathbf{v})\mathbf{w}. \tag{2.25}$$

Proof. Let $\mathbf{c}$ be an arbitrary constant vector. Then, using (2.22),

$$\begin{aligned}\mathbf{c}\cdot\mathrm{div}_{(\sigma)}(\phi\mathbf{A}) &= \mathrm{div}_{(\sigma)}(\phi\mathbf{A}^T\mathbf{c}) = \mathrm{tr}(\mathrm{grad}(\phi\mathbf{A}^T\mathbf{c})\mathbf{P})\\ &= \phi\mathrm{tr}(\mathrm{grad}(\mathbf{A}^T\mathbf{c})\mathbf{P}) + \mathbf{c}\cdot\mathbf{A}\mathbf{P}\mathrm{grad}\phi\\ &= \phi\mathrm{div}_{(\sigma)}(\mathbf{A}^T\mathbf{c}) + \mathbf{c}\cdot\mathbf{A}\mathrm{grad}_{(\sigma)}\phi = \mathbf{c}\cdot(\phi\mathrm{div}_{(\sigma)}(\mathbf{A}) + \mathbf{A}\mathrm{grad}_{(\sigma)}\phi)\end{aligned}$$

which proves (2.24). For (2.25) we proceed in a similar way:

$$\begin{aligned}\mathbf{c}\cdot\mathrm{div}_{(\sigma)}(\mathbf{v}\otimes\mathbf{w}) &= \mathrm{tr}(\mathrm{grad}((\mathbf{c}\cdot\mathbf{v})\mathbf{w})\mathbf{P}) = \mathrm{tr}([(\mathbf{c}\cdot\mathbf{v})\mathrm{grad}\mathbf{w} + \mathbf{w}\otimes\mathrm{grad}(\mathbf{c}\cdot\mathbf{v})]\mathbf{P})\\ &= (\mathbf{c}\cdot\mathbf{v})\mathrm{div}_{(\sigma)}(\mathbf{w}) + \mathbf{w}\cdot(\mathrm{grad}\mathbf{v}\mathbf{P})^T\mathbf{c}\\ &= \mathbf{c}\cdot(\mathbf{v}\mathrm{div}_{(\sigma)}\mathbf{w} + (\mathrm{grad}_{(\sigma)}\mathbf{v})\mathbf{w}).\end{aligned}$$

□

For a detailed discussion of the theory of elastic material surfaces see [23, 24, 37, 47]. We can now find an explicit expression for $\mathrm{div}_{(\sigma)}\mathbf{T}^{(\sigma)}$. If we assume that the surface stress $\mathbf{T}^{(\sigma)}$ is given by $\mathbf{T}^{(\sigma)} = \tilde{\gamma}\mathbf{P}$, where $\mathbf{P}$ is the projection tensor defined by (2.19), then (2.24) yields

$$\mathrm{div}_{(\sigma)}\mathbf{T}^{(\sigma)} = \mathrm{grad}_{(\sigma)}\tilde{\gamma} + \tilde{\gamma}\mathrm{div}_{(\sigma)}\mathbf{P}. \tag{2.26}$$

Now, combining (2.19) and (2.25) one has

$$\mathrm{div}_{(\sigma)}\mathbf{P} = -\mathrm{div}_{(\sigma)}\mathbf{n}\otimes\mathbf{n} = -\mathbf{n}\mathrm{div}_{(\sigma)}\mathbf{n}. \tag{2.27}$$

Here we have used the fact that

$$(\mathrm{grad}_{(\sigma)}\mathbf{n})\mathbf{n} = (\mathrm{grad}\mathbf{n})\,\mathbf{P}\mathbf{n} = \mathbf{0}.$$

Let us now define the *curvature* of Σ by

$$H = -\frac{1}{2}\mathrm{div}_{(\sigma)}\mathbf{n}, \tag{2.28}$$

where, in order to avoid ambiguity of the definition, we are going to choose the direction of $\mathbf{n}$ so that $\mathbf{n}$ points into $\mathcal{P}^+$ (Fig. 2.2). Note that $\mathrm{div}_{(\sigma)}\mathbf{P}$ is independent of how we choose the direction of $\mathbf{n}$. Then we can express $\mathrm{div}_{(\sigma)}\mathbf{P}$ in the following way

$$\mathrm{div}_{(\sigma)}\mathbf{P} = 2H\mathbf{n}. \tag{2.29}$$

Combining (2.15), (2.26) and (2.29) one concludes that the jump momentum balance for Case 1 takes the form

$$\mathrm{grad}_{(\sigma)}\tilde{\gamma} + 2\tilde{\gamma}H\mathbf{n}^- + [\![\mathbf{T}]\!]\mathbf{n}^- = \mathbf{0}. \tag{2.30}$$

Consider first the upper crack surface. It can be described by the scalar equation

$$f(\mathbf{x}) = x_2 - h(x_1) = 0 \qquad \text{for } -1 < x_1 < 1.$$

Then the unit normal vector pointing into the bulk material ($\mathcal{P}^+$) is given by

$$\mathbf{n}^- = \frac{1}{\sqrt{1+h'^2}}\langle -h', 1, 0\rangle^T. \tag{2.31}$$

This and (2.19) yield the following expression for the projection tensor $\mathbf{P}$

$$\mathbf{P} = \frac{1}{1+h'^2}\begin{pmatrix} 1 & h' & 0 \\ h' & h'^2 & 0 \\ 0 & 0 & 1+h'^2 \end{pmatrix}.$$

Then, by (2.20), the surface gradient of $\tilde{\gamma}(x_1)$ can be expressed as follows:

$$\mathrm{grad}_{(\sigma)}\tilde{\gamma} = \mathbf{P}\mathrm{grad}\tilde{\gamma} = \frac{\tilde{\gamma}'}{1+h'^2}\langle 1, h', 0\rangle^T. \tag{2.32}$$

Next, consider $\mathrm{div}_{(\sigma)}\mathbf{n}^-$. Using (2.22) one arrives at

$$\mathrm{div}_{(\sigma)}\mathbf{n}^- = -\frac{1}{(1+h'^2)^{5/2}}\mathrm{tr}\left(\begin{pmatrix} h'' & h'h'' & 0 \\ h'h'' & (h')^2h'' & 0 \\ 0 & 0 & 0 \end{pmatrix}\right) = \frac{-h''}{(1+h'^2)^{3/2}}. \tag{2.33}$$

In the case of plane stress, one obtains the following component form for the jump momentum balance equations using (2.28), (2.30), (2.31), (2.32), and (2.33):

$$\begin{aligned} &\frac{\tilde{\gamma}'}{(1+h'^2)^{1/2}} - \frac{\tilde{\gamma}h'h''}{(1+h'^2)^{3/2}} + (-h'\tau_{11} + \tau_{12}) = 0 \\ &\frac{\tilde{\gamma}'h'}{(1+h'^2)^{1/2}} + \frac{\tilde{\gamma}h''}{(1+h'^2)^{3/2}} + (-h'\tau_{12} + \tau_{22}) = 0, \end{aligned} \tag{2.34}$$

where τ_{ij} are the components of the Cauchy stress $\mathbf{T}$ in Cartesian coordinates.

2.6. Localization of Φ and $\tilde{\gamma}$ Using Perturbation Theory

In this section we derive an approximation to the correction potential Φ and the excess property $\tilde{\gamma}$. Since they depend on the crack opening profile, we work in the current configuration as reference. Let $\mathbf{x} = \langle x_1, x_2\rangle \in \mathcal{B}$ be a point in the current configuration $\mathcal{B}$ of the body. As derived above (cf. (2.14) and (2.30)), the quasistatic differential balance of linear momentum becomes

$$\mathrm{div}(\mathbf{T}) = \mathrm{grad}\Phi \tag{2.35}$$

and the jump momentum balance across the crack faces can be written in the following form:

$$\mathrm{grad}_{(\sigma)}\tilde{\gamma} + 2\tilde{\gamma}H\mathbf{n}^- + [\![\mathbf{T}]\!]\mathbf{n}^- = \mathbf{0}, \tag{2.36}$$

where $\mathbf{n}^-$ is the unit normal vector to the crack surface Σ pointing into the bulk material.

For the bulk material, elastic constitutive behavior modeled by Hooke's law (2.3) is assumed. In addition, we assume homogeneous tensile far-field loading, i.e.,

$$\begin{aligned} \lim_{x_2\to\infty} \tau_{11}(x_1,x_2) &= 0 \\ \lim_{x_2\to\infty} \tau_{12}(x_1,x_2) &= 0 \\ \lim_{x_2\to\infty} \tau_{22}(x_1,x_2) &= \sigma. \end{aligned} \tag{2.37}$$

Two different approaches are employed to solve the given problem. The first one is presented in Chapter III and is based on the *Method of Integral Transforms*. This approach allows us to prove that a model incorporating nonzero curvature-dependent surface tension, together with the appropriate boundary condition in the form of the jump momentum balance, leads to bounded stresses in a neighborhood of the crack tip in contrast to the results of the classical theory of Linear Elastic Fracture Mechanics.

The second approach uses singular perturbation methods (similar to boundary layer theory in fluid mechanics) to approximate the solution. Since the mutual body force term in (2.35) and the boundary condition (2.36) lead to a highly non-linear problem, the potential Φ and the excess property $\tilde{\gamma}$, which can be viewed as non-local operators on the crack profile h, are approximated by local operators.

In order to simplify the notation, let $\phi(r^\star/\delta^\star) := \dfrac{a^3}{E}\phi_f^{(A,A)}(r/\delta)$ where $r^\star$ denotes the nondimensional intermolecular distance:

$$r^\star = \sqrt{(x_1^\star - x^\star)^2 + (x_2^\star - y^\star)^2 + z^{\star 2}}, \tag{2.38}$$

δ is a parameter, associated with the interatomic length scale and $\delta^\star = \delta/a$. (Recall that the crack profile in the current configuration can be parameterized by

$\{(x_1, x_2) \,|\, x_1 \in (-a, a), x_2 = \pm h(x_1)\}$.)

Assume that a suitable relation between the parameters can be found which turns $\phi(r^\star/\delta^\star)$ into a delta sequence as $\delta^\star \to 0$, i.e.,

$$\tilde{\phi}(r^\star) := (\delta^\star)^{-3}\phi(\frac{r^\star}{\delta^\star}). \tag{2.39}$$

Assume also that the potential $\tilde{\phi}(r^\star) \in L^1(\mathbb{R}^3)$.

Let $r^\star$ be as in (2.38). After a change of variables $\Phi^\star(x_1^\star, x_2^\star)$ can be written in the following way:

$$\begin{aligned}\Phi^\star(x_1^\star, x_2^\star, \{h^\star(\cdot,\delta^\star)\}, \delta^\star) &= \int_{-1}^{1}\int_{-h^\star(x^\star)}^{h^\star(x^\star)}\int_{-\infty}^{\infty}\phi\left(r^\star\right)dz^\star dy^\star dx^\star \\ &= \int_{-1}^{x_1^\star}\int_{-h^\star(x^\star)}^{h^\star(x^\star)}\int_{-\infty}^{\infty}\phi\left(r^\star\right)dz^\star dy^\star dx^\star + \int_{x_1^\star}^{1}\int_{-h^\star(x^\star)}^{h^\star(x^\star)}\int_{-\infty}^{\infty}\phi\left(r^\star\right)dz^\star dy^\star dx^\star.\end{aligned} \tag{2.40}$$

Here the notation $\{h^\star(\cdot,\delta^\star)\}$ is used to signify that $\Phi^\star$ is a non-local functional of $h^\star(\cdot,\delta^\star)$ rather than one depending only on its point values for a given $x_1^\star$. Consider first

$$\begin{aligned}&\int_{x_1^\star}^{1}\int_{-h^\star(x^\star)}^{h^\star(x^\star)}\int_{-\infty}^{\infty}\phi\left(\sqrt{(x_1^\star - x^\star)^2 + (x_2^\star - y^\star)^2 + z^{\star 2}}\right)dz^\star dy^\star dx^\star \\ &= \int_{0}^{1-x_1^\star}\int_{x_2^\star - h^\star(x_1^\star + x^\star)}^{x_2^\star + h^\star(x_1^\star + x^\star)}\int_{-\infty}^{\infty}\phi\left(\sqrt{x^{\star 2} + y^{\star 2} + z^{\star 2}}\right)dz^\star dy^\star dx^\star \\ &= \int_{0}^{(1-x_1^\star)/\delta^\star}\int_{(x_2^\star - h^\star(x_1^\star + \delta^\star x^\star))/\delta^\star}^{(x_2^\star + h^\star(x_1^\star + \delta^\star x^\star))/\delta^\star}\int_{-\infty}^{\infty}\tilde{\phi}\left(\sqrt{x^{\star 2} + y^{\star 2} + z^{\star 2}}\right)dz^\star dy^\star dx^\star \\ &=: I_1(x_1^\star, x_2^\star, \{h^\star(\cdot,\delta^\star)\}, \delta^\star).\end{aligned} \tag{2.41}$$

For the last equality property (2.39) is used. Thus

$$\Phi^\star(x_1^\star, x_2^\star, \{h^\star(\cdot,\delta^\star)\}, \delta^\star) = I_1(x_1^\star, x_2^\star, \{h^\star(\cdot,\delta^\star)\}, \delta^\star) + I_2(x_1^\star, x_2^\star, \{h^\star(\cdot,\delta^\star)\}, \delta^\star) \tag{2.42}$$

where

$$I_2(x_1^\star, x_2^\star, \{h^\star(\cdot,\delta^\star)\},\delta^\star) := \int_0^{(1+x_1^\star)/\delta^\star} \int_{(x_2^\star - h^\star(x_1^\star - \delta^\star x^\star))/\delta^\star}^{(x_2^\star + h^\star(x_1^\star - \delta^\star x^\star))/\delta^\star} \int_{-\infty}^{\infty} \tilde{\phi}\left(\sqrt{x^{\star 2} + y^{\star 2} + z^{\star 2}}\right) dz^\star dy^\star dx^\star. \tag{2.43}$$

Since we are interested in the behavior of $\Phi^\star(x_1^\star, x_2^\star)$ in a small neighborhood around the crack surface, we make the following change of variables

$$y_2^{\star\star} = \frac{x_2^\star - h^\star(x_1^\star)}{\delta^\star}.$$

Assuming that the expansion of the crack profile $h^\star(\cdot,\delta^\star)$ in terms of the *small* parameter $\delta^\star$ is given by

$$h^\star(\cdot,\delta^\star) = h_0^\star(\cdot) + \delta^\star h_1^\star(\cdot) + O(\delta^{\star 2}), \tag{2.44}$$

we look for expansions

$$I_i(x_1^\star, x_2^\star, \{h^\star(\cdot,\delta^\star)\},\delta^\star) = I_i^{(0)}(x_1^\star, y_2^{\star\star}) + \delta^\star I_i^{(1)}(x_1^\star, y_2^{\star\star}) + O(\delta^{\star 2}), \quad i = 1,2 \tag{2.45}$$

where

$$I_i^{(0)}(x_1^\star, y_2^{\star\star}) = \lim_{\delta^\star \to 0} I_i(x_1^\star, x_2^\star, \{h^\star(\cdot,\delta^\star)\},\delta^\star) \tag{2.46}$$

and

$$I_i^{(1)}(x_1^\star, y_2^{\star\star}) = \lim_{\delta^\star \to 0} \frac{\partial}{\partial \delta^\star} I_i(x_1^\star, x_2^\star, \{h^\star(\cdot,\delta^\star)\},\delta^\star). \tag{2.47}$$

We consider $-1 < x_1^\star < 1$, in which case $h^\star(x_1^\star) > 0$ whenever the applied loading is nonzero. Then

$$\frac{x_2^\star + h^\star(x_1^\star \pm \delta^\star x^\star)}{\delta^\star} = \frac{\delta^\star y_2^{\star\star} + h^\star(x_1^\star) + h^\star(x_1^\star \pm \delta^\star x^\star)}{\delta^\star} \to \infty \quad \text{as } \delta^\star \to 0 \tag{2.48}$$

and

$$\begin{aligned}\frac{x_2^\star - h^\star(x_1^\star \pm \delta^\star x^\star)}{\delta^\star} &= \frac{\delta^\star y_2^{\star\star} + h^\star(x_1^\star) - h^\star(x_1^\star \pm \delta^\star x^\star)}{\delta^\star} \\ &\to y_2^{\star\star} \mp x^\star h_0^{\star\prime}(x_1^\star) \quad \text{as } \delta^\star \to 0.\end{aligned} \tag{2.49}$$

Using equations (2.46), (2.48) and (2.49) and the fact that $\tilde{\phi}(r^\star) \in L^1(\mathbb{R}^3)$, one concludes

$$\begin{aligned}I_1^{(0)}(x_1^\star, y_2^{\star\star}) &= \int_0^\infty \int_{y_2^{\star\star} - x^\star h_0^{\star\prime}(x_1^\star)}^\infty \int_{-\infty}^\infty \tilde{\phi}\left(\sqrt{x^{\star 2} + y^{\star 2} + z^{\star 2}}\right) dz^\star dy^\star dx^\star \\ &= \tilde{I_1}^{(0)}(h_0^{\star\prime}(x_1^\star), y_2^{\star\star}) \\ I_2^{(0)}(x_1^\star, y_2^{\star\star}) &= \int_0^\infty \int_{y_2^{\star\star} + x^\star h_0^{\star\prime}(x_1^\star)}^\infty \int_{-\infty}^\infty \tilde{\phi}\left(\sqrt{x^{\star 2} + y^{\star 2} + z^{\star 2}}\right) dz^\star dy^\star dx^\star \\ &= \tilde{I_2}^{(0)}(h_0^{\star\prime}(x_1^\star), y_2^{\star\star}).\end{aligned} \tag{2.50}$$

Remark 2. *The zero order approximation of the correction potential $\Phi^\star(x_1^\star, x_2^\star)$ on the crack surface is given by*

$$\begin{aligned}&\Phi_0^\star(x_1^\star, h^\star(x_1^\star)) = I_1^{(0)}(x_1^\star, 0) + I_2^{(0)}(x_1^\star, 0) \\ &= 2\int_0^\infty \int_{-x^\star h_0^{\star\prime}(x_1^\star)}^\infty \int_{-\infty}^\infty \tilde{\phi}\left(\sqrt{x^{\star 2} + y^{\star 2} + z^{\star 2}}\right) dz^\star dy^\star dx^\star \\ &+ \int_0^\infty \int_{x^\star h_0^{\star\prime}(x_1^\star)}^{-x^\star h_0^{\star\prime}(x_1^\star)} \int_{-\infty}^\infty \tilde{\phi}\left(\sqrt{x^{\star 2} + y^{\star 2} + z^{\star 2}}\right) dz^\star dy^\star dx^\star \\ &= 2\int_0^\infty \int_0^\infty \int_{-\infty}^\infty \tilde{\phi}\left(\sqrt{x^{\star 2} + y^{\star 2} + z^{\star 2}}\right) dz^\star dy^\star dx^\star = const.\end{aligned} \tag{2.51}$$

One should note here that even though the zero order approximation of the potential is constant on the crack surface, it does depend on $y_2^{\star\star}$ and the point values of the slope of the crack profile $h^{\star\prime}(x_1^\star)$ away from the crack surface.

Let

$$
\begin{aligned}
&a(x_1^\star, y_2^{\star\star}, x^\star, \delta^\star) := \frac{\delta^\star y_2^{\star\star} + h^\star(x_1^\star) - h^\star(x_1^\star + \delta^\star x^\star)}{\delta^\star} \\
&= y_2^{\star\star} + \frac{h_0^\star(x_1^\star) + \delta^\star h_1^\star(x_1^\star) - h_0^\star(x_1^\star + \delta^\star x^\star) - \delta^\star h_1^\star(x_1^\star + \delta^\star x^\star)}{\delta^\star} + O(\delta^\star) \quad \Rightarrow \\
&a(x_1^\star, y_2^{\star\star}, x^\star, \delta^\star) = y_2^{\star\star} - x^\star h_0^{\star\prime}(x_1^\star) - \delta^\star \left(\frac{x^{\star 2}}{2} h_0^{\star\prime\prime}(x_1^\star) + x^\star h_1^{\star\prime}(x_1^\star) \right) + O(\delta^{\star 2}) \\
&\frac{\partial}{\partial \delta^\star} a(x_1^\star, y_2^{\star\star}, x^\star, \delta^\star) = - \left(\frac{x^{\star 2}}{2} h_0^{\star\prime\prime}(x_1^\star) + x^\star h_1^{\star\prime}(x_1^\star) \right) + O(\delta^\star)
\end{aligned}
\tag{2.52}
$$

and

$$
\begin{aligned}
&b(x_1^\star, y_2^{\star\star}, x^\star, \delta^\star) := \frac{\delta^\star y_2^{\star\star} + h^\star(x_1^\star) + h^\star(x_1^\star + \delta^\star x^\star)}{\delta^\star} \\
&= y_2^{\star\star} + \frac{h_0^\star(x_1^\star) + \delta^\star h_1^\star(x_1^\star) + h_0^\star(x_1^\star + \delta^\star x^\star) + \delta^\star h_1^\star(x_1^\star + \delta^\star x^\star)}{\delta^\star} + O(\delta^\star) \quad \Rightarrow \\
&b(x_1^\star, y_2^{\star\star}, x^\star, \delta^\star) = \frac{2h_0^\star(x_1^\star)}{\delta^\star} + y_2^{\star\star} + 2h_1^\star(x_1^\star) + x^\star h_0^{\star\prime}(x_1^\star) + O(\delta^\star) \\
&\frac{\partial}{\partial \delta^\star} b(x_1^\star, y_2^{\star\star}, x^\star, \delta^\star) = -\frac{2h_0^\star(x_1^\star)}{\delta^{\star 2}} + 2h_2^\star(x_1^\star) + x^\star h_1^{\star\prime}(x_1^\star) + \frac{x^{\star 2}}{2} h_0^{\star\prime\prime}(x_1^\star) \\
&\qquad\qquad + O(\delta^\star).
\end{aligned}
\tag{2.53}
$$

We proceed with the calculation of $I_1^{(1)}(x_1^\star, y_2^{\star\star})$:

$$
\begin{aligned}
&\frac{\partial}{\partial \delta^\star} I_1(x_1^\star, x_2^\star, \{h^\star(\cdot, \delta^\star)\}, \delta^\star) \\
&= \frac{\partial}{\partial \delta^\star} \int_0^{(1-x_1^\star)/\delta^\star} \int_{a(x_1^\star, y_2^{\star\star}, x^\star, \delta^\star)}^{b(x_1^\star, y_2^{\star\star}, x^\star, \delta^\star)} \int_{-\infty}^{\infty} \tilde{\phi}\left(\sqrt{x^{\star 2} + y^{\star 2} + z^{\star 2}} \right) dz^\star dy^\star dx^\star \\
&= \frac{-1 + x_1^\star}{\delta^{\star 2}} \int_{a(x_1^\star, y_2^{\star\star}, \frac{1-x_1^\star}{\delta^\star}, \delta^\star)}^{b(x_1^\star, y_2^{\star\star}, \frac{1-x_1^\star}{\delta^\star}, \delta^\star)} \int_{-\infty}^{\infty} \tilde{\phi}\left(\sqrt{\left(\frac{1 - x_1^\star}{\delta^\star} \right)^2 + y^{\star 2} + z^{\star 2}} \right) dz^\star dy^\star \\
&+ \int_0^{\frac{1-x_1^\star}{\delta^\star}} \int_{-\infty}^{\infty} \left(\tilde{\phi}\left(\sqrt{x^{\star 2} + (b(x_1^\star, y_2^{\star\star}, x^\star, \delta^\star))^2 + z^{\star 2}} \right) \frac{\partial}{\partial \delta^\star} b(x_1^\star, y_2^{\star\star}, x^\star, \delta^\star) \right. \\
&\qquad \left. - \tilde{\phi}\left(\sqrt{x^{\star 2} + (a(x_1^\star, y_2^{\star\star}, x^\star, \delta^\star))^2 + z^{\star 2}} \right) \frac{\partial}{\partial \delta^\star} a(x_1^\star, y_2^{\star\star}, x^\star, \delta^\star) \right) dz^\star dx^\star.
\end{aligned}
\tag{2.54}
$$

The first and the second terms in the right hand side of (2.54) vanish as $\delta^\star$ tends to

zero provided

$$r^2\tilde{\phi}(r) \to 0 \quad \text{as } r \to \infty. \tag{2.55}$$

Combining (2.52), (2.54) and (2.55) one concludes

$$\begin{aligned} I_1^{(1)}(x_1^\star, y_2^{\star\star}) &= \lim_{\delta^\star \to 0} \frac{\partial}{\partial \delta^\star} I_1(x_1^\star, x_2^\star, \{h^\star(\cdot, \delta^\star)\}, \delta^\star) \\ &= \int_0^\infty \int_{-\infty}^\infty \tilde{\phi}\left(\sqrt{x^{\star 2} + \left(y_2^{\star\star} - x^\star h_0^{\star\prime}(x_1^\star)\right)^2 + z^{\star 2}}\right) \\ &\qquad \times \left(\frac{x^{\star 2}}{2} h_0^{\star\prime\prime}(x_1^\star) + x^\star h_1^{\star\prime}(x_1^\star)\right) dz^\star dx^\star. \end{aligned} \tag{2.56}$$

In a similar way one can show that

$$\begin{aligned} I_2^{(1)}(x_1^\star, y_2^{\star\star}) &= \lim_{\delta^\star \to 0} \frac{\partial}{\partial \delta^\star} I_2(x_1^\star, x_2^\star, \{h^\star(\cdot, \delta^\star)\}, \delta^\star) \\ &= \int_0^\infty \int_{-\infty}^\infty \tilde{\phi}\left(\sqrt{x^{\star 2} + \left(y_2^{\star\star} + x^\star h_0^{\star\prime}(x_1^\star)\right)^2 + z^{\star 2}}\right) \\ &\qquad \times \left(\frac{x^{\star 2}}{2} h_0^{\star\prime\prime}(x_1^\star) - x^\star h_1^{\star\prime}(x_1^\star)\right) dz^\star dx^\star. \end{aligned} \tag{2.57}$$

Let $\psi(r^\star/\delta^\star) := \dfrac{a^3}{E}\phi_n^{(A,A)}(r/\delta)$ and assume that it satisfies a property analogous to (2.39), i.e.,

$$\tilde{\psi}(r^\star) := (\delta^\star)^{-3}\psi(\frac{r^\star}{\delta^\star}). \tag{2.58}$$

Combining equations (2.4) and the equivalent of (2.50)[2] for $\tilde{\psi}$, one obtains the fol-

[2]Use of the inner variables and the approximation of $\Phi^{(n)}$ given by the analogue of (2.50) is valid, since $\tilde{\gamma}$ is constructed by collapsing a small neighborhood of the interfacial region to the dividing surface Σ and ascribing the part of the point-to-point potential active in this neighborhood as an excess property $\tilde{\gamma}$ of Σ. Thus, integration in (2.4) along the entire ray $\Gamma\{h(x_1)\}$ is used only due to the fast decay of the potential $\Phi^{(n)}$.

lowing expression for the zero order approximation of the excess property $\tilde{\gamma}$

$$\begin{aligned}\tilde{\gamma}_0^\star(x_1^\star) &= \int_0^\infty \Bigg\{ \int_0^\infty \int_{y_2^{\star\star}-x^\star h_0^{\star\prime}(x_1^\star)}^\infty \int_{-\infty}^\infty \psi\left(\sqrt{x^{\star 2}+y^{\star 2}+z^{\star 2}}\right) dz^\star dy^\star dx^\star \\ &\qquad + \int_0^\infty \int_{y_2^{\star\star}+x^\star h_0^{\star\prime}(x_1^\star)}^\infty \int_{-\infty}^\infty \psi\left(\sqrt{x^{\star 2}+y^{\star 2}+z^{\star 2}}\right) dz^\star dy^\star dx^\star \Bigg\} dy_2^{\star\star} \\ &= \int_0^\infty \int_0^\infty \int_{y_2^{\star\star}}^\infty \int_{-\infty}^\infty \Bigg(\psi\left(\sqrt{x^{\star 2}+\left(y^\star - x^\star h_0^{\star\prime}(x_1^\star)\right)^2+z^{\star 2}}\right) \\ &\qquad + \psi\left(\sqrt{x^{\star 2}+\left(y^\star + x^\star h_0^{\star\prime}(x_1^\star)\right)^2+z^{\star 2}}\right) \Bigg) dz^\star dy^\star dx^\star dy_2^{\star\star}.\end{aligned} \tag{2.59}$$

Switching the order of integration with respect to $y^\star$ and $y_2^{\star\star}$, one obtains $\int_0^\infty \int_{y_2^{\star\star}}^\infty (...) dy^\star dy_2^{\star\star} = \int_0^\infty \int_0^{y^\star} (...) dy_2^{\star\star} dy^\star$. As the integrand has no $y_2^{\star\star}$ dependence, (2.59) reduces to

$$\begin{aligned}\tilde{\gamma}_0^\star(x_1^\star) &= 2\int_0^\infty \int_0^\infty \int_0^\infty y^\star \Bigg(\tilde{\psi}\left(x^\star \sqrt{1+\left(\frac{y^\star}{x^\star} - h_0^{\star\prime}(x_1^\star)\right)^2 + \left(\frac{z^\star}{x^\star}\right)^2} \right) \\ &\qquad + \tilde{\psi}\left(x^\star \sqrt{1+\left(\frac{y^\star}{x^\star} + h_0^{\star\prime}(x_1^\star)\right)^2 + \left(\frac{z^\star}{x^\star}\right)^2} \right) \Bigg) dz^\star dy^\star dx^\star \\ &= 2\int_0^\infty \int_0^\infty \int_0^\infty (x^\star)^3 y^\star \Bigg(\tilde{\psi}\left(x^\star \sqrt{1+\left(y^\star - h_0^{\star\prime}(x_1^\star)\right)^2 + z^{\star 2}} \right) \\ &\qquad + \tilde{\psi}\left(x^\star \sqrt{1+\left(y^\star + h_0^{\star\prime}(x_1^\star)\right)^2 + z^{\star 2}} \right) \Bigg) dz^\star dy^\star dx^\star.\end{aligned} \tag{2.60}$$

We now split the integral into two parts. In the first we make a change of variables

$$s = x^\star \sqrt{1+\left(y^\star - h_0^{\star\prime}(x_1^\star)\right)^2 + z^{\star 2}},$$

in the second -

$$s = x^\star \sqrt{1+\left(y^\star + h_0^{\star\prime}(x_1^\star)\right)^2 + z^{\star 2}}.$$

Finally, for the zero order approximation of the excess property $\tilde{\gamma}$ we obtain

$$\begin{aligned}\tilde{\gamma}_0^\star(x_1^\star) &= 2\int_0^\infty s^3\tilde{\psi}(s)ds\int_0^\infty\int_0^\infty\left\{\frac{y^\star}{\left(1+(y^\star-h_0^{\star\prime}(x_1^\star))^2+z^{\star 2}\right)^2}\right.\\ &\qquad\left.+\frac{y^\star}{\left(1+(y^\star+h_0^{\star\prime}(x_1^\star))^2+z^{\star 2}\right)^2}\right\}dz^\star dy^\star \qquad (2.61)\\ &= \pi\sqrt{1+(h_0^{\star\prime}(x_1^\star))^2}\int_0^\infty s^3\tilde{\psi}(s)ds,\end{aligned}$$

provided $s^3\tilde{\psi}(s)\in L^1(0,\infty)$.

We proceed with computing the first order approximation of $\tilde{\gamma}$. Combining equation (2.4) with the analogs of (2.56) and (2.57) for $\tilde{\psi}$ we obtain

$$\begin{aligned}\tilde{\gamma}_1^\star(x_1^\star) &= \int_0^\infty\left(I_1^{(1)}(x_1^\star,y_2^{\star\star})+I_2^{(1)}(x_1^\star,y_2^{\star\star})\right)dy_2^{\star\star}\\ &= h_0^{\star\prime\prime}(x_1^\star)\int_0^\infty dz^\star\int_0^\infty dx^\star\left(\int_{-x^\star h_0^{\star\prime}}^\infty dy_2^{\star\star}+\int_{x^\star h_0^{\star\prime}}^\infty dy_2^{\star\star}\right)\\ &\qquad\times\left\{x^{\star 2}\tilde{\psi}\left(\sqrt{x^{\star 2}+y_2^{\star\star 2}+z^{\star 2}}\right)\right\} \qquad (2.62)\\ &+2h_1^{\star\prime}(x_1^\star)\int_0^\infty dz^\star\int_0^\infty dx^\star\left(\int_{-x^\star h_0^{\star\prime}}^\infty dy_2^{\star\star}-\int_{x^\star h_0^{\star\prime}}^\infty dy_2^{\star\star}\right)\\ &\qquad\times\left\{x^\star\tilde{\psi}\left(\sqrt{x^{\star 2}+y_2^{\star\star 2}+z^{\star 2}}\right)\right\}.\end{aligned}$$

Notice that since the integrand is an even function of $y_2^{\star\star}$,

$$\begin{aligned}&\int_{-x^\star h_0^{\star\prime}}^\infty dy_2^{\star\star}+\int_{x^\star h_0^{\star\prime}}^\infty dy_2^{\star\star}=2\int_{-x^\star h_0^{\star\prime}}^\infty dy_2^{\star\star}+\int_{x^\star h_0^{\star\prime}}^{-x^\star h_0^{\star\prime}} dy_2^{\star\star}\\ =&2\int_{-x^\star h_0^{\star\prime}}^\infty dy_2^{\star\star}+2\int_0^{-x^\star h_0^{\star\prime}} dy_2^{\star\star}=2\int_0^\infty dy_2^{\star\star},\end{aligned}$$

and

$$\int_{-x^\star h_0^{\star\prime}}^\infty dy_2^{\star\star}-\int_{x^\star h_0^{\star\prime}}^\infty dy_2^{\star\star}=-\int_{x^\star h_0^{\star\prime}}^{-x^\star h_0^{\star\prime}} dy_2^{\star\star}=-2\int_0^{-x^\star h_0^{\star\prime}} dy_2^{\star\star}.$$

Using the above equality we simplify the second term of (2.62) in the following way

$$\begin{aligned}
&\int_0^\infty \int_0^\infty \int_0^{-x^\star h_0^{\star\prime}} \left(x^\star \tilde{\psi}\left(\sqrt{x^{\star 2} + y_2^{\star\star 2} + z^{\star 2}} \right) \right) dy_2^{\star\star} dx^\star dz^\star \\
=&\int_0^\infty \int_0^\infty \int_0^{-h_0^{\star\prime}} \left(x^{\star 2} \tilde{\psi}\left(\sqrt{(1+y^{\star 2})x^{\star 2} + z^{\star 2}} \right) \right) dy^\star dx^\star dz^\star \\
=&\int_0^\infty \int_0^{-h_0^{\star\prime}} \int_0^\infty \left(\frac{s^2}{(1+y^{\star 2})^{3/2}} \tilde{\psi}\left(\sqrt{s^2 + z^{\star 2}} \right) \right) ds dy^\star dz^\star \\
=&\frac{-h_0^{\star\prime}}{\sqrt{1+(h_0^{\star\prime})^2}} \int_0^\infty \int_0^\infty \left(s^2 \tilde{\psi}\left(\sqrt{s^2 + z^{\star 2}} \right) \right) ds dz^\star \\
=&\frac{-\pi h_0^{\star\prime}}{4\sqrt{1+(h_0^{\star\prime})^2}} \int_0^\infty r^3 \tilde{\psi}(r) dr.
\end{aligned} \tag{2.63}$$

For the first term, notice that after several changes of variables it simplifies to

$$\begin{aligned}
&\int_0^\infty \int_0^\infty \int_0^\infty \left(x^{\star 2} \tilde{\psi}\left(\sqrt{x^{\star 2} + y^{\star 2} + z^{\star 2}} \right) \right) dy^\star dx^\star dz^\star \\
=&\int_0^\infty \int_0^\infty \int_0^\infty \left(\frac{x^{\star 3}}{(1+y^{\star 2})^2} \tilde{\psi}\left(\sqrt{x^{\star 2} + z^{\star 2}} \right) \right) dy^\star dx^\star dz^\star \\
=&\frac{\pi}{4} \int_0^\infty \int_0^\infty \left(x^{\star 3} \tilde{\psi}\left(\sqrt{x^{\star 2} + z^{\star 2}} \right) \right) dx^\star dz^\star \\
=&\frac{\pi}{4} \int_0^\infty \int_0^\infty \left(\frac{r^4}{(1+z^{\star 2})^{5/2}} \tilde{\psi}(r) \right) dr dz^\star = \frac{\pi}{6} \int_0^\infty r^4 \psi(r) dr.
\end{aligned} \tag{2.64}$$

Finally, we conclude that provided $r^4 \tilde{\psi}(r) \in L^1(0,\infty)$,

$$\tilde{\gamma}_1^\star(x_1^\star) = h_0^{\star\prime\prime} \frac{\pi}{3} \int_0^\infty r^4 \tilde{\psi}(r) dr + \frac{h_0^{\star\prime} h_1^{\star\prime}}{\sqrt{1+(h_0^{\star\prime})^2}} \pi \int_0^\infty r^3 \tilde{\psi}(r) dr. \tag{2.65}$$

CHAPTER III

METHOD OF INTEGRAL TRANSFORMS

3.1. Formulation of the Problem in the Reference Configuration

Since the body force correction potential $\Phi(x_1, x_2)$ becomes active in the current configuration, as does the excess property $\tilde{\gamma}(x_1)$ of the dividing surface, the differential and jump momentum balance equations were formulated previously in the deformed configuration. As derived in Chapter II (cf. (2.14) and (2.30)), they take the following form:

$$\mathrm{div}(\mathbf{T}) = \mathrm{grad}\Phi \tag{3.1}$$

$$\mathrm{grad}_{(\sigma)}\tilde{\gamma} + 2\tilde{\gamma}H\mathbf{n}^- + [\![\mathbf{T}]\!]\mathbf{n}^- = \mathbf{0}, \tag{3.2}$$

where $\mathbf{n}^-$ is the unit normal to the fracture surface Σ pointing into the bulk material.

In view of the fact that the Method of Integral Transforms is most easily applied when the problem is formulated in a reference configuration where the crack is just a slit, in this chapter we work in the unloaded reference configuration of the body.

Consider a map $\mathbf{f} : \mathcal{B}_\kappa \to \mathcal{B}$ which takes a point $\mathbf{X}$ in the reference configuration $\mathcal{B}_\kappa$ into a point

$$\mathbf{x} = \mathbf{f}(\mathbf{X}) \in \mathcal{B}$$

in the current configuration (Fig. 3.1). As introduced in Section 2.2, we denote by $\mathbf{F}$ the deformation gradient, and by $\mathbf{u}(\mathbf{X})$ - the displacement of $\mathbf{X}$. In order to simplify the presentation, assume that $\mathbf{X}$ is nondimensionalized by crack length, so that the crack in the reference configuration is parameterized by

$$\Sigma_\kappa^\pm = \{\mathbf{X} : \ -1 \le X_1 \le 1, X_2 = 0^\pm\}.$$

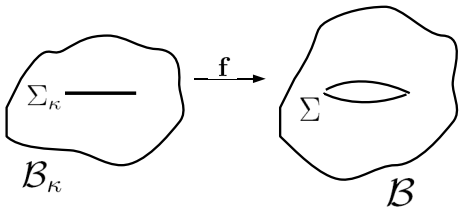

Fig. 3.1. $\mathbf{f} : \mathcal{B}_\kappa \to \mathcal{B}$.

Consequently, in the current configuration, the upper/lower crack surface can be parameterized by

$$\Sigma^{\pm} = \{\mathbf{x} : \; x_1 = X_1 + u_1(X_1, 0^{\pm}), \; x_2 = u_2(X_1, 0^{\pm}), -1 \leq X_1 \leq 1\}. \qquad (3.3)$$

Let $\mathcal{P}_\kappa \subset \mathcal{B}_\kappa$ be a part in the reference configuration of the body, $\mathcal{P} = \mathbf{f}(\mathcal{P}_\kappa)$, Σ_κ be the crack surface in the reference configuration, $\Sigma = \mathbf{f}(\Sigma_\kappa)$ be the crack surface in the current configuration, $\partial\Sigma = \partial\mathcal{B} \bigcap \Sigma$, and let $\mathbf{b}$ denote the mutual body force term in the current configuration (in the previous analysis we took $\mathbf{b} = -\text{grad}\Phi$).

Then the force acting on $\mathcal{P}$ is[1] ((2.13) and [22], p. 178)

$$\begin{aligned}\mathbf{f}(\mathcal{P}) &= \int_{\partial\mathcal{P}} \mathbf{T}\mathbf{n}\, da + \int_{\mathcal{P}} \mathbf{b}\, dv + \int_{\partial(\Sigma \bigcap \mathcal{P})} \mathbf{T}^{(\sigma)}\boldsymbol{\nu} ds \\ &= \int_{\partial\mathcal{P}} \mathbf{T}\mathbf{n}\, da + \int_{\mathcal{P}} \mathbf{b}\, dv + \int_{\Sigma \bigcap \mathcal{P}} \mathrm{div}_{(\sigma)}\mathbf{T}^{(\sigma)}\, da \\ &= \int_{\partial\mathcal{P}_\kappa} J\mathbf{T}_m\mathbf{F}^{-T}\mathbf{N}\, dA + \int_{\mathcal{P}_\kappa} J\mathbf{b}\, dV \\ &+ \int_{\Sigma_\kappa \bigcap \mathcal{P}_\kappa} J(\mathrm{div}_{(\sigma)}\mathbf{T}^{(\sigma)} \otimes \mathbf{n}^-)_m\mathbf{F}^{-T}\mathbf{N}^- dA,\end{aligned} \tag{3.4}$$

where $\mathbf{n}$ is the outward unit normal vector to $\partial\mathcal{P}$ and $\mathbf{n}^-$, as above, is the unit normal to the crack profile Σ pointing into the bulk material, $\mathbf{N}$ is the outward unit normal vector to $\partial\mathcal{P}_\kappa$ and $\mathbf{N}^-$ is the unit normal to the reference crack profile Σ_κ pointing into the bulk material, $\boldsymbol{\nu}$ is the conormal to $\partial\Sigma$, while $\mathbf{T}_m$ is the material description of $\mathbf{T}$, i.e., $\mathbf{T}_m(\mathbf{X}) = \mathbf{T}(\mathbf{f}(\mathbf{X}))$.

Recall that the first Piola-Kirchhoff stress tensor is given by (2.2). Letting $\mathbf{b}_\kappa = J\mathbf{b}$ and using (2.10), we transform (3.4) in

$$\mathbf{f}(\mathcal{P}) = \int_{\mathcal{P}_\kappa} (\mathrm{Div}\mathbf{T}_\kappa + \mathbf{b}_\kappa) dV + \int_{\Sigma_\kappa \bigcap \mathcal{P}_\kappa} J(\mathrm{div}_{(\sigma)}\mathbf{T}^{(\sigma)} \otimes \mathbf{n}^- + [\![\mathbf{T}]\!])_m\mathbf{F}^{-T}\mathbf{N}^- dA. \tag{3.5}$$

Since $\mathbf{f}(\mathcal{P}) = \mathbf{0}$, application of the Localization Theorem to the first term in (3.5) implies that the differential momentum balance in the reference configuration can be expressed as

$$\mathrm{Div}\mathbf{T}_\kappa + \mathbf{b}_\kappa = \mathbf{0}, \tag{3.6}$$

[1]The force acting on a part $\mathcal{P}$ is given by (3.4) provided either $\mathcal{P}$ does not contain the fracture tip or there are no excess properties ascribed to the fracture tip. Otherwise there is an additional contribution to $f(\mathcal{P})$ due to the excess properties at the crack tip. In this case the differential and jump momentum balances remain unchanged, however there is an additional momentum balance equation at the crack tip (Chapter V, Section 5.4). Since this additional momentum balance equation does not affect the solution of the boundary value problem, its consideration is postponed until Chapter V.

where the form of the mutual body force term $\mathbf{b}_\kappa$ will be specified later.

Consider now the second term in (3.5):

$$\begin{aligned}\mathbf{0} &= \int_{\Sigma_\kappa \bigcap \mathcal{P}_\kappa} J(\mathrm{div}_{(\sigma)}\mathbf{T}^{(\sigma)} \otimes \mathbf{n}^- + [\![\mathbf{T}]\!])_m \mathbf{F}^{-T}\mathbf{N}^- dA \\ &= \int_{\Sigma_\kappa \bigcap \mathcal{P}_\kappa} \Big(J(\mathrm{div}_{(\sigma)}\mathbf{T}^{(\sigma)} \otimes \mathbf{n}^-)_m \mathbf{F}^{-T}\mathbf{N}^- + [\![\mathbf{T}_\kappa]\!]\mathbf{N}^- \Big) dA.\end{aligned} \tag{3.7}$$

Equations (2.26) and (2.27) yield

$$\mathrm{div}_{(\sigma)}\mathbf{T}^{(\sigma)} = \mathrm{grad}_{(\sigma)}\tilde{\gamma} + \tilde{\gamma}\mathrm{div}_{(\sigma)}\mathbf{P} = \mathrm{grad}_{(\sigma)}\tilde{\gamma} - \tilde{\gamma}\mathbf{n}^-\mathrm{div}_{(\sigma)}\mathbf{n}^-. \tag{3.8}$$

Now, from equation (3.3) one concludes that the unit normal vector to Σ pointing into the bulk material has the following component form

$$\mathbf{n}^- = \frac{1}{\sqrt{(1+u_{1,1})^2 + u_{2,1}^2}} \langle -u_{2,1}, 1+u_{1,1} \rangle^T, \tag{3.9}$$

consequently

$$\mathbf{P} = \mathbf{I} - \mathbf{n}^- \otimes \mathbf{n}^- = \frac{1}{(1+u_{1,1})^2 + u_{2,1}^2} \begin{pmatrix} (1+u_{1,1})^2 & (1+u_{1,1})u_{2,1} \\ (1+u_{1,1})u_{2,1} & u_{2,1}^2 \end{pmatrix}. \tag{3.10}$$

Here $u_{i,j}$ are evaluated at points $\mathbf{X}$ on Σ_κ, i.e., $-1 \leq X_1 \leq 1, X_2 = 0$. Whenever this is clear, for simplicity of notation, this dependence is suppressed. Combining equations (2.20) and (3.10), one arrives at the following expression for $\mathrm{grad}_{(\sigma)}\tilde{\gamma}$:

$$\mathrm{grad}_{(\sigma)}\tilde{\gamma} = \frac{\tilde{\gamma}'(x_1)}{(1+u_{1,1})^2 + u_{2,1}^2} \langle (1+u_{1,1})^2, (1+u_{1,1})u_{2,1} \rangle^T. \tag{3.11}$$

Further, equations (2.22) and (3.10) yield

$$\mathrm{div}_{(\sigma)}\mathbf{n}^- = \frac{u_{2,1}^2 u_{1,12} + u_{2,1}(1+u_{1,1})(u_{1,11} - u_{2,12}) - (1+u_{1,1})^2 u_{2,11}}{\big((1+u_{1,1})^2 + u_{2,1}^2\big)^{3/2}}. \tag{3.12}$$

It only remains to evaluate the term $J\mathbf{F}^{-T}\mathbf{N}^- \cdot \mathbf{n}^-$. The matrix of the deformation

gradient in Cartesian coordinates can be written in the following form

$$[\mathbf{F}] = \begin{pmatrix} 1+u_{1,1} & u_{1,2} \\ u_{2,1} & 1+u_{2,2} \end{pmatrix}.$$

Using this, the fact that $\mathbf{N}^- = \langle 0,1 \rangle^T$ and equation (3.9) for $\mathbf{n}^-$, one arrives at

$$J\mathbf{F}^{-T}\mathbf{N}^- \cdot \mathbf{n}^- = \frac{(1+u_{1,1})^2 + u_{1,2}u_{2,1}}{\sqrt{(1+u_{1,1})^2 + u_{2,1}^2}}. \tag{3.13}$$

Finally, equations (3.8), (3.9), (3.11) and (3.13) and application of the Localization Theorem to (3.7) lead to the following expression for the jump momentum balance equations formulated in the reference configuration:

$$\begin{aligned}
\sigma_{12} &= -\frac{(1+u_{1,1})^2 + u_{1,2}u_{2,1}}{\sqrt{(1+u_{1,1})^2 + u_{2,1}^2}} \left(\frac{\tilde{\gamma}'(x_1)(1+u_{1,1})^2}{(1+u_{1,1})^2 + u_{2,1}^2} \right. \\
&\quad \left. + \frac{\tilde{\gamma} u_{2,1} \Big(u_{2,1}^2 u_{1,12} + u_{2,1}(1+u_{1,1})(u_{1,11} - u_{2,12}) - (1+u_{1,1})^2 u_{2,11} \Big)}{\Big((1+u_{1,1})^2 + u_{2,1}^2 \Big)^2} \right), \\
\sigma_{22} &= -\frac{(1+u_{1,1})^2 + u_{1,2}u_{2,1}}{\sqrt{(1+u_{1,1})^2 + u_{2,1}^2}} \left(\frac{\tilde{\gamma}'(x_1)(1+u_{1,1})u_{2,1}}{(1+u_{1,1})^2 + u_{2,1}^2} \right. \\
&\quad \left. - \frac{\tilde{\gamma}(1+u_{1,1}) \Big(u_{2,1}^2 u_{1,12} + u_{2,1}(1+u_{1,1})(u_{1,11} - u_{2,12}) - (1+u_{1,1})^2 u_{2,11} \Big)}{\Big((1+u_{1,1})^2 + u_{2,1}^2 \Big)^2} \right)
\end{aligned} \tag{3.14}$$

where σ_{ij} are the components of the matrix of the first Piola-Kirchhoff stress tensor $\mathbf{T}_\kappa$ in Cartesian coordinates,

$$[\mathbf{T}_\kappa] = \begin{pmatrix} \sigma_{11} & \sigma_{12} \\ \sigma_{12} & \sigma_{22} \end{pmatrix}.$$

The jump momentum balance provides us with boundary conditions on the crack surfaces. Because of symmetry, it suffices to consider the problem on the upper half plane only. In this case, additional boundary conditions are needed on $\{\mathbf{X} : |X_1| >$

$1, X_2 = 0\}$. Symmetry implies

$$\begin{aligned} u_2(X_1, 0) &= 0, \qquad |X_1| > 1 \\ \sigma_{12}(X_1, 0) &= 0, \qquad |X_1| > 1. \end{aligned} \tag{3.15}$$

We assume that the constitutive behavior of the material can be modeled by Hooke's law in the reference configuration, that is, the Piola-Kirchhoff stress tensor $\mathbf{T}_\kappa$ is given by

$$\mathbf{T}_\kappa = 2\mu\mathbf{E} + \lambda \mathrm{tr}(\mathbf{E})\mathbf{I}, \tag{3.16}$$

where

$$\mathbf{E} = \frac{1}{2}(\nabla\mathbf{u} + \nabla\mathbf{u}^T)$$

is the infinitesimal strain tensor.

Also, a homogeneous tensile far-field loading is assumed, i.e.,

$$\begin{aligned} \lim_{X_2\to\infty} \sigma_{11}(X_1, X_2) &= 0 \\ \lim_{X_2\to\infty} \sigma_{12}(X_1, X_2) &= 0 \\ \lim_{X_2\to\infty} \sigma_{22}(X_1, X_2) &= \sigma. \end{aligned} \tag{3.17}$$

Thus, the problem we are going to consider is formulated in the reference configuration (the upper half plane) and consists of

1. a differential momentum balance given by (3.6),
2. boundary conditions on $\{\mathbf{X} : |X_1| \leq 1, X_2 = 0\}$ given by the jump momentum balance - equations (3.14),
3. boundary conditions on $\{\mathbf{X} : |X_1| > 1, X_2 = 0\}$ given by equations (3.15),
4. a constitutive equation given by (3.16),
5. a far filed loading condition given by (3.17).

3.2. Method of Integral Transforms Applied to the Navier Equations

Following [53], we proceed as follows. The component form of the differential momentum balance (3.6) is given by

$$\begin{aligned} \sigma_{11,1} + \sigma_{12,2} + b_{\kappa 1} &= 0 \\ \sigma_{21,1} + \sigma_{22,2} + b_{\kappa 2} &= 0, \end{aligned} \tag{3.18}$$

where, from Hooke's law (3.16),

$$\begin{aligned} \sigma_{11} &= (\lambda + 2\mu) u_{1,1} + \lambda u_{2,2} \\ \sigma_{12} &= \mu (u_{1,2} + u_{2,1}) \\ \sigma_{22} &= \lambda u_{1,1} + (\lambda + 2\mu) u_{2,2}. \end{aligned} \tag{3.19}$$

After substituting (3.19) into (3.18) and differentiating with respect to X_1, one obtains

$$\begin{aligned} (\lambda + 2\mu) u_{1,111} + \mu u_{1,122} + (\lambda + \mu) u_{2,112} + b_{\kappa 1,1} &= 0 \\ (\lambda + \mu) u_{1,112} + \mu u_{2,111} + (\lambda + 2\mu) u_{2,122} + b_{\kappa 2,1} &= 0. \end{aligned} \tag{3.20}$$

For simplicity, from here on X_2 is denoted by y. Taking Fourier transform of (3.20) with respect to X_1 results in the following system of ordinary differential equations

$$\begin{aligned} \mu \frac{d^2}{dy^2} \hat{u}_{1,1} + ip(\lambda + \mu) \frac{d}{dy} \hat{u}_{2,1} - p^2 (\lambda + 2\mu) \hat{u}_{1,1} + ip \hat{b}_{\kappa 1} &= 0 \\ (\lambda + 2\mu) \frac{d^2}{dy^2} \hat{u}_{2,1} + ip(\lambda + \mu) \frac{d}{dy} \hat{u}_{1,1} - p^2 \mu \hat{u}_{2,1} + ip \hat{b}_{\kappa 2} &= 0, \end{aligned} \tag{3.21}$$

where the Fourier transform of an integrable function f on $\mathbb{R}$ is defined by

$$\mathcal{F}[f](p) = \hat{f}(p) = \int_{-\infty}^{\infty} f(x) e^{-ipx} dx \tag{3.22}$$

and use is made of the property

$$\mathcal{F}[f'] = ip\mathcal{F}[f] \tag{3.23}$$

for f - a continuous and piecewise smooth function such that $f' \in L^1(\mathbb{R})$ ([14]). System (3.21) is equivalent to a first order system of ordinary differential equations

$$\mathbf{Y}' = \mathbf{A}\mathbf{Y} + \mathbf{B}, \tag{3.24}$$

where

$$\mathbf{Y} = \langle \hat{u}_{1,1}, \hat{u}_{2,1}, \frac{d}{dy}\hat{u}_{1,1}, \frac{d}{dy}\hat{u}_{2,1} \rangle^T,$$

$$\mathbf{B} = \langle 0, 0, -ip\hat{b}_{\kappa 1}, -ip\hat{b}_{\kappa 2} \rangle^T$$

and

$$\mathbf{A} = \begin{pmatrix} 0 & 0 & 1 & 0 \\ 0 & 0 & 0 & 1 \\ \frac{p^2(\lambda+2\mu)}{\mu} & 0 & 0 & -\frac{ip(\lambda+\mu)}{\mu} \\ 0 & \frac{p^2\mu}{\lambda+2\mu} & -\frac{ip(\lambda+\mu)}{\lambda+2\mu} & 0 \end{pmatrix}.$$

The general solution of the homogeneous system is

$$\begin{aligned}
Y_{h1} &= i\left(-A_1 + \frac{\lambda+3\mu}{p(\lambda+\mu)}A_2\right)e^{-py} - iA_2 y e^{-py} \\
&\quad + i\left(A_3 + \frac{\lambda+3\mu}{p(\lambda+\mu)}A_4\right)e^{py} + iA_4 y e^{py} \\
Y_{h2} &= A_1 e^{-py} + A_2 y e^{-py} + A_3 e^{py} + A_4 y e^{py} \\
Y_{h3} &= i\left(pA_1 - \frac{2(\lambda+2\mu)}{\lambda+\mu}A_2\right)e^{-py} + ipA_2 y e^{-py} \\
&\quad + i\left(pA_3 + \frac{2(\lambda+2\mu)}{\lambda+\mu}A_4\right)e^{py} + ipA_4 y e^{py} \\
Y_{h4} &= (-pA_1 + A_2)\,e^{-py} - pA_2 y e^{-py} + (pA_3 + A_4)\,e^{py} + pA_4 y e^{py}
\end{aligned}$$

with $A_i = A_i(p)$, $i = 1, .., 4$. Then, the general solution of (3.24) is given by $\mathbf{Y} =$

$\mathbf{Y}_h + \mathbf{P}$, where $\mathbf{P}(p,y) = \langle \alpha_1(p,y), \alpha_2(p,y), \alpha_3(p,y), \alpha_4(p,y) \rangle^T$ is a particular solution such that $\lim_{y\to\infty} \mathbf{P}(p,y) = \mathbf{0}$. Thus, the general solution of (3.21), defined on the upper half plane, which vanishes as $y \to \infty$ is

$$\begin{aligned} \hat{u}_{1,1}(p,y) &= i\left(-\mathrm{sgn}(p)A_1 + \frac{\lambda+3\mu}{p(\lambda+\mu)}A_2\right)e^{-|p|y} - i\mathrm{sgn}(p)A_2 y e^{-|p|y} + \alpha_1(p,y) \\ \hat{u}_{2,1}(p,y) &= A_1 e^{-|p|y} + A_2 y e^{-|p|y} + \alpha_2(p,y). \end{aligned} \tag{3.25}$$

From (3.23) we have

$$\begin{aligned} \hat{u}_{1,1}(p,y) = ip\hat{u}_1(p,y) \qquad &\Rightarrow \qquad \hat{u}_{1,2}(p,y) = -\frac{i}{p}\frac{d}{dy}\hat{u}_{1,1}(p,y) \\ \hat{u}_{2,1}(p,y) = ip\hat{u}_2(p,y) \qquad &\Rightarrow \qquad \hat{u}_{2,2}(p,y) = -\frac{i}{p}\frac{d}{dy}\hat{u}_{2,1}(p,y). \end{aligned}$$

The above equations together with (3.19) and (3.25) lead to

$$\begin{aligned} \hat{\sigma}_{12}(p,y) &= \mu\left(-\frac{i}{p}\frac{d}{dy}\hat{u}_{1,1} + \hat{u}_{2,1}\right) \\ &= 2\mu\left(A_1 - \frac{\lambda+2\mu}{|p|(\lambda+\mu)}A_2 + A_2 y\right)e^{-|p|y} - \frac{i}{p}\mu\frac{d}{dy}\alpha_1(p,y) + \mu\alpha_2(p,y) \\ \hat{\sigma}_{22}(p,y) &= \lambda\hat{u}_{1,1} - \frac{i}{p}(\lambda+2\mu)\frac{d}{dy}\hat{u}_{2,1} \\ &= 2\mu i\left(\mathrm{sgn}(p)A_1 - \frac{\mu}{p(\lambda+\mu)}A_2 + \mathrm{sgn}(p)A_2 y\right)e^{-|p|y} \\ &+ \lambda\alpha_1(p,y) - \frac{i}{p}(\lambda+2\mu)\frac{d}{dy}\alpha_2(p,y). \end{aligned} \tag{3.26}$$

We can solve (3.25) for $A_1(p)$ and $A_2(p)$

$$\begin{aligned} A_1(p) &= \hat{u}_{2,1}(p,0) - \alpha_2(p,0) \\ A_2(p) &= -\frac{ip(\lambda+\mu)}{\lambda+3\mu}\left(\hat{u}_{1,1}(p,0) + i\mathrm{sgn}(p)\hat{u}_{2,1}(p,0) - i\mathrm{sgn}(p)\alpha_2(p,0) - \alpha_1(p,0)\right) \end{aligned}$$

and substitute these into (3.26) to arrive at

$$\begin{aligned}
\hat{\sigma}_{12}(p,0) &= \frac{2\mu^2}{\lambda+3\mu}\hat{u}_{2,1}(p,0) + i\mathrm{sgn}(p)\frac{2\mu(\lambda+2\mu)}{\lambda+3\mu}\left(\hat{u}_{1,1}(p,0) - \alpha_1(p,0)\right) \\
&\quad + \frac{\mu(\lambda+\mu)}{\lambda+3\mu}\alpha_2(p,0) - \frac{i}{p}\mu\frac{d}{dy}\alpha_1(p,0) \\
\hat{\sigma}_{22}(p,0) &= -\frac{2\mu^2}{\lambda+3\mu}\hat{u}_{1,1}(p,0) + i\mathrm{sgn}(p)\frac{2\mu(\lambda+2\mu)}{\lambda+3\mu}\left(\hat{u}_{2,1}(p,0) - \alpha_2(p,0)\right) \\
&\quad + \frac{(\lambda+2\mu)(\lambda+\mu)}{\lambda+3\mu}\alpha_1(p,0) - \frac{i}{p}(\lambda+2\mu)\frac{d}{dy}\alpha_2(p,0).
\end{aligned} \tag{3.27}$$

Next, we apply the inverse Fourier transform to equations (3.27), using

$$\mathcal{F}^{-1}[i\mathrm{sgn}(p)\hat{f}(p)](x) = \frac{1}{\pi}⨍_{-\infty}^{\infty}\frac{f(r)}{r-x}dr = \mathcal{H}[f](x), \tag{3.28}$$

where $⨍$ denotes a Cauchy principal value integral. The operator $\mathcal{H}[f]$ defined in (3.28) is known as the Hilbert transform. This leads us to the so called *Dirichlet to Neumann* map:

$$\begin{aligned}
\sigma_{12}(x,0) &= \frac{2\mu^2}{\lambda+3\mu}u_{2,1}(x,0) + \frac{2\mu(\lambda+2\mu)}{\pi(\lambda+3\mu)}⨍_{-\infty}^{\infty}\frac{u_{1,1}(r,0) - \breve{\alpha}_1(r,0)}{r-x}dr \\
&\quad + \frac{\mu(\lambda+\mu)}{\lambda+3\mu}\breve{\alpha}_2(x,0) + \mu\frac{d}{dy}\int_0^x \breve{\alpha}_1(s,0)ds \\
\sigma_{22}(x,0) &= -\frac{2\mu^2}{\lambda+3\mu}u_{1,1}(x,0) + \frac{2\mu(\lambda+2\mu)}{\pi(\lambda+3\mu)}⨍_{-\infty}^{\infty}\frac{u_{2,1}(r,0) - \breve{\alpha}_2(r,0)}{r-x}dr \\
&\quad + \frac{(\lambda+2\mu)(\lambda+\mu)}{\lambda+3\mu}\breve{\alpha}_1(x,0) + (\lambda+2\mu)\frac{d}{dy}\int_0^x \breve{\alpha}_2(s,0)ds,
\end{aligned} \tag{3.29}$$

where $\breve{f} = \mathcal{F}^{-1}[f]$ denotes the inverse Fourier transform of f. In order to construct

the inverse map of (3.29), one solves equations (3.27) for $\hat{u}_{1,1}$ and $\hat{u}_{1,2}$

$$\begin{aligned}
\hat{u}_{1,1}(p,0) &= -i\mathrm{sgn}(p)\frac{\lambda+2\mu}{2\mu(\lambda+\mu)}(\hat{\sigma}_{12}(p,0)-\mu\alpha_2(p,0))+\frac{1}{2(\lambda+\mu)}\hat{\sigma}_{22}(p,0)\\
&\quad+\frac{\lambda+2\mu}{2(\lambda+\mu)}\left(\alpha_1(p,0)+\frac{\mathrm{sgn}(p)}{p}\frac{d}{dy}\alpha_1(p,0)+\frac{i}{p}\frac{d}{dy}\alpha_2(p,0)\right)\\
\hat{u}_{2,1}(p,0) &= -i\mathrm{sgn}(p)\frac{\lambda+2\mu}{2\mu(\lambda+\mu)}(\hat{\sigma}_{22}(p,0)-\lambda\alpha_1(p,0))-\frac{1}{2(\lambda+\mu)}\hat{\sigma}_{12}(p,0)\\
&\quad+\frac{2\lambda+3\mu}{2(\lambda+\mu)}\alpha_2(p,0)+\frac{\mathrm{sgn}(p)}{p}\frac{(\lambda+2\mu)^2}{2\mu(\lambda+\mu)}\frac{d}{dy}\alpha_2(p,0)\\
&\quad-\frac{i}{p}\frac{\mu}{2(\lambda+\mu)}\frac{d}{dy}\alpha_1(p,0).
\end{aligned}\tag{3.30}$$

After applying the inverse Fourier transform to (3.30) one obtains the *Neumann to Dirichlet* map:

$$\begin{aligned}
u_{1,1}(x,0) &= -\frac{\lambda+2\mu}{2\mu(\lambda+\mu)\pi}\fint_{-\infty}^{\infty}\frac{\sigma_{12}(r,0)-\mu\breve{\alpha}_2(r,0)}{r-x}dr+\frac{1}{2(\lambda+\mu)}\sigma_{22}(x,0)\\
&\quad+\frac{\lambda+2\mu}{2(\lambda+\mu)}\left(\breve{\alpha}_1(x,0)+\frac{1}{\pi}\frac{d}{dy}\fint_{-\infty}^{\infty}\int_0^r\breve{\alpha}_1(s,0)ds\frac{dr}{r-x}\right.\\
&\qquad\left.-\frac{d}{dy}\int_0^x\breve{\alpha}_2(s,0)ds\right)\\
u_{2,1}(x,0) &= -\frac{\lambda+2\mu}{2\mu(\lambda+\mu)\pi}\fint_{-\infty}^{\infty}\frac{\sigma_{22}(r,0)-\lambda\breve{\alpha}_1(r,0)}{r-x}dr-\frac{1}{2(\lambda+\mu)}\sigma_{12}(x,0)\\
&\quad+\frac{2\lambda+3\mu}{2(\lambda+\mu)}\breve{\alpha}_2(x,0)+\frac{(\lambda+2\mu)^2}{2\mu(\lambda+\mu)\pi}\frac{d}{dy}\fint_{-\infty}^{\infty}\int_0^r\frac{\breve{\alpha}_2(s,0)}{r-x}dsdr\\
&\quad+\frac{\mu}{2(\lambda+\mu)}\frac{d}{dy}\int_0^x\breve{\alpha}_1(s,0)ds.
\end{aligned}\tag{3.31}$$

3.3. Model with Constant Surface Tension and Zero Mutual Body Force Term

As a first step in our analysis we consider a model with constant surface tension ($\tilde{\gamma}\equiv$ const) and zero mutual body force, i.e., $\mathbf{b}_\kappa=\mathbf{0}$ in (3.6). In particular, $\alpha_j(p,y)\equiv 0$, $j=1,2$ and the Dirichlet to Neumann and Neumann to Dirichlet maps reduce

respectively to

$$\begin{aligned}\sigma_{12}(x,0) &= \frac{2\mu^2}{\lambda+3\mu}u_{2,1}(x,0) + \frac{2\mu(\lambda+2\mu)}{(\lambda+3\mu)\pi}\int_{-\infty}^{\infty}\frac{u_{1,1}(r,0)}{r-x}dr \\ \sigma_{22}(x,0) &= -\frac{2\mu^2}{\lambda+3\mu}u_{1,1}(x,0) + \frac{2\mu(\lambda+2\mu)}{(\lambda+3\mu)\pi}\int_{-\infty}^{\infty}\frac{u_{2,1}(r,0)}{r-x}dr\end{aligned} \tag{3.32}$$

and

$$\begin{aligned}u_{1,1}(x,0) &= -\frac{\lambda+2\mu}{2\mu(\lambda+\mu)\pi}\int_{-\infty}^{\infty}\frac{\sigma_{12}(r,0)}{r-x}dr + \frac{1}{2(\lambda+\mu)}\sigma_{22}(x,0) \\ u_{2,1}(x,0) &= -\frac{\lambda+2\mu}{2\mu(\lambda+\mu)\pi}\int_{-\infty}^{\infty}\frac{\sigma_{22}(r,0)}{r-x}dr - \frac{1}{2(\lambda+\mu)}\sigma_{12}(x,0).\end{aligned} \tag{3.33}$$

Substituting the first equation of (3.33) into the second of (3.32) and using the boundary conditions on $|x|>1$ - (3.15), one arrives at

$$\begin{aligned}\sigma_{22}(x,0) &= \frac{2\mu(\lambda+\mu)}{(\lambda+2\mu)\pi}\int_{-1}^{1}\frac{u_{2,1}(r,0)}{r-x}dr + \frac{\mu}{(\lambda+2\mu)\pi}\int_{-1}^{1}\frac{\sigma_{12}(r,0)}{r-x}dr \\ &= \frac{E}{2(1-\nu^2)\pi}\int_{-1}^{1}\frac{u_{2,1}(r,0)}{r-x}dr + \frac{1-2\nu}{2(1-\nu)\pi}\int_{-1}^{1}\frac{\sigma_{12}(r,0)}{r-x}dr.\end{aligned} \tag{3.34}$$

Here E and ν denote Young's modulus and Poisson's ratio respectively:

$$E = \frac{\mu(3\lambda+2\mu)}{\lambda+\mu}, \qquad \nu = \frac{\lambda}{2(\lambda+\mu)}.$$

We now linearize the jump momentum balance boundary conditions (3.14) under the assumption that $u_{i,j}(x,0)$ and $u_{i,jk}(x,0)$ are small. The solution of the linearized problem will then be checked for consistency with the assumptions made.

From (3.14) it is evident that the asymptotic form of the jump momentum balance equations is

$$\begin{aligned}\sigma_{12}(x,0) &= 0 + h.o.t., \qquad |x|\le 1 \\ \sigma_{22}(x,0) &= -\tilde{\gamma}u_{2,11}(x,0) + h.o.t., \qquad |x|\le 1.\end{aligned} \tag{3.35}$$

Note that the Dirichlet to Neumann and the Neumann to Dirichlet maps (and consequently equation (3.34)) were derived under the assumption that $\hat{u}_{1,1}(p,y)$ and

$\hat{u}_{2,1}(p,y)$ vanish in the limit as $y \to \infty$, whereas the far field loading condition for our problem is given by (3.17). In order to reduce the considered problem to a problem which satisfies the above assumptions, we use the linearity of the differential momentum balance and the (linearized) boundary conditions and introduce $\mathbf{u}^f$ and $\mathbf{u}^0$ such that $\mathbf{u} = \mathbf{u}^f + \mathbf{u}^0$ with $\mathbf{u}^f$ being the displacement field corresponding to the homogeneous stress field

$$\mathbf{T}^f_\kappa = \begin{pmatrix} 0 & 0 \\ 0 & \sigma \end{pmatrix}. \tag{3.36}$$

Since the stress and strain tensors corresponding to $\mathbf{u}^f$ are related constitutively by Hooke's law, i.e., $\mathbf{T}^f_\kappa = 2\mu\mathbf{E}^f + \lambda \mathrm{tr}(\mathbf{E}^f)$, where $\mathbf{E}^f = \frac{1}{2}(\nabla\mathbf{u}^f + (\nabla\mathbf{u}^f)^T)$, one easily finds

$$\begin{aligned} u^f_1(x,y) &= -\frac{\lambda\sigma}{4\mu(\lambda+\mu)}x \\ u^f_2(x,y) &= \frac{(\lambda+2\mu)\sigma}{4\mu(\lambda+\mu)}y. \end{aligned} \tag{3.37}$$

The stress corresponding to $\mathbf{u}^0$ vanishes in the limit as $y \to \infty$, and consequently

$$\lim_{y\to\infty} \hat{u}^0_{1,1}(p,y) = 0, \qquad \text{and} \qquad \lim_{y\to\infty} \hat{u}^0_{2,1}(p,y) = 0,$$

that is, $\mathbf{u}^0$ satisfies the assumptions under which equation (3.34) was derived. From the definition of $\mathbf{u}^0$ and equations (3.35) and (3.36) one concludes that

$$\begin{aligned} \sigma^0_{12}(x,0) &= 0 + h.o.t., \qquad |x| \le 1 \\ \sigma^0_{22}(x,0) &= -\sigma - \tilde{\gamma} u_{2,11}(x,0) + h.o.t., \qquad |x| \le 1. \end{aligned} \tag{3.38}$$

Substituting the above equations into (3.34) one arrives at

$$-\sigma - \tilde{\gamma} u^0_{2,11}(x,0) = \frac{E}{2(1-\nu^2)\pi} \fint_{-1}^{1} \frac{u^0_{2,1}(r,0)}{r-x} dr. \tag{3.39}$$

Let us define

$$\phi(x) = u^0_{2,1}(x, 0), \qquad \zeta = \frac{E}{2(1-\nu^2)}. \tag{3.40}$$

Then equation (3.39) takes the form

$$\tilde{\gamma}\phi'(x) + \frac{\zeta}{\pi}\int_{-1}^{1} \frac{\phi(r)}{r-x} dr = -\sigma, \qquad x \in [-1, 1]. \tag{3.41}$$

This is a Cauchy singular, linear integro-differential equation. It arises, for example, when modeling combined infrared gaseous radiations and molecular conduction. Abdou ([1]) and Badr ([6]) derive the solution as a series of Legendre polynomials, while Frankel in his 1995 paper [16] derives the solution of an equation of the type (3.41) as a series of Chebyshev polynomials. It should be noted that while Frankel considers some numerical experiments, he does not study the convergence of the obtained infinite system of linear algebraic equations. Various numerical approaches to solving equations of a similar type were considered in [5, 41].

3.3.1. Chebyshev Polynomials

In this section we summarize some well-known properties of the Chebyshev polynomials ([32]).

The Chebyshev polynomials of the first and second kind $T_n(x)$ and $U_n(x)$ are polynomials in x of degree n, defined respectively by

$$T_n(x) = \cos n\theta \qquad \text{when} \qquad x = \cos\theta$$

and

$$U_n(x) = \frac{\sin(n+1)\theta}{\sin\theta} \qquad \text{when} \qquad x = \cos\theta.$$

Both $\{T_n\}$ and $\{U_n\}$ form sequences of orthogonal polynomials on the interval $[-1, 1]$. The first kind Chebyshev polynomials are orthogonal with respect to the weight

function $w_1(x) = (1-x^2)^{-1/2}$, i.e.,

$$\langle T_m, T_n \rangle_{w_1} = \int_{-1}^{1} \frac{T_m(x)T_n(x)}{\sqrt{1-x^2}} dx = \begin{cases} 0, & m \neq n \\ \pi, & m = n = 0 \\ \frac{\pi}{2}, & m = n \neq 0. \end{cases} \tag{3.42}$$

Similarly, the second kind Chebyshev polynomials are orthogonal with respect to the weight function $w_2(x) = (1-x^2)^{1/2}$:

$$\langle U_m, U_n \rangle_{w_2} = \int_{-1}^{1} U_m(x)U_n(x)\sqrt{1-x^2} dx = \frac{\pi}{2}\delta_{mn},$$

where δ_{mn} is the Kronecker symbol.

Using the definition of $T_n(x)$ one readily obtains

$$T_m(x)T_n(x) = \frac{1}{2}(T_{m+n}(x) + T_{|m-n|}(x)). \tag{3.43}$$

By means of the usual substitution $x = \cos\theta$,

$$\int T_n(x)dx = \frac{1}{2}\left(\frac{\cos(n+1)\theta}{n+1} - \frac{\cos|n-1|\theta}{n-1}\right)$$

where, in the case $n = 1$, the second term is omitted. Hence

$$\int_{-1}^{1} T_n(x)dx = \begin{cases} \frac{2}{1-n^2},\ n = 0, 2, ... \\ 0,\ n = 1, 3, ... \ . \end{cases} \tag{3.44}$$

The formula for the derivative of $T_n(x)$ in terms of the second kind polynomials is given by

$$\frac{d}{dx}T_n = nU_{n-1}(x). \tag{3.45}$$

Another class of formulas we need concerns integration of the Chebyshev polynomials

against certain Hilbert-type kernels, namely

$$\fint_{-1}^{1} \frac{T_n(r)}{\sqrt{1-r^2}(r-x)} dr = \pi U_{n-1}(x) \tag{3.46}$$

and

$$\fint_{-1}^{1} U_{n-1}(r) \frac{\sqrt{1-r^2}}{(r-x)} dr = -\pi T_n(x). \tag{3.47}$$

3.3.2. Solution Method

One can show ([53]) that the general solution of the singular integral equation

$$\psi(x) = \frac{1}{\pi} \fint_{-1}^{1} \frac{\phi(r)}{r-x} dr \tag{3.48}$$

is given by

$$\phi(x) = -\frac{1}{\sqrt{1-x^2}} \left(\frac{1}{\pi} \fint_{-1}^{1} \psi(r) \frac{\sqrt{1-r^2}}{r-x} dr + C \right). \tag{3.49}$$

In essence, formula (3.49) gives an inverse of the finite Hilbert transform operator (3.48). Applying (3.49) to equation (3.41) yields

$$\phi(x) = \frac{1}{\zeta \pi \sqrt{1-x^2}} \fint_{-1}^{1} (\phi'(r) - f) \frac{\sqrt{1-r^2}}{r-x} dr + \frac{C}{\zeta \sqrt{1-x^2}}. \tag{3.50}$$

Recall that $\phi(x)$ is defined by (3.40) and that $u_2(\pm 1, 0) = 0$ due to (3.15). Consequently, using (3.37) one obtains

$$\int_{-1}^{1} \phi(x) dx = \int_{-1}^{1} (u_{2,1}(x,0) - u_{2,1}^f(x,0)) dx = 0.$$

Hence, integration over (3.49) on $[-1, 1]$ implies that

$$\begin{aligned} 0 &= \int_{-1}^{1} \frac{1}{\sqrt{1-x^2}} \left(\frac{1}{\pi} \fint_{-1}^{1} \psi(r) \frac{\sqrt{1-r^2}}{r-x} dr + C \right) dx \\ &= \frac{1}{\pi} \int_{-1}^{1} \psi(r) \sqrt{1-r^2} \left(\fint_{-1}^{1} \frac{1}{\sqrt{1-x^2}(r-x)} dx \right) dr + C \int_{-1}^{1} \frac{1}{\sqrt{1-x^2}} dx \\ &= \pi C \end{aligned}$$

from where one concludes that $C = 0$. Here we have used

$$\int_{-1}^{1} \frac{1}{\sqrt{1-x^2}} dx = \pi$$

and

$$⨍_{-1}^{1} \frac{1}{\sqrt{1-x^2}(r-x)} dx = 0 \qquad \text{for} \qquad |r| < 1.$$

For a proof of the latter see [53].

Further, because of the symmetry of the problem, $\phi(x)$ is an odd function of x. Using the fact that T_{2k} is an even polynomial, while T_{2k+1} is odd, we assume that $\phi(x)$ has an expansion of the form

$$\phi(x) = \sum_{k=0}^{\infty} a_{2k+1} T_{2k+1}(x). \tag{3.51}$$

Formally taking the derivative of (3.51) and using (3.45) one obtains

$$\phi'(x) = \sum_{k=0}^{\infty} (2k+1) a_{2k+1} U_{2k}(x).$$

Substitution of these into (3.50) yields

$$\sqrt{1-x^2} \sum_{k=0}^{\infty} a_{2k+1} T_{2k+1}(x) = \frac{1}{\zeta\pi} ⨍_{-1}^{1} \left(\sum_{k=0}^{\infty} (2k+1) a_{2k+1} U_{2k}(r) - f U_0 \right) \frac{\sqrt{1-r^2}}{r-x} dr$$

where we have used that $f \equiv \text{const}$ and $U_0(x) \equiv 1$. Now, application of (3.47) to the above equation leads to

$$\sqrt{1-x^2} \sum_{k=0}^{\infty} a_{2k+1} T_{2k+1}(x) = -\frac{1}{\zeta} \left(\sum_{k=0}^{\infty} (2k+1) a_{2k+1} T_{2k+1}(x) - f T_1(x) \right).$$

Use of the orthogonality property of the first kind Chebyshev polynomials (3.42) implies

$$\sum_{k=0}^{\infty} a_{2k+1} \int_{-1}^{1} T_{2k+1}(x) T_n(x) dx = -\frac{\pi}{2\zeta} \left(\sum_{k=0}^{\infty} (2k+1) a_{2k+1} \delta_{2k+1,n} - f \delta_{1n} \right).$$

Further, this together with (3.43) and (3.44) leads to the following infinite system of equations for the expansion coefficients a_m

$$\sum_{m=2k+1} a_m \left(\frac{1}{1-(m+n)^2} + \frac{1}{1-(m-n)^2} + \frac{\pi m}{2\zeta}\delta_{mn} \right) = -\frac{\pi\sigma}{2\zeta\tilde{\gamma}}\delta_{1n}, \tag{3.52}$$

where $n = 2l+1, l \in \mathbb{N}$.

Our goal now is to show convergence of the above system of equations, i.e., that the solutions of the truncated systems converge to the solution of (3.52). In addition, we need to find under what conditions the solution $\phi(x)$ of (3.41) is bounded on $[-1,1]$, that is, unlike the solution of the classical crack problem, the two crack surfaces come together at an edge, rather than a blunt tip. Taking into account the series representation (3.51) of $\phi(x)$ and that $T_n(1) = 1$ and $T_n(-1) = (-1)^n$, one concludes that a necessary and sufficient condition for this is

$$\sum |a_k| < \infty,$$

i.e., $\{a_k\} \in l_1$. These issues will be investigated in detail in the following section.

3.3.3. Convergence Results

Let $\mathcal{L}(X)$ denote the algebra of bounded linear operators A on a Banach space X with domains $\mathcal{D}(A) = X$. For a matrix $A = (a_{ij})$, let $A = D + F$, where $D = \text{diag}(a_{11}, a_{22}, ...)$ and $F = A - D$. The identity operator on X is denoted by I. The following theorem is due to Farid (Theorem 2.1, [11]) and Farid and Lancaster (Theorem 2.2, [12]).

Theorem 1. *Let $A = (a_{ij})$ be a matrix operator on l_p, $1 \le p \le \infty$, and assume that:*

1. *$a_{ii} \neq 0$ for all $i \in \mathbb{N}$ and $|a_{ii}| \to \infty$ as $i \to \infty$.*

2. *There is a* $s \in [0,1)$ *such that for all* $i \in \mathbb{N}$,

$$P_i = \sum_{j \neq i} |a_{ij}| = s_i |a_{ii}|, \quad \textit{where } s_i \in [0,s].$$

3. *Either* $FD^{-1} \in \mathcal{L}(l_p)$ *and* $(I + \theta FD^{-1})^{-1}$ *exists and is in* $\mathcal{L}(l_p)$ *for every* $\theta \in [0,1]$, *or* $D^{-1}F \in \mathcal{L}(l_p)$ *and* $(I + \theta D^{-1}F)^{-1}$ *exists and is in* $\mathcal{L}(l_p)$ *for every* $\theta \in [0,1]$.

Then:

1. *The spectrum* $\sigma(A)$ *of the closed operator* A *is nonempty and consists of a discrete, countable set of nonzero eigenvalues* $\{\lambda_i : i \in N\}$ *lying in the set* $\bigcup_{i=1}^{\infty} R_i$, *where* $\mathcal{R}_i = \{z \in \mathbb{C} : |z - a_{ii}| \leq P_i\}$.

2. *Furthermore, any set of* r *Gershgorin discs whose union is disjoint from all other Gershgorin discs intersects* $\sigma(A)$ *in a finite set of eigenvalues of* A *with total algebraic multiplicity* r.

3. *There exists a sequence of compact operators converging in norm to* A^{-1}.

Let $B = (b_{lk})$, where b_{kl} are the nonzero coefficients of the infinite linear system (3.52), i.e.,

$$b_{kl} = \left(\frac{1}{1-(2k+2l+2)^2} + \frac{1}{1-(2k-2l)^2} + \frac{\pi(2k+1)}{2\zeta}\delta_{kl} \right). \tag{3.53}$$

Let $I_n = (e_{ij}^{(n)})$ with

$$e_{ij}^{(n)} = \begin{cases} \delta_{ij}, & \text{if } i,j \leq n \\ 0, & \text{otherwise.} \end{cases}$$

We next show that, provided n is chosen large enough, $A = B + I_n$ satisfies the conditions of Theorem 1 with $p = 1$. Let, as above, F denote the off-diagonal part of

A, i.e., $F = ((1-\delta_{kl})b_{kl})$. Condition (1) is clearly satisfied. Next, note that

$$\sum_{k=0,k\neq l}^{\infty}\left(\frac{1}{|1-(2k+2l+2)^2|}+\frac{1}{|1-(2k-2l)^2|}\right)=1-\frac{1}{4(2l+1)^2-1}.$$

Thus

$$P_l=\sum_{k\neq l}|b_{kl}|=\sum_{k}|F_{kl}|\leq 1-\frac{1}{4(2l+1)^2-1}<1. \tag{3.54}$$

The diagonal elements of A are given by

$$a_{kk}=\begin{cases} b_{kk}+1=2-\dfrac{1}{4(2k+1)^2-1}+\dfrac{\pi(2k+1)}{2\zeta}>\dfrac{5}{3}+\dfrac{\pi}{\zeta}k, & \text{if } \ k\leq n \\ b_{kk}=1-\dfrac{1}{4(2k+1)^2-1}+\dfrac{\pi(2k+1)}{2\zeta}>\dfrac{2}{3}+\dfrac{\pi}{\zeta}k, & \text{if } \ k>n. \end{cases} \tag{3.55}$$

Thus A is strictly diagonally dominant and satisfies condition (2), provided we choose $n>\dfrac{\zeta}{3\pi}$.

Further, note that $F\in\mathcal{L}(l_1)$. Indeed, let $||\cdot||_1$ denote the norm in l_1, i.e., for $x=(x_1,x_2,...)\in l_1$, $||x||_1=\sum_i|x_i|$. Then

$$\begin{aligned} ||F||_1 &= \sup_{||x||_1=1}||Fx||_1=\sup_{||x||_1=1}\sum_k\left|\sum_l F_{kl}x_l\right|\leq\sup_{||x||_1=1}\sum_l\left(|x_l|\sum_k|F_{kl}|\right) \\ &\leq 1, \end{aligned} \tag{3.56}$$

where we used equation (3.54) and the symmetry of F. The change of the order of summation is justified by the absolute convergence of the last sum in (3.56).

Also, (3.55) implies that $||D^{-1}||_1<1$ and consequently, $||FD^{-1}||_1<1$ which ensures that $(I+\theta FD^{-1})^{-1}$ exists and is in $\mathcal{L}(l_1)$ for all $\theta\in[0,1]$. Thus, the operator $A=B+I_n$ with $n>\dfrac{\zeta}{3\pi}$ satisfies all the hypotheses of Theorem 1.

Finally, from hypothesis (3) and since D^{-1} is a compact operator on l_1 (see condition (1)), it follows that A^{-1} exists and is compact on l_1. In addition, the proof provided in [12] constructs an explicit sequence of compact operators converging in norm to A^{-1}.

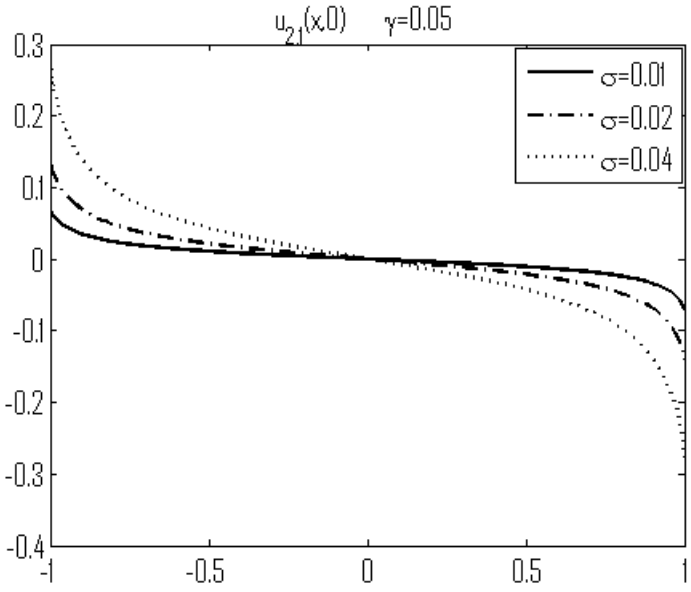

Fig. 3.2. Approximation of $u_{2,1}(x,0)$ by a finite sum of Chebyshev polynomials (400 terms) for $\gamma = 0.05$ and far-field loading $\sigma = 0.01,\ 0.02,\ 0.04$.

Returning to our system of interest (3.52), it can be written in the form

$$\begin{aligned} Bx &= y \qquad \Longleftrightarrow \\ (I - A^{-1}I_n)x &= A^{-1}y \end{aligned} \tag{3.57}$$

where the components of B are given by (3.53). Note that $I - A^{-1}I_n$ is a finite rank perturbation of the identity operator, so that (3.57) is in essence reduced to solving a finite dimensional system of linear equations.

3.3.4. Numerical Experiments

In Table 3.1 the values at the crack tip of $u_{2,1}(x,0)$, obtained using the method described in Section 3.3.2, are compared for various values of the (nondimensionalized) far field loading parameter σ and surface excess property $\tilde{\gamma}$. One can observe that

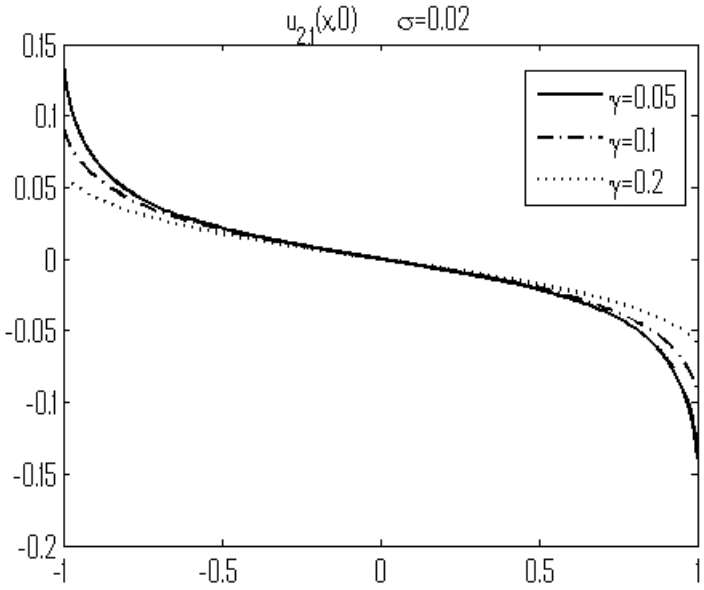

Fig. 3.3. Approximation of $u_{2,1}(x,0)$ by a finite sum of Chebyshev polynomials (400 terms) for far-field loading $\sigma_0 = 0.02$ and $\tilde{\gamma} = 0.005,\ 0.01,\ 0.02$.

the larger the value of the surface excess property, the smaller the slope of the crack profile at the crack tip.

From the numerical experiments (Fig. 3.2 and Fig. 3.3) it is clear that the described method yields a solution $u_2(x,0)$ for the crack profile such that $u_2(x,0)$ is a monotonically increasing function on $(-1,0)$ and monotonically decreasing on $(0,1)$. Furthermore, the slope of the crack profile at the crack tip increases with an increase in the far field loading. In addition, the surface excess property $\tilde{\gamma}$, with the appropriate boundary condition, given by the jump momentum balance leads to a finite opening angle at the crack tip. However, (3.41) implies that if the crack surfaces do not come together at a cusp, i.e., $\phi(\pm 1) = u_{2,1}(\pm 1, 0)$ is nonzero, then $\phi'(x) = u_{2,11}(x,0)$ has a logarithmic singularity at the crack tips. Using (3.35) one concludes that this leads to a logarithmically singular stress at the crack tip. This is an improvement from the

Table 3.1. Values of $u_{2,1}(1,0)$ for various values of the (non-dimensional) far-field loading σ and (non-dimensional) excess property $\tilde{\gamma}$.

$\tilde{\gamma}$	σ	$u_{2,1}(1,0)$
0.05	0.01	-0.0694
	0.02	-0.1388
	0.04	-0.2776
0.1	0.01	-0.0463
	0.02	-0.0927
	0.04	-0.1853
0.2	0.01	-0.0297
	0.02	-0.0595
	0.04	-0.1190

classical LEFM model which leads to a square-root singularity of the crack tip stress, however, as in LEFM, any singular stress is inconsistent with the assumptions made to linearize the equations and derive (3.41).

Remark 3. *Note that if the surface excess property is modeled using (2.4), applying perturbation theory techniques (Section 2.6), we can approximate $\tilde{\gamma}(x)$ by (2.61). Therefore, in the linearized model $\tilde{\gamma}(x)$ is reduced to*

$$\tilde{\gamma}(x) \approx \pi \int_0^\infty s^3 \tilde{\psi}(s)\, ds \equiv const,$$

which, as shown above, leads to a finite, nonzero crack tip angle and a cleavage stress which has a logarithmic singularity at the crack tip.

3.4. Model with Curvature Dependence in the Surface Tension and Zero Mutual Body Force Term

In this section, as a next step, we study a model in which the mutual body force is assumed to be zero but we allow for curvature dependence in the excess property $\tilde{\gamma}$ of the fracture surface, i.e.,

$$\tilde{\gamma} = \tilde{\gamma}(H). \tag{3.58}$$

Even though curvature-dependent surface tension models are not common in the fracture literature, the effect of curvature-dependent surface tension has been widely studied in the context of nucleation theory ([35, 36, 42]).

Recall that the curvature H is given by (2.28). Assuming that stresses and strains remain small and combining (3.12) and (3.58) one concludes that one has the following asymptotic expansion for $\tilde{\gamma}$:

$$\tilde{\gamma}(x) = \gamma_0 + \gamma_1 u_{2,11}(x,0) + h.o.t. \tag{3.59}$$

where $\gamma_0 \equiv \text{const}$ and $\gamma_1 \equiv \text{const}$. After substituting (3.59) into (3.14) and linearizing the jump momentum balance equations under the assumption that $u_{i,j}(x,0)$ and $u_{i,jk}(x,0)$, $i,j,k = 1,2$ are small, we obtain

$$\begin{aligned} \sigma_{12}(x,0) &= \gamma_1 u_{2,111}(x,0) + h.o.t. \\ \sigma_{22}(x,0) &= -\gamma_0 u_{2,11}(x,0) + h.o.t. \ . \end{aligned} \tag{3.60}$$

We proceed in a similar way to the approach taken in the case of constant $\tilde{\gamma}$ (Section 3.3). Using (3.34) and splitting the displacement vector into $\mathbf{u} = \mathbf{u}^0 + \mathbf{u}^f$, where the components of $\mathbf{u}^f$ are given by (3.37), we arrive at the following linear

integro-differential equation for $\phi(x) = u^0_{2,1}(x,0) = u_{2,1}(x,0)$:

$$\gamma_0\phi'(x) + \frac{1}{\pi}\fint_{-1}^{1} \frac{\zeta_1\phi(r) + \zeta_2\gamma_1\phi''(r)}{r-x}\,dr = -\sigma, \quad x \in (-1,1), \tag{3.61}$$

where

$$\zeta_1 = \frac{E}{2(1-\nu^2)} \quad \text{and} \quad \zeta_2 = \frac{1-2\nu}{2(1-\nu)}.$$

First notice that unlike in the case with $\tilde{\gamma} \equiv \text{const}$ (cf. (3.41)), (3.61) cannot have a solution $\phi(x)$, such that $\phi'(x)$ is singular at the endpoints. The reason being that this would imply $\phi''(x) \notin L^1([-1,1])$ and consequently the Cauchy principal value integral in (3.61) would not exist. In its turn, this implies that every solution $\phi(x)$ of (3.61) satisfies

$$\zeta_1\phi(\pm 1) + \zeta_2\gamma_1\phi''(\pm 1) = 0. \tag{3.62}$$

Thus, the solution $\phi(x)$ "adjusts itself" so that (3.62) is satisfied. Note that (3.62) cannot be viewed as a boundary condition.

Further, taking into account $(3.15)_1$ we look for a solution of (3.61) subject to

$$\phi(-1) = \phi(1) = 0 \tag{3.63}$$

so that $u_{2,1}(x,0)$ is continuous at the crack tips. Furthermore, the symmetry of the problem requires that the crack profile $u_2(x,0)$ be an even function of x and therefore we look for a solution ϕ of (3.61) such that

$$\phi(x) = -\phi(-x), \quad x \in (-1,1). \tag{3.64}$$

Theorem 2. *Problem (3.61), subject to (3.63) and (3.64), has a unique solution for all, apart from countably many, values of the parameters γ_0 and γ_1.*

Proof. We use a standard technique introduced by Mikhlin and Prössdorf in [34], Chapter VII, to reduce (3.61) to canonical form.

Let $\psi(x) := \phi''(x)$. Then

$$\phi'(x) = \int_{-1}^{1} \omega_0(x,r)\psi(r)\,dr + c_1 \tag{3.65}$$

and

$$\phi(x) = \int_{-1}^{1} \omega_1(x,r)\psi(r)\,dr + c_1(x+1) + c_2, \tag{3.66}$$

where

$$\omega_0(x,r) = \begin{cases} 1,\ r \in (-1,x) \\ 0,\ r \in (x,1), \end{cases} \qquad \omega_1(x,r) = \int_{-1}^{1} \omega_0(x,t)\omega_0(t,r)\,dt$$

and $c_1 = \phi'(-1)$, $c_2 = \phi(-1)$. After substituting (3.65) and (3.66) into (3.61) we arrive at a singular integral equation for $\psi(x)$ of the form

$$\frac{\gamma_1\zeta_2}{\pi}\!\!\int_{-1}^{1} \frac{\psi(r)}{r-x}\,dr + \int_{-1}^{1} k(x,r)\psi(r)\,dr = -\sigma - \gamma_0 c_1 - \frac{\zeta_1}{\pi}\!\!\int_{-1}^{1} \frac{c_1(r+1)+c_2}{r-x}\,dr, \tag{3.67}$$

where

$$k(x,r) = \gamma_0\omega_0(x,r) + \frac{\zeta_1}{\pi}\!\!\int_{-1}^{1} \frac{\omega_1(t,r)}{t-x}\,dr.$$

Using the boundary conditions (3.63), we have $c_2 = 0$. Also, combining (3.63), (3.64) and (3.65) we find

$$0 = \int_0^1 \phi'(x)\,dx = \int_0^1 \int_{-1}^{1} \omega_0(x,r)\psi(r)\,dr\,dx + c_1. \tag{3.68}$$

Thus, using (3.63) and (3.64), (3.67) can be written in the (canonical) form

$$R[\psi](x) := \frac{\gamma_1\zeta_2}{\pi}\!\!\int_{-1}^{1} \frac{\psi(r)}{r-x}\,dr + \int_{-1}^{1} \tilde{k}(x,r)\psi(r)\,dr = -\sigma, \tag{3.69}$$

where

$$\tilde{k}(x,r) = \gamma_0\omega_0(x,r) + \frac{\zeta_1}{\pi}\!\!\int_{-1}^{1} \frac{\omega_1(t,r)}{t-x}\,dt - \gamma_0\int_0^1 \omega_0(t,r)\,dt - \frac{\zeta_1}{\pi}\!\!\int_{-1}^{1}\int_0^1 \omega_0(s,r)\frac{t+1}{t-x}\,ds\,dt.$$

Let $L^2_\varrho([-1,1])$ denote the weighted space of functions having a finite norm

$$||v||_\varrho = \left(\int_{-1}^{1} (1-x^2)^{1/2} |v(x)|^2 \, dx \right)^{1/2}.$$

It is well known ([34, 38, 41]) that the singular integral operator $R[\psi]$ is a Fredholm operator from $L^2_\varrho([-1,1])$ to $L^2_\varrho([-1,1])$ of index 1. The index depends only on the dominant part of the operator - the singular integral operator

$$R_1[\psi](x) := \frac{1}{\pi} \int\!\!\!\!\!\!- _{-1}^{1} \frac{\psi(r)}{r-x} \, dr,$$

and is independent of any compact perturbation, in particular, it is independent of

$$R_2[\psi](x) := \int_{-1}^{1} \tilde{k}(x,r)\psi(r) \, dr.$$

Now, recall formula (3.49) which provides an inverse of the finite Hilbert transform. Using an argument similar to the one given in Section 3.3.2, we conclude that $R_1[\psi](x)$, restricted to the space of functions ψ with $\int_{-1}^{1} \psi(x) \, dx = 0$, has a trivial null space. Therefore, (3.69) is equivalent to

$$\gamma_1 \zeta_2 \psi(x) + R_2^{-1} R_1[\psi](x) = R_2^{-1}[\sigma](x).$$

Note that $R_2^{-1}R_1$ is a compact operator, being the composition of a compact with a continuous operator, and consequently, it has a countable spectrum $\sigma(R_2^{-1}R_1)$. Furthermore, $\gamma_1\zeta_2 I + R_2^{-1}R_1$, where I is the identity operator, is invertible, unless $-\gamma_1\zeta_2 \in \sigma(R_2^{-1}R_1)$. This concludes the proof. □

3.4.1. Numerical Experiments

To find a numerical solution to problem (3.61), subject to (3.63) and (3.64), we employ a *spline collocation method*, similar to the one introduced by Samoĭlova in [40], where a first order singular integro-differential equation (SIDE) is solved. Spline

collocation methods for SIDEs were considered by many others, including Schmidt ([43]). Using (3.64), it suffices to solve the problem on $(0,1)$. Further, the boundary conditions (3.63) combined with (3.62) imply that $\phi(1) = \phi''(1) = 0$ and (3.64) yields $\phi(0) = \phi''(0) = 0$. Consequently we can use a natural cubic spline $S(x)$ to approximate the solution $\phi(x)$. Let $0 = x_1 < x_2 < ... < x_{N+1} = 1$ be the evenly-spaced spline nodes, i.e.,

$$S(x) = \begin{cases} S_1(x), \ x \in [x_1, x_2] \\ S_2(x), \ x \in [x_2, x_3] \\ ... \\ S_N(x), \ x \in [x_N, x_{N+1}] \end{cases}$$

with ([7])

$$\begin{aligned} S_i(x) = \frac{z_{i+1}(x - x_i)^3 + z_i(x_{i+1} - x)^3}{6h} + \left(\frac{y_{i+1}}{h} - \frac{h}{6}z_{i+1}\right)(x - x_i) \\ + \left(\frac{y_i}{h} - \frac{h}{6}z_i\right)(x_{i+1} - x). \end{aligned} \tag{3.70}$$

Here $h = 1/N$, y_i approximates $\phi(x_i)$ and the coefficients z_i can be found by solving the tridiagonal system of equations

$$\begin{aligned} z_1 &= 0 \\ z_{i-1} + 4z_i + z_{i+1} &= \frac{6}{h^2}(y_{i+1} - 2y_i + y_{i-1}) \\ z_{N+1} &= 0. \end{aligned}$$

Using (3.64), we transform (3.61) into

$$\gamma_0\phi'(x) + \frac{2}{\pi}\int_0^1 \frac{(\zeta_1\phi(r) + \zeta_2\gamma_1\phi''(r))r}{r^2 - x^2}\, dr = -\sigma, \quad x \in (0,1). \tag{3.71}$$

The Cauchy principal value integral is calculated with the help of a *product integration*

method ([9, 54]), i.e.,

$$\int_0^1 \frac{(\zeta_1 S(r) + \zeta_2\gamma_1 S''(r))r}{r^2 - x^2}\, dr = \sum_{i=1}^{N} \int_{x_i}^{x_{i+1}} \frac{(\zeta_1 S_i(r) + \zeta_2\gamma_1 S_i''(r))r}{r^2 - x^2}\, dr,$$

and, using (3.70), each of the integrals on $[x_i, x_{i+1}]$ is evaluated exactly.

In the end, the following $(N-1)\times(N-1)$ linear system of equations for the unknowns y_2, y_3, ..., y_N is solved

$$\gamma_0 S_i'(t_i) + \sum_{j=1}^{N} \int_{x_j}^{x_{j+1}} \frac{(\zeta_1 S_j(r) + \zeta_2\gamma_1 S_j''(r))r}{r^2 - t_i^2}\, dr = -\sigma, \quad i = 2...N, \tag{3.72}$$

where t_i is the midpoint of the interval $[x_i, x_{i+1}]$.

Provided below are graphs of the slope of the crack profile $u_{2,1}(x,0)$ and of $\gamma_1 u_{2,11}(x,0)$ for $\nu = 0.33$ and various values of the parameters γ_0, γ_1 and the far-field loading σ. Note that the parameters are nondimensionalized as in (2.7) and $\zeta_1^\star = \zeta_1/E$, but for simplicity of notation the superscript $\star$ is dropped.

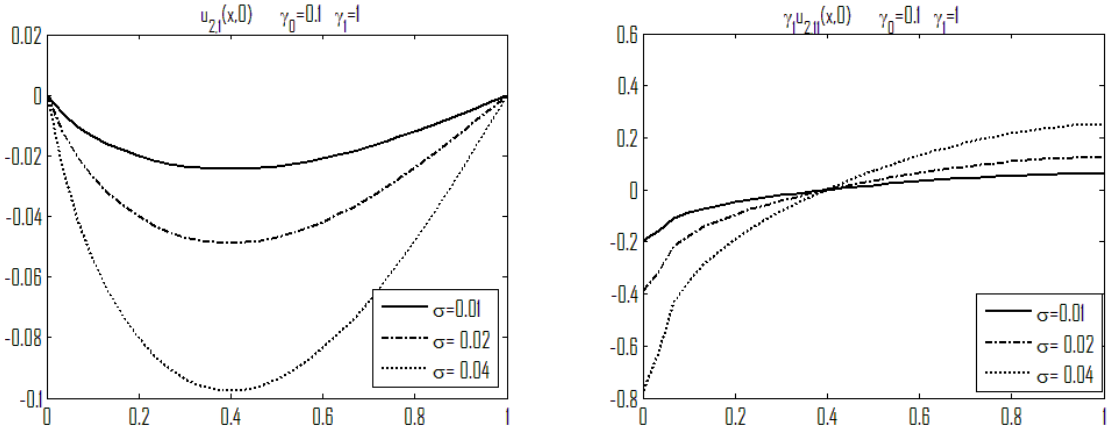

Fig. 3.4. Graph of $u_{2,1}(x,0)$ and of $\gamma_1 u_{2,11}(x,0)$ for $\gamma_0 = 0.1$, $\gamma_1 = 1$ and far-field loading $\sigma = 0.01$, 0.02, 0.04.

From the numerical experiments (Fig. 3.4) it is clear that $|\sigma_{22}(1,0)|$ - the stress

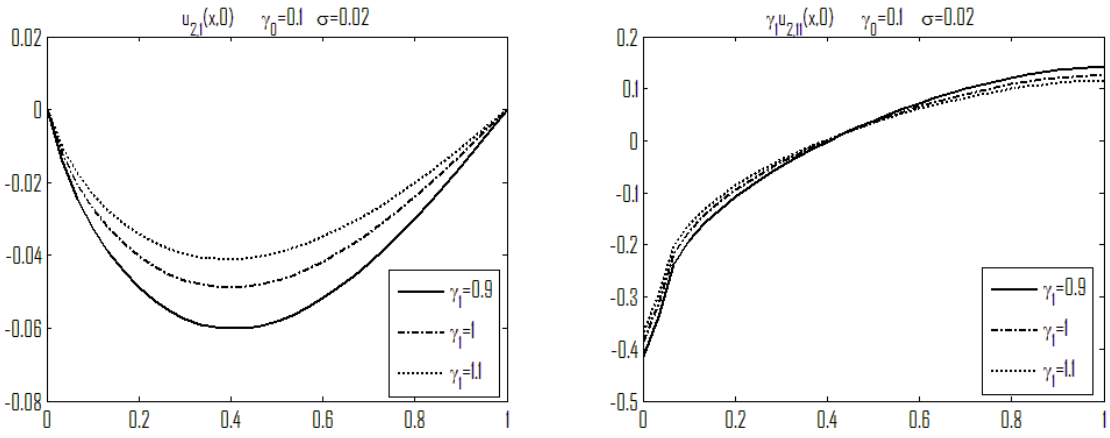

Fig. 3.5. Graph of $u_{2,1}(x,0)$ and of $\gamma_1 u_{2,11}(x,0)$ for $\gamma_0 = 0.1$, far-field loading $\sigma = 0.02$ and $\gamma_1 = 0.9,\ 1,\ 1.1$.

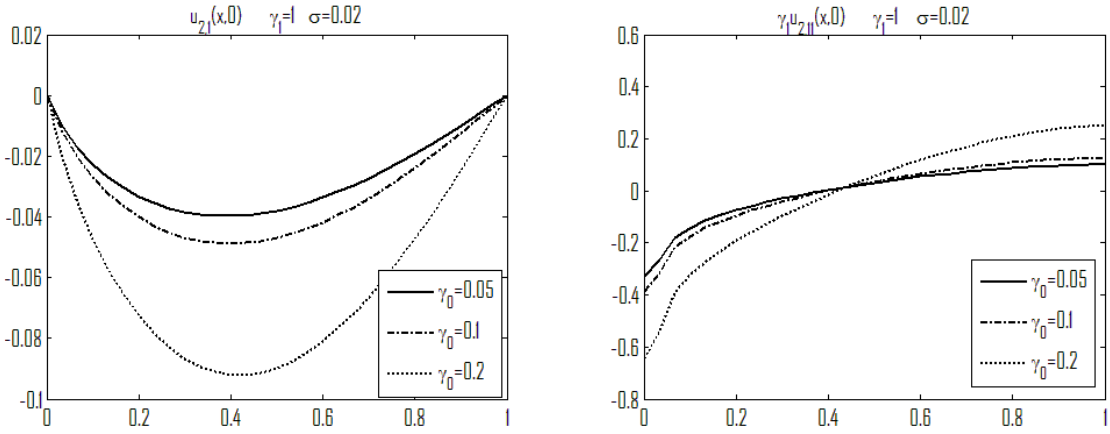

Fig. 3.6. Graph of $u_{2,1}(x,0)$ and of $\gamma_1 u_{2,11}(x,0)$ for $\gamma_1 = 1$, far-field loading $\sigma = 0.02$ and $\gamma_0 = 0.05,\ 0.1,\ 0.2$.

Table 3.2. Value of $\phi'(1) = u_{2,11}(1,0)$ for various values of the (non-dimensional) far–field loading σ and (nondimensionalized) γ_0 and γ_1.

γ_0	γ_1	σ	$\phi'(1)$	γ_0	γ_1	σ	$\phi'(1)$	γ_0	γ_1	σ	$\phi'(1)$
0.05	0.9	0.01	0.0600	0.1	0.9	0.01	0.0789	0.2	0.9	0.01	0.2021
		0.02	0.1199			0.02	0.1577			0.02	0.4042
		0.04	0.2398			0.04	0.3154			0.04	0.8084
	1	0.01	0.0503		1	0.01	0.0631		1	0.01	0.1251
		0.02	0.1006			0.02	0.1262			0.02	0.2501
		0.04	0.2012			0.04	0.2525			0.04	0.5003
	1.1	0.01	0.0433		1.1	0.01	0.0526		1.1	0.01	0.0902
		0.02	0.0866			0.02	0.1051			0.02	0.1803
		0.04	0.1732			0.04	0.2102			0.04	0.3607

at the crack tip (in absolute value) is an increasing function of the far field loading (cf. (3.60)). Furthermore, the larger the value of γ_1, the smaller the crack tip stress (Fig. 3.5). Interestingly, unlike in the constant surface tension model (Section 3.3), the crack tip stress is an *increasing function* of γ_0 (Fig. 3.6). In Table 3.2 the values at the crack tip of $\phi'(x) = u_{2,11}(x,0)$, in the case of curvature-dependent surface tension, are compared for various values of the (nondimensionalized) far field loading parameter σ and the parameters γ_0 and γ_1 which determine the surface excess property $\tilde{\gamma}(x)$.

It should be noted here that for certain values of the parameters, namely when γ_0 is not much smaller than γ_1, the model yields unphysical solutions and predicts interpenetration of the upper and lower crack surfaces (Fig. 3.7). Further, models for which γ_0 is much larger than γ_1 predict highly oscillatory solutions.

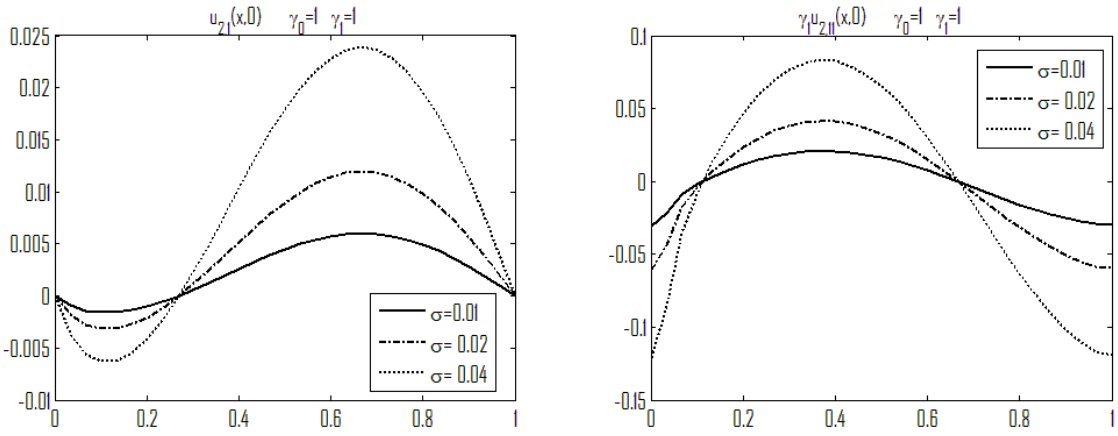

Fig. 3.7. Graph of $u_{2,1}(x,0)$ and of $\gamma_1 u_{2,11}(x,0)$ for $\gamma_0 = 0.1$, $\gamma_1 = 1$ and far-field loading $\sigma = 0.01,\ 0.02,\ 0.04$.

Most importantly, introducing curvature dependence into the surface tension removes the crack tip stress singularity and leads to a crack profile such that the two crack surfaces meet at a cusp at the crack tip. Moreover, models with curvature-dependent surface tension yield solutions such that $u_{2,1}(x,0)$ and $u_{2,11}(x,0)$ remain small (when σ is small enough), which is consistent with the assumptions made to derive (3.61).

3.5. Model Including Mutual Body Force Correction

In order to construct the Dirichlet to Neumann (3.29) and the Neumann to Dirichlet (3.31) maps for the model with nonzero mutual body force correction, one first needs to find a particular solution of (3.21). The system (3.21) can be written in the form

$$\begin{aligned} \mu\frac{d^2}{dy^2}Y_1 + ip(\lambda+\mu)\frac{d}{dy}Y_2 - p^2(\lambda+2\mu)\hat{u}_{1,1} &= B_3(y) \\ (\lambda+2\mu)\frac{d^2}{dy^2}Y_2 + ip(\lambda+\mu)\frac{d}{dy}Y_1 - p^2\mu Y_1 &= B_4(y), \end{aligned} \tag{3.73}$$

with

$$Y_1(p,y) = \hat{u}_{1,1}(p,y), \quad Y_2(p,y) = \hat{u}_{2,1}(p,y),$$
$$B_3(p,y) = -ip\hat{b}_{\kappa 1}(p,y), \quad B_4(p,y) = -ip\hat{b}_{\kappa 2}(p,y).$$

We often suppress the dependence on p whenever this dependence is clear from the context. We look for a particular solution $\mathbf{P}(p,y) = \langle \alpha_1(p,y), \alpha_2(p,y) \rangle^T$ of the form

$$\begin{aligned} \alpha_1(p,y) &= \int_y^\infty \left(g_1(p,s) + (y-s)g_2(p,s)\right) e^{|p|(y-s)} ds \\ \alpha_2(p,y) &= \int_y^\infty \left(g_3(p,s) + (y-s)g_4(p,s)\right) e^{|p|(y-s)} ds. \end{aligned} \tag{3.74}$$

Let $g_j'(p,y)$ denote $\dfrac{\partial g_j}{\partial y}(p,y)$, $j = 1, ..., 4$. Substituting (3.74) into (3.73) we obtain that $g_i(y)$, $i = 1, ..., 4$ have to satisfy

$$\begin{aligned} &-\mu(g_1' + |p|g_1 + g_2) - ip(\lambda+\mu)g_3 \\ &+ |p|\mu \int_y^\infty \Big(|p|g_1(s) + 2g_2(s) + |p|(y-s)g_2(s)\Big) e^{|p|(y-s)} ds \\ &+ ip(\lambda+\mu) \int_y^\infty \Big(|p|g_3(s) + g_4(s) + |p|(y-s)g_4(s)\Big) e^{|p|(y-s)} ds \\ &- p^2(\lambda+2\mu) \int_y^\infty \Big(g_1(s) + (y-s)g_2(s)\Big) e^{|p|(y-s)} ds = B_3(p,y), \end{aligned} \tag{3.75}$$

and

$$\begin{aligned} &-(\lambda+2\mu)(g_3' + |p|g_3 + g_4) - ip(\lambda+\mu)g_1 \\ &+ |p|(\lambda+2\mu) \int_y^\infty \Big(|p|g_3(s) + 2g_4(s) + |p|(y-s)g_4(s)\Big) e^{|p|(y-s)} ds \\ &+ ip(\lambda+\mu) \int_y^\infty \Big(|p|g_1(s) + g_2(s) + |p|(y-s)g_2(s)\Big) e^{|p|(y-s)} ds \\ &- p^2\mu \int_y^\infty \Big(g_3(s) + (y-s)g_4(s)\Big) e^{|p|(y-s)} ds = B_4(p,y). \end{aligned} \tag{3.76}$$

One can easily check that (3.75) and (3.76) reduce respectively to

$$-\mu(g_1' + |p|g_1 + g_2) - ip(\lambda+\mu)g_3 = B_3(p,y) \tag{3.77}$$

and

$$-(\lambda+2\mu)(g_3'+|p|g_3+g_4)-ip(\lambda+\mu)g_1=B_4(p,y) \tag{3.78}$$

provided

$$\begin{aligned} g_4(p,y)&=-\frac{\lambda+\mu}{\lambda+3\mu}(ipg_1(p,y)+|p|g_3(p,y))\\ g_2(p,y)&=i\mathrm{sgn}(p)g_4(p,y)=\frac{\lambda+\mu}{\lambda+3\mu}(|p|g_1(p,y)-ipg_3(p,y)). \end{aligned} \tag{3.79}$$

Using (3.79), (3.77) and (3.78) one concludes that $g_1(y)$ and $g_3(y)$ have to satisfy the following system of equations

$$\begin{aligned} g_1'+\frac{2|p|(\lambda+2\mu)}{\lambda+3\mu}g_1+\frac{ip(\lambda+\mu)(\lambda+2\mu)}{\mu(\lambda+3\mu)}g_3&=-\frac{B_3}{\mu}\\ g_3'+\frac{ip(\lambda+\mu)\mu}{(\lambda+2\mu)(\lambda+3\mu)}g_1+\frac{2|p|\mu}{\lambda+3\mu}g_3&=-\frac{B_4}{\lambda+2\mu}. \end{aligned} \tag{3.80}$$

One readily shows that

$$\begin{aligned} g_1(p,s)=\int_0^s e^{-|p|(s-t)}\Bigg(&\frac{B_3(t)}{\mu}\Big(-1+\frac{|p|(\lambda+\mu)}{\lambda+3\mu}(s-t)\Big)\\ &+\frac{ip(\lambda+\mu)}{\mu(\lambda+3\mu)}B_4(t)(s-t)\Bigg)dt \end{aligned}$$

and

$$\begin{aligned} g_3(p,s)=\int_0^s e^{-|p|(s-t)}\Bigg(&\frac{ip(\lambda+\mu)}{(\lambda+2\mu)(\lambda+3\mu)}B_3(t)(s-t)\\ &-\frac{B_4(t)}{\lambda+2\mu}\Big(1+\frac{|p|(\lambda+\mu)}{\lambda+3\mu}(s-t)\Big)\Bigg)dt \end{aligned}$$

satisfy (3.80). Using (3.79), for $g_2(s)$ and $g_4(s)$ we obtain

$$\begin{aligned} g_2(p,s)=\frac{\lambda+\mu}{\lambda+3\mu}\int_0^s e^{-|p|(s-t)}\Bigg(&\frac{|p|B_3(t)}{\mu}\Big(-1+\frac{|p|(\lambda+\mu)}{\lambda+2\mu}(s-t)\Big)\\ &+\frac{ip}{\lambda+2\mu}B_4(t)\Big(1+\frac{|p|(\lambda+\mu)}{\mu}(s-t)\Big)\Bigg)dt \end{aligned}$$

and

$$g_4(p,s)=\frac{\lambda+\mu}{\lambda+3\mu}\int_0^s e^{-|p|(s-t)}\Bigg(\frac{ip}{\mu}B_3(t)\Big(1-\frac{|p|(\lambda+\mu)}{\lambda+2\mu}(s-t)\Big)\\ +\frac{|p|B_4(t)}{\lambda+2\mu}\Big(1+\frac{|p|(\lambda+\mu)}{\mu}(s-t)\Big)\Bigg)dt.$$

Let us introduce

$$\begin{aligned}f_1(x)=&-\frac{2\mu(\lambda+2\mu)}{\lambda+3\mu}\mathcal{H}[\breve{\alpha}_1](x,0)+\frac{\mu(\lambda+\mu)}{\lambda+3\mu}\breve{\alpha}_2(x,0)+\mu\frac{d}{dy}\int_0^x\breve{\alpha}_1(s,0)ds\\ f_2(x)=&-\frac{2\mu(\lambda+2\mu)}{\lambda+3\mu}\mathcal{H}[\breve{\alpha}_2](x,0)+\frac{(\lambda+2\mu)(\lambda+\mu)}{\lambda+3\mu}\breve{\alpha}_1(x,0)\\ &+(\lambda+2\mu)\frac{d}{dy}\int_0^x\breve{\alpha}_2(s,0)ds.\end{aligned}\tag{3.81}$$

With these notations the Dirichlet to Neumann map (3.29) takes the form

$$\begin{aligned}\sigma_{12}(x,0)&=\frac{2\mu^2}{\lambda+3\mu}u_{2,1}(x,0)+\frac{2\mu(\lambda+2\mu)}{\lambda+3\mu}\mathcal{H}[u_{1,1}](x,0)+f_1(x)\\ \sigma_{22}(x,0)&=-\frac{2\mu^2}{\lambda+3\mu}u_{1,1}(x,0)+\frac{2\mu(\lambda+2\mu)}{\lambda+3\mu}\mathcal{H}[u_{2,1}](x,0)+f_2(x),\end{aligned}\tag{3.82}$$

while the Neumann to Dirichlet map (3.31) becomes

$$\begin{aligned}u_{1,1}(x,0)=&-\frac{\lambda+2\mu}{2\mu(\lambda+\mu)}\left(\mathcal{H}[\sigma_{12}](x,0)-\mathcal{H}[f_1](x)\right)\\ &+\frac{1}{2(\lambda+\mu)}(\sigma_{22}(x,0)-f_2(x))\\ u_{2,1}(x,0)=&-\frac{\lambda+2\mu}{2\mu(\lambda+\mu)}\left(\mathcal{H}[\sigma_{22}](x,0)-\mathcal{H}[f_2](x)\right)\\ &-\frac{1}{2(\lambda+\mu)}(\sigma_{12}(x,0)-f_1(x)).\end{aligned}\tag{3.83}$$

Here $\mathcal{H}[\cdot]$ is the Hilbert transform operator defined in (3.28).

Taking a similar approach to the one presented in Section 3.3, we substitute equation $(3.83)_1$ into $(3.82)_2$ to obtain

$$\sigma_{22}(x,0)=\frac{2\mu(\lambda+\mu)}{\lambda+2\mu}\mathcal{H}[u_{2,1}](x,0)+\frac{\mu}{\lambda+2\mu}(\mathcal{H}[\sigma_{12}](x,0)-\mathcal{H}[f_1](x))+f_2(x).\tag{3.84}$$

Next, we need to evaluate the term arising because of the nonzero mutual body force:

$$z(x) := -\frac{\mu}{\lambda + 2\mu}\mathcal{H}[f_1](x) + f_2(x). \tag{3.85}$$

For this purpose, let us list some properties of the Hilbert and Fourier transforms to be subsequently used. The inverse Fourier transform of $e^{-a|p|}$ is given by

$$\mathcal{F}^{-1}[e^{-a|p|}](x) = \frac{a}{\pi(x^2 + a^2)}, \qquad a > 0. \tag{3.86}$$

Using (3.28) one shows that $\mathcal{H}^2 = -I$, where I is the identity operator, i.e.,

$$\mathcal{H}[\mathcal{H}[f]] = -f. \tag{3.87}$$

Also, the Hilbert transform commutes with differentiation

$$\mathcal{H}[\frac{d^n}{dx^n}f(x)] = \frac{d^n}{dx^n}\mathcal{H}[f](x). \tag{3.88}$$

Let $*$ denote the convolution operation, i.e.,

$$f * g(x) = \int_{-\infty}^{\infty} f(x-y)g(y)\,dy$$

then

$$\mathcal{F}^{-1}[\hat{f}(p)\hat{g}(p)](x) = f * g(x). \tag{3.89}$$

For the Hilbert transform of a convolution of two functions one can easily show that

$$\mathcal{H}[f * g] = \mathcal{H}[f] * g = f * \mathcal{H}[g]. \tag{3.90}$$

In addition, for $f = \dfrac{a}{\pi(x^2+a^2)}$ with $a > 0$,

$$\begin{array}{rlrl} f &= \dfrac{a}{\pi(x^2+a^2)} & \mathcal{H}[f] &= -\dfrac{x}{\pi(x^2+a^2)} \\ \dfrac{df}{dx} &= -\dfrac{2ax}{\pi(x^2+a^2)^2} & \dfrac{d}{dx}\mathcal{H}[f] &= \dfrac{(x^2-a^2)}{\pi(x^2+a^2)^2} \\ \dfrac{d^2f}{dx^2} &= \dfrac{2a(3x^2-a^2)}{\pi(x^2+a^2)^3} & \dfrac{d^2}{dx^2}\mathcal{H}[f] &= -\dfrac{2x(x^2-3a^2)}{\pi(x^2+a^2)^3} \\ \dfrac{d^3f}{dx^3} &= \dfrac{24ax(a^2-x^2)}{\pi(x^2+a^2)^4} & \dfrac{d^3}{dx^3}\mathcal{H}[f] &= \dfrac{6(a^2+2ax-x^2)(a^2-2ax-x^2)}{\pi(x^2+a^2)^4}. \end{array} \tag{3.91}$$

Substituting (3.81) into (3.85) and using (3.87), one obtains

$$\begin{aligned} z(x) =& \lambda\breve{\alpha}_1(x,0) - \frac{\mu(\lambda+\mu)(2\lambda+5\mu)}{(\lambda+2\mu)(\lambda+3\mu)}\mathcal{H}[\breve{\alpha}_2](x,0) \\ & - \frac{\mu^2}{\lambda+2\mu}\frac{d}{dy}\Big|_{y=0}\mathcal{H}\left[\int_0^x \breve{\alpha}_1(a,y)da\right] + (\lambda+2\mu)\frac{d}{dy}\Big|_{y=0}\int_0^x \breve{\alpha}_2(a,y)da. \end{aligned} \tag{3.92}$$

For the last two terms in (3.92), differentiation of (3.74) with respect to y yields

$$\begin{aligned} \frac{d}{dy}\Big|_{y=0}\alpha_1(p,y) &= |p|\alpha_1(p,0) + \int_0^\infty g_2(p,s)e^{-|p|s}ds \\ \frac{d}{dy}\Big|_{y=0}\alpha_2(p,y) &= |p|\alpha_2(p,0) + \int_0^\infty g_4(p,s)e^{-|p|s}ds \end{aligned}$$

from where, after taking the inverse Fourier transform with respect to p and using (3.23) and (3.28), one obtains

$$\begin{aligned} \frac{d}{dy}\breve{\alpha}_1(x,0) &= -\frac{\partial}{\partial x}\mathcal{H}[\breve{\alpha}_1](x,0) + \int_0^\infty \mathcal{F}^{-1}[g_2(p,s)e^{-|p|s}](x,s)ds \\ \frac{d}{dy}\breve{\alpha}_2(x,0) &= -\frac{\partial}{\partial x}\mathcal{H}[\breve{\alpha}_2](x,0) + \int_0^\infty \mathcal{F}^{-1}[g_4(p,s)e^{-|p|s}](x,s)ds. \end{aligned}$$

Using (3.87) and (3.88) one concludes

$$\begin{aligned} \frac{d}{dy}\Big|_{y=0}\mathcal{H}\left[\int_0^x \breve{\alpha}_1(a,y)da\right] &= \breve{\alpha}_1(x,0) \\ &\quad + \int_0^\infty\int_0^x \mathcal{H}[\mathcal{F}^{-1}[g_2(p,s)e^{-|p|s}]](a,s)da\,ds \end{aligned} \tag{3.93}$$

and

$$\frac{d}{dy}\Big|_{y=0}\int_0^x \breve{\alpha}_2(a,y)da = -\mathcal{H}[\breve{\alpha}_2](x,0) + \int_0^\infty\int_0^x \mathcal{F}^{-1}[g_4(p,s)e^{-|p|s}](a,s)da\,ds. \quad (3.94)$$

It is easy to see that $(3.79)_2$, (3.28) and (3.87) imply

$$\mathcal{H}[\mathcal{F}^{-1}[g_2]] = -\mathcal{F}^{-1}[g_4].$$

Thus, substitution of (3.93) and (3.94) into (3.92) gives

$$\begin{aligned} z(x) =& \frac{\lambda^2+2\lambda\mu-\mu^2}{\lambda+2\mu}\breve{\alpha}_1(x,0) - \left(\frac{\mu(\lambda+\mu)(2\lambda+5\mu)}{(\lambda+2\mu)(\lambda+3\mu)} + \lambda + 2\mu\right)\mathcal{H}[\breve{\alpha}_2](x,0) \\ &+ \frac{\mu^2+(\lambda+2\mu)^2}{\lambda+2\mu}\int_0^\infty\int_0^x \mathcal{F}^{-1}[g_4(p,s)e^{-|p|s}](a,s)da\,ds. \end{aligned} \quad (3.95)$$

Using (3.86)-(3.91), after straightforward computations one finds

$$\begin{aligned} \breve{\alpha}_1(x,0) = \int_0^\infty \Bigg[& b_{\kappa 1}(x,t) * \left(\frac{-x}{2\pi\mu(x^2+t^2)} + \frac{(\lambda+\mu)x(x^2+3t^2)}{4\pi\mu(\lambda+2\mu)(x^2+t^2)^2}\right) \\ & + b_{\kappa 2}(x,t) * \Bigg(\frac{-(\lambda+\mu)^2t^3}{2\pi\mu(\lambda+2\mu)(\lambda+3\mu)(x^2+t^2)^2} \\ & + \frac{(\lambda+\mu)t}{4\pi\mu(\lambda+3\mu)(x^2+t^2)} + \frac{(\lambda+\mu)t(x^2-3t^2)}{4\pi(\lambda+2\mu)(\lambda+3\mu)(x^2+t^2)^2}\Bigg)\Bigg]\,dt \end{aligned} \quad (3.96)$$

where the convolution is with respect to x. In a similar way one concludes that

$$\begin{aligned} &\mathcal{H}[\breve{\alpha}_2](x,0) = \\ &\int_0^\infty \Bigg[b_{\kappa 1}(x,t) * \Bigg(\frac{-(\lambda+\mu)x}{4\pi(\lambda+2\mu)(\lambda+3\mu)(x^2+t^2)} \\ &\quad + \frac{(\lambda+\mu)x^3}{4\pi(\lambda+2\mu)(\lambda+3\mu)(x^2+t^2)^2} + \frac{(\lambda+\mu)(2\lambda+7\mu)xt^2}{4\pi\mu(\lambda+2\mu)(\lambda+3\mu)(x^2+t^2)^2}\Bigg) \\ &\quad + b_{\kappa 2}(x,t) * \left(\frac{-t}{2\pi(\lambda+2\mu)(x^2+t^2)} - \frac{(\lambda+\mu)t^3}{2\pi\mu(\lambda+2\mu)(x^2+t^2)^2}\right)\Bigg]\,dt. \end{aligned} \quad (3.97)$$

It is straightforward to show that the last term of (3.95) can be expressed as follows:

$$\begin{aligned}&\int_0^\infty \int_0^x \mathcal{F}^{-1}[g_4(p,s)e^{-|p|s}](a,s)da\,ds = \\ &\frac{\lambda+\mu}{4\pi\mu(\lambda+2\mu)}\int_0^\infty \left[b_{\kappa 1}(x,t) * \frac{x}{x^2+t^2} - b_{\kappa 2}(x,t) * \frac{t}{x^2+t^2}\right] dt.\end{aligned} \tag{3.98}$$

One concludes from (3.95) together with (3.96), (3.97) and (3.98) that $z(t)$ is of the form

$$\begin{aligned}z(x) = \int_0^\infty \Bigg[&b_{\kappa 1}(x,t) * \left(c_1\frac{x}{x^2+t^2} + c_2\frac{x^3}{(x^2+t^2)^2} + c_3\frac{xt^2}{(x^2+t^2)^2}\right) \\ &+b_{\kappa 2}(x,t) * \left(d_1\frac{t}{x^2+t^2} + d_2\frac{t^3}{(x^2+t^2)^2} + d_3\frac{tx^2}{(x^2+t^2)^2}\right)\Bigg] dt\end{aligned} \tag{3.99}$$

where the constants c_i and d_i, $i = 1, 2, 3$ depend only on the Lamé parameters λ and μ.

Next, we linearize the components of the body force term $\mathbf{b}_\kappa(x,t)$ under the assumption that $u_{i,j}(x,0)$ and $u_{i,jk}(x,0)$ are small. Recall that the body force in the current configuration is $\mathbf{b} = -\text{grad}\Phi$ with $\Phi(x_1,x_2)$ - a correction potential of the form (cf. (2.6) and (2.40))

$$\Phi(x_1,x_2) = \int_{-1}^1 \int_{-h(a)}^{h(a)} \int_{-\infty}^\infty \varphi(\sqrt{(x_1-a)^2+(x_2-b)^2+c^2})dc\,db\,da \tag{3.100}$$

and that the body force in the reference configuration is $\mathbf{b}_\kappa = J\mathbf{b}$ where J is the determinant of the deformation gradient. Note that the approximation given by (2.51) cannot be used here as (3.99) requires information about $\Phi(\cdot,t)$ for all $t \geq 0$, not only in a neighborhood of the crack surface.

Then, using

$$(x_1,\, h(x_1)) = (X_1 + u_1(X_1,0), u_2(X_1,0)),$$

it is easy to see that the components of $\mathbf{b}_\kappa$ are

$$b_{\kappa 1}(X_1, X_2) = J \int_{-1}^{1} \int_{-u_2(a,0)}^{u_2(a,0)} \int_{-\infty}^{\infty} \frac{\varphi'(r)}{\sqrt{r}} (X_1 + u_1(X_1, X_2) - a) dc\, db\, da \tag{3.101}$$

and

$$b_{\kappa 2}(X_1, X_2) = J \int_{-1}^{1} \int_{-u_2(a,0)}^{u_2(a,0)} \int_{-\infty}^{\infty} \frac{\varphi'(r)}{\sqrt{r}} (X_2 + u_2(X_1, X_2) - b) dc\, db\, da \tag{3.102}$$

where r stands for $\sqrt{(X_1 + u_1(X_1, X_2) - a)^2 + (X_2 + u_2(X_1, X_2) - b)^2 + c^2}$ and $J = (1 + u_{1,1})(1 + u_{2,2}) - u_{1,2}u_{2,1}$. Linearization of $\mathbf{b}_\kappa$ under the assumption of small displacement gradient leads to

$$b_{\kappa 1}(X_1, X_2) \sim \int_{-1}^{1} \vartheta \left(\sqrt{(X_1 - a)^2 + X_2^2} \right) (X_1 - a) u_2(a, 0)\, da \tag{3.103}$$

and

$$b_{\kappa 2}(X_1, X_2) \sim \int_{-1}^{1} \vartheta \left(\sqrt{(X_1 - a)^2 + X_2^2} \right) X_2 u_2(a, 0)\, da \tag{3.104}$$

with

$$\vartheta(s) = 4 \int_0^{\infty} \frac{\varphi'(\sqrt{s^2 + c^2})}{\sqrt{s^2 + c^2}}\, dc.$$

Thus, in the case of small strains,

$$\begin{aligned} z(x) \sim T[u_2](x) = \int_0^{\infty} \int_{-1}^{1} u_2(a, 0) \Bigg[& \\ & (x - a)\vartheta(\sqrt{(x - a)^2 + t^2}) * \left(\frac{c_1 x}{x^2 + t^2} + \frac{c_2 x^3}{(x^2 + t^2)^2} + \frac{c_3 x t^2}{(x^2 + t^2)^2} \right) \\ & + t\vartheta(\sqrt{(x - a)^2 + t^2}) * \left(\frac{d_1 t}{x^2 + t^2} + \frac{d_2 t^3}{(x^2 + t^2)^2} + \frac{d_3 t x^2}{(x^2 + t^2)^2} \right) \Bigg] da\, dt \\ = \int_{-1}^{1} u_2(a, 0) K(x, a)\, da. & \end{aligned} \tag{3.105}$$

Let $\phi \in C[-1, 1]$ and $||\phi(x)|| = \sup_{-1<x<1} |\phi(x)|$, where $C[-1, 1]$ is the space of continuous functions on $[-1, 1]$. Note that $K : [-1, 1] \times [-1, 1] \to \mathbb{R}$ is a continuous

function. Consequently, T is a Fredholm integral operator of the first kind.

3.5.1. Model with Constant Surface Tension and a Mutual Body Force Term

First consider the case where the surface excess property $\tilde{\gamma}$ is a constant. As in Section 3.3, we split $\mathbf{u} = \mathbf{u}^0 + \mathbf{u}^f$ where $\mathbf{u}^f$ is the displacement field corresponding to the homogeneous stress field determined by the far field loading σ. Proceeding in the same way as for the derivation of (3.39), one concludes that $u^0_{2,1}(x,0)$ satisfies

$$-\sigma - \tilde{\gamma} u^0_{2,11}(x,0) = \frac{E}{2(1-\nu^2)\pi} \fint_{-1}^{1} \frac{u^0_{2,1}(r,0)}{r-x} dr + \mathcal{K}[u^0_{2,1}](x) \tag{3.106}$$

where

$$\mathcal{K}[u^0_{2,1}](x) = T\left[\int_{-1}^{x} u^0_{2,1}(r,0)\, dr\right] \tag{3.107}$$

is a compact operator on $C[-1,1]$, being the composition of the compact operator T ([56], p. 55) and a bounded operator on $C[-1,1]$. Let

$$\phi(x) := u^0_{2,1}(x,0)$$

and let the singular integro-differential operator $\mathcal{S}$ be defined by

$$\mathcal{S}[\phi](x) := \tilde{\gamma}\phi'(x) + \frac{E}{2(1-\nu^2)\pi} \fint_{-1}^{1} \frac{\phi(r)}{r-x} dr.$$

Then (3.106) is equivalent to

$$\mathcal{S}[\phi](x) + \mathcal{K}[\phi](x) = -\sigma. \tag{3.108}$$

Conjecture 1. *If $\tilde{\gamma} = 0$, then for any physically reasonable correction potential the solution ϕ of the singular integral equation (3.108) exhibits a square root singularity at the crack tip.*

3.5.2. Model with Curvature-dependent Surface Tension and a Mutual Body Force Term

In the case when the surface excess property is curvature-dependent and the model includes a body force correction term, after linearizing the differential and jump momentum balances, using arguments similar to the ones given in the previous section, it is straightforward to show that $u^0_{2,1}(x,0)$ satisfies

$$\gamma_0 u^0_{2,11}(x,0) + \frac{1}{\pi}\fint_{-1}^{1} \frac{\zeta_1 u^0_{2,1}(r,0) + \zeta_2\gamma_1 u^0_{2,111}(r,0)}{r-x}\,dr + \mathcal{K}[u^0_{2,1}](x) = -\sigma. \tag{3.109}$$

Let

$$\tilde{\mathcal{S}}[\phi](x) := \gamma_0 u^0_{2,11}(x,0) + \frac{1}{\pi}\fint_{-1}^{1} \frac{\zeta_1 u^0_{2,1}(r,0) + \zeta_2\gamma_1 u^0_{2,111}(r,0)}{r-x}\,dr.$$

Here the notation introduced in Section 3.4 is used. Then (3.109) can be written in the form

$$\tilde{\mathcal{S}}[\phi](x) + \mathcal{K}[\phi](x) = -\sigma. \tag{3.110}$$

Conjecture 2. *If $\tilde{\gamma}(x) \approx \gamma_0 + \gamma_1 u_{2,11}(x,0)$ with $\gamma_1 \neq 0$, i.e., there is nonzero curvature-dependent surface tension introduced as an excess property of the fracture surfaces, then (3.109) has a unique solution $\phi(x) = u^0_{2,1}(x,0)$ for all, apart from countably many values of the parameters γ_0 and γ_1. Moreover, $\phi(x)$ and $\phi'(x)$ are bounded on $[-1,1]$, i.e., the operator $\tilde{\mathcal{S}}[\cdot] + \mathcal{K}[\cdot]$, where $\mathcal{K}$ is the compact operator given by (3.107), behaves in a similar way to the singular integro-differential operator $\tilde{\mathcal{S}}[\cdot]$.*

In other words, it is the surface tension $\tilde{\gamma}$ of the fracture surfaces, together with the appropriate fracture surface boundary conditions in the form of the jump momentum balance that is responsible for removing the square root singularities at the fracture tips, characteristic of the classical LEFM model. Furthermore, including a mutual body force term in the model, after linearization of the jump momentum bal-

ance conditions, results in a compact perturbation of the singular integro-differential equation. We conjecture that this compact perturbation does not affect the fundamental result, namely a model with curvature-dependent surface tension ascribed to the crack surfaces yields bounded stresses and strains for any physically reasonable body force correction.

CHAPTER IV

SINGULAR PERTURBATION ANALYSIS

In this chapter an alternative approach for finding the crack profile in the deformed configuration is offered. This strategy leads to a simple way of approximating the stresses and strains in a neighborhood of the fracture surfaces.

The fracture boundary value problem, formulated with the deformed configuration as reference, can be studied through a perturbation analysis with a parameter δ, corresponding to atomic length scale, as a small parameter.

The point-to-point potential, which determines the body force correction term and the excess properties is set up only when chemical bonds have been broken. On the other hand, δ determines the length scale over which the potential is active, thus the problem corresponding to $\delta = 0$ is what one would have in the absence of the potential, i.e., it describes the case when no covalent bonds have been broken. Consequently, one can choose the outer solution in the perturbation analysis to be the loaded but uncracked body.

As before, by $\mathbf{x} = \langle x_1, x_2 \rangle \in \mathcal{B}$ we denote a point in the deformed configuration $\mathcal{B}$ of the body and $\mathbf{u} = \mathbf{u}(\mathbf{x})$ denotes the spatial description of the displacement. A constitutive equation of the form (2.3) is assumed and a nondimensionalization of the parameters given by (2.7) is used.

4.1. Outer Solution

The *outer solution* corresponds to uniaxial extension of the uncracked body whose stress field is easily seen to be

$$\begin{aligned} 0 = \tau^\star_{11} &= (\lambda^\star + 2\mu^\star)\frac{\partial u^\star_1}{\partial x^\star_1} + \lambda^\star \frac{\partial u^\star_2}{\partial x^\star_2} = \frac{2\mu^\star}{1-2\nu}\left((1-\nu)\frac{\partial u^\star_1}{\partial x^\star_1} + \nu\frac{\partial u^\star_2}{\partial x^\star_2}\right) \\ 0 = \tau^\star_{12} &= \mu^\star\left(\frac{\partial u^\star_1}{\partial x^\star_2} + \frac{\partial u^\star_2}{\partial x^\star_1}\right) \\ \sigma^\star = \tau^\star_{22} &= (\lambda^\star + 2\mu^\star)\frac{\partial u^\star_2}{\partial x^\star_2} + \lambda^\star \frac{\partial u^\star_1}{\partial x^\star_1} = \frac{2\mu^\star}{1-2\nu}\left(\nu\frac{\partial u^\star_1}{\partial x^\star_1} + (1-\nu)\frac{\partial u^\star_2}{\partial x^\star_2}\right). \end{aligned} \tag{4.1}$$

It follows that the components of the displacement for the outer solution have the form

$$u^\star_1 = -\frac{\nu\sigma^\star}{2\mu^\star}x^\star_1 + k(x^\star_2) \quad u^\star_2 = \frac{(1-\nu)\sigma^\star}{2\mu^\star}x^\star_2 + m(x^\star_1), \tag{4.2}$$

where $k'(x^\star_2) + m'(x^\star_1) = 0$. Symmetry implies that $u^\star_1(0, x^\star_2) = 0$, consequently

$$u^\star_1 = -\frac{\nu\sigma^\star}{2\mu^\star}x^\star_1 \qquad u^\star_2 = \frac{(1-\nu)\sigma^\star}{2\mu^\star}x^\star_2 + \text{const.} \tag{4.3}$$

4.2. Inner Solution

Let

$$\mathbf{x}^\star = \langle x^\star_1, x^\star_2 \rangle.$$

In order to find the solution within the immediate neighborhood of the crack, we "stretch" the coordinates through the following change of variables

$$\begin{aligned} \mathbf{y} = \langle y^\star_1, y^{\star\star}_2 \rangle &= \left\langle x^\star_1, \frac{x^\star_2 - h^\star(x^\star_1)}{\delta^\star} \right\rangle \\ v^\star_1(y^\star_1, y^{\star\star}_2) = u^\star_1(x^\star_1, x^\star_2), &\quad v^\star_2(y^\star_1, y^{\star\star}_2) = \frac{u^\star_2(x^\star_1, x^\star_2) - h^\star(x^\star_1)}{\delta^\star}. \end{aligned} \tag{4.4}$$

One then readily shows that

$$\operatorname{grad}_{\mathbf{x}^\star}\mathbf{f}(\mathbf{x}^\star) = \operatorname{grad}_{\mathbf{y}}\bar{\mathbf{f}}(\mathbf{y}) \circ \operatorname{grad}_{\mathbf{x}^\star}\mathbf{y} \tag{4.5}$$

$$\operatorname{grad}_{\mathbf{x}^\star}\mathbf{y} = \begin{bmatrix} 1 & 0 \\ -h^{\star\prime}(x_1^\star)/\delta^\star & 1/\delta^\star \end{bmatrix} \tag{4.6}$$

$$\begin{aligned} \operatorname{div}_{\mathbf{x}^\star}\mathbf{f}(\mathbf{x}^\star) &= \operatorname{tr}\left(\operatorname{grad}_{\mathbf{x}^\star}\mathbf{f}(\mathbf{x}^\star)\right) = \operatorname{tr}(\operatorname{grad}_{\mathbf{y}}\bar{\mathbf{f}}(\mathbf{y}) \circ \operatorname{grad}_{\mathbf{x}^\star}\mathbf{y}) \\ &= (\operatorname{grad}_{\mathbf{x}^\star}\mathbf{y})^T \cdot \operatorname{grad}_{\mathbf{y}}\bar{\mathbf{f}}(\mathbf{y}) \end{aligned} \tag{4.7}$$

$$\mathbf{T}^\star = \begin{bmatrix} \boldsymbol{\tau}_1^{\star T} \\ \boldsymbol{\tau}_2^{\star T} \end{bmatrix}, \text{ where } \quad \boldsymbol{\tau}_1^\star = \begin{bmatrix} \tau_{11}^\star \\ \tau_{12}^\star \end{bmatrix}, \quad \boldsymbol{\tau}_2^\star = \begin{bmatrix} \tau_{12}^\star \\ \tau_{22}^\star \end{bmatrix}. \tag{4.8}$$

Equations (4.7) and (4.8) imply

$$\operatorname{div}_{\mathbf{x}^\star}\mathbf{T}^\star = \begin{bmatrix} \operatorname{div}_{\mathbf{x}^\star}\boldsymbol{\tau}_1^\star \\ \operatorname{div}_{\mathbf{x}^\star}\boldsymbol{\tau}_2^\star \end{bmatrix} = \begin{bmatrix} (\operatorname{grad}_{\mathbf{x}^\star}\mathbf{y})^T \cdot \operatorname{grad}_{\mathbf{y}}\bar{\boldsymbol{\tau}}_1(\mathbf{y}) \\ (\operatorname{grad}_{\mathbf{x}^\star}\mathbf{y})^T \cdot \operatorname{grad}_{\mathbf{y}}\bar{\boldsymbol{\tau}}_2(\mathbf{y}) \end{bmatrix}, \tag{4.9}$$

$$\begin{bmatrix} 1 & -h^{\star\prime}(x_1^\star)/\delta^\star \\ 0 & 1/\delta^\star \end{bmatrix} \cdot \begin{bmatrix} \bar{\tau}_{11,1} & \bar{\tau}_{11,2} \\ \bar{\tau}_{12,1} & \bar{\tau}_{12,2} \end{bmatrix} = \bar{\tau}_{11,1} - \delta^{\star -1} h^{\star\prime}\bar{\tau}_{11,2} + \delta^{\star -1}\bar{\tau}_{12,2}, \tag{4.10}$$

and

$$\begin{bmatrix} 1 & -h^{\star\prime}(x_1^\star)/\delta^\star \\ 0 & 1/\delta^\star \end{bmatrix} \cdot \begin{bmatrix} \bar{\tau}_{12,1} & \bar{\tau}_{12,2} \\ \bar{\tau}_{22,1} & \bar{\tau}_{22,2} \end{bmatrix} = \bar{\tau}_{12,1} - \delta^{\star -1} h^{\star\prime}\bar{\tau}_{12,2} + \delta^{\star -1}\bar{\tau}_{22,2}. \tag{4.11}$$

Combining equations (4.6), (4.8), (4.10) and (4.11) one obtains the components of $\operatorname{div}_{\mathbf{x}^\star}\mathbf{T}^\star$ in the scaled coordinates

$$\operatorname{div}_{\mathbf{x}^\star}\mathbf{T}^\star = \begin{bmatrix} \bar{\tau}_{11,1} - \delta^{\star -1} h^{\star\prime}\bar{\tau}_{11,2} + \delta^{\star -1}\bar{\tau}_{12,2} \\ \bar{\tau}_{12,1} - \delta^{\star -1} h^{\star\prime}\bar{\tau}_{12,2} + \delta^{\star -1}\bar{\tau}_{22,2} \end{bmatrix}. \tag{4.12}$$

Similarly, for the scalar valued function $\Phi^\star(x_1^\star, x_2^\star) = \bar{\Phi}(y_1^\star, y_2^{\star\star})$,

$$\begin{aligned}\mathrm{grad}_{\mathbf{x}^\star}\Phi^\star(\mathbf{x}^\star) = (\mathrm{grad}_{\mathbf{x}^\star}\mathbf{y})^T \mathrm{grad}_{\mathbf{y}}\bar{\Phi}(\mathbf{y}) &= \begin{bmatrix} 1 & -h^{\star\prime}(x_1^\star)/\delta^\star \\ 0 & 1/\delta^\star \end{bmatrix} \begin{bmatrix} \bar{\Phi}_{,1} \\ \bar{\Phi}_{,2} \end{bmatrix} \\ &= \begin{bmatrix} \bar{\Phi}_{,1} - \delta^{\star -1} h^{\star\prime}(x_1^\star)\bar{\Phi}_{,2} \\ \delta^{\star -1}\bar{\Phi}_{,2} \end{bmatrix}.\end{aligned} \tag{4.13}$$

Thus, equations (4.10), (4.11) and (4.13) imply that, in the scaled coordinates, the differential momentum balance $\mathrm{div}_{\mathbf{x}^\star}\mathbf{T}^\star = \mathrm{grad}_{\mathbf{x}^\star}\Phi^\star$ takes the form

$$\begin{aligned}\bar{\tau}_{11,1} - \delta^{\star -1} h^{\star\prime}\bar{\tau}_{11,2} + \delta^{\star -1}\bar{\tau}_{12,2} &= \bar{\Phi}_{,1} - \delta^{\star -1} h^{\star\prime}(x_1^\star)\bar{\Phi}_{,2} \\ \bar{\tau}_{12,1} - \delta^{\star -1} h^{\star\prime}\bar{\tau}_{12,2} + \delta^{\star -1}\bar{\tau}_{22,2} &= \delta^{\star -1}\bar{\Phi}_{,2}.\end{aligned} \tag{4.14}$$

We have the following asymptotic expansions in terms of $\delta^\star$,

$$\begin{aligned} h^\star(y_1^\star) &= h_0^\star(y_1^\star) + \delta^\star h_1^\star(y_1^\star) + ... \\ \bar{\Phi}(y_1^\star, y_2^{\star\star}) &= \bar{\Phi}_0(y_1^\star, y_2^{\star\star}) + \delta^\star \bar{\Phi}_1(y_1^\star, y_2^{\star\star}) + ... \\ v_1^\star(y_1^\star, y_2^{\star\star}) &= v_1^{(0)}(y_1^\star, y_2^{\star\star}) + \delta^\star v_1^{(1)}(y_1^\star, y_2^{\star\star}) + ... \\ v_2^\star(y_1^\star, y_2^{\star\star}) &= v_2^{(0)}(y_1^\star, y_2^{\star\star}) + \delta^\star v_2^{(1)}(y_1^\star, y_2^{\star\star}) + ... \,. \end{aligned} \tag{4.15}$$

These together with the differential momentum balance imply

$$\bar{\tau}_{ij}(y_1^\star, y_2^{\star\star}) = \bar{\tau}_{ij}^{(0)}(y_1^\star, y_2^{\star\star}) + \delta^\star \bar{\tau}_{ij}^{(1)}(y_1^\star, y_2^{\star\star}) + ... \,.$$

4.2.1. Zeroth Order Approximation of the Differential Momentum Balance

Substituting (4.15) into (4.14) and equating the lowest order terms, one obtains the zeroth order approximation to the differential momentum balance:

$$\begin{aligned} -h_0^{\star\prime}\bar{\tau}_{11,2}^{(0)} + \bar{\tau}_{12,2}^{(0)} &= -h_0^{\star\prime}\bar{\Phi}_{0,2} \\ -h_0^{\star\prime}\bar{\tau}_{12,2}^{(0)} + \bar{\tau}_{22,2}^{(0)} &= \bar{\Phi}_{0,2}. \end{aligned} \tag{4.16}$$

By integrating the above equations with respect to $y_2^{\star\star}$, one obtains

$$\begin{aligned} -h_0^{\star\prime}\bar{\tau}_{11}^{(0)} + \bar{\tau}_{12}^{(0)} &= -h_0^{\star\prime}\bar{\Phi}_0 + m(y_1^\star) \\ -h_0^{\star\prime}\bar{\tau}_{12}^{(0)} + \bar{\tau}_{22}^{(0)} &= \bar{\Phi}_0 + n(y_1^\star). \end{aligned} \tag{4.17}$$

We determine the functions $m(y_1^\star)$ and $n(y_1^\star)$ by matching the inner and outer solutions. The stress for the outer solution is given by[1]

$$\mathbf{T}^{\star outer} = \begin{bmatrix} 0 & 0 \\ 0 & \sigma^\star \end{bmatrix}, \tag{4.18}$$

where $\sigma^\star$ is the far filed loading. Substituting (4.18) into (4.17) and using

$$\lim_{y_2^{\star\star}\to\infty} \bar{\Phi}(y_1^\star, y_2^{\star\star}) = 0$$

one obtains

$$m(y_1^\star) = 0 \qquad \text{and} \qquad n(y_1^\star) = \sigma^\star.$$

---

[1] If one needs to consider a more general form of the outer solution, e.g.,

$$\mathbf{T}^{\star outer} = \begin{bmatrix} \tau_{11}^\infty(x_1^\star, x_2^\star) & \tau_{12}^\infty(x_1^\star, x_2^\star) \\ \tau_{12}^\infty(x_1^\star, x_2^\star) & \tau_{22}^\infty(x_1^\star, x_2^\star) \end{bmatrix},$$

the values of the functions $m(y_1^\star)$ and $n(y_1^\star)$ change ($m(y_1^\star) = -h_0^{\star\prime}(y_1^\star)\tau_{11}^\infty(y_1^\star, 0) + \tau_{11}^\infty(y_1^\star, 0)$ and $n(y_1^\star) = -h_0^{\star\prime}(y_1^\star)\tau_{12}^\infty(y_1^\star, 0) + \tau_{22}^\infty(y_1^\star, 0)$) but the rest of the analysis remains unchanged.

Consequently, the zeroth order approximation to the differential momentum balance yields

$$\begin{aligned} -h_0^{\star\prime}\bar{\tau}_{11}^{(0)} + \bar{\tau}_{12}^{(0)} &= -h_0^{\star\prime}\bar{\Phi}_0 \\ -h_0^{\star\prime}\bar{\tau}_{12}^{(0)} + \bar{\tau}_{22}^{(0)} &= \bar{\Phi}_0 + \sigma^\star. \end{aligned} \tag{4.19}$$

4.2.2. First Order Approximation of the Differential Momentum Balance

In a similar way, one readily obtains that the first order approximation to the differential momentum balance is given by

$$\begin{aligned} &\bar{\tau}_{11,1}^{(0)} - h_0^{\star\prime}\bar{\tau}_{11,2}^{(1)} - h_1^{\star\prime}\bar{\tau}_{11,2}^{(0)} + \bar{\tau}_{12,2}^{(1)} = \bar{\Phi}_{0,1} - h_0^{\star\prime}\bar{\Phi}_{1,2} - h_1^{\star\prime}\bar{\Phi}_{0,2} \\ &\bar{\tau}_{12,1}^{(0)} - h_0^{\star\prime}\bar{\tau}_{12,2}^{(1)} - h_1^{\star\prime}\bar{\tau}_{12,2}^{(0)} + \bar{\tau}_{22,2}^{(1)} = \bar{\Phi}_{1,2}. \end{aligned} \tag{4.20}$$

Integration of $(4.20)_2$ with respect to $y_2^{\star\star}$ leads to

$$-h_0^{\star\prime}\bar{\tau}_{12}^{(1)} - h_1^{\star\prime}\bar{\tau}_{12}^{(0)} + \bar{\tau}_{22}^{(1)} = \bar{\Phi}_1 - \int \bar{\tau}_{12,1}^{(0)} dy_2^{\star\star} + c. \tag{4.21}$$

Matching to the outer solution and using $\lim_{y_2^{\star\star}\to\infty}\bar{\Phi} = 0$ one determines the constant of integration

$$c = \lim_{y_2^{\star\star}\to\infty} \int \bar{\tau}_{12,1}^{(0)} dy_2^{\star\star}. \tag{4.22}$$

4.2.3. Crack Profile

We now turn to the jump momentum balance equation (2.36). In its non-dimensional form it is

$$\mathrm{grad}_{(\sigma)}\tilde{\gamma}^\star + 2H^\star\tilde{\gamma}^\star\mathbf{n} + [\![\mathbf{T}^\star]\!]\mathbf{n} = \mathbf{0}, \tag{4.23}$$

where

$$\begin{aligned} \mathrm{grad}_{(\sigma)}\tilde{\gamma}^\star &= \frac{d\tilde{\gamma}^\star}{dx_1^\star}\frac{1}{1+h^{\star\prime 2}}\langle 1, h^{\star\prime}\rangle^T \\ \mathbf{n} &= \frac{1}{\sqrt{1+h^{\star\prime 2}}}\langle -h^{\star\prime}, 1\rangle^T \\ H^\star &= \frac{1}{2}h^{\star\prime\prime}(1+h^{\star\prime 2})^{-3/2}. \end{aligned} \tag{4.24}$$

Using (4.24) one obtains the component form of (4.23)

$$\begin{aligned} &\frac{d\tilde{\gamma}^\star}{dx_1^\star}(1+h^{\star\prime 2})^{-1/2} - \tilde{\gamma}^\star h^{\star\prime}h^{\star\prime\prime}(1+h^{\star\prime 2})^{-3/2} + (-h^{\star\prime}\tau_{11}^\star + \tau_{12}^\star) = 0 \\ &\frac{d\tilde{\gamma}^\star}{dx_1^\star}(1+h^{\star\prime 2})^{-1/2}h^{\star\prime} + \tilde{\gamma}^\star h^{\star\prime\prime}(1+h^{\star\prime 2})^{-3/2} + (-h^{\star\prime}\tau_{12}^\star + \tau_{22}^\star) = 0. \end{aligned} \tag{4.25}$$

Substitution of (4.19) into the zeroth order approximation of (4.25) yields

$$\begin{aligned} &\frac{d\tilde{\gamma}_0^\star}{dx_1^\star}(1+h_0^{\star\prime 2})^{-1/2} - \tilde{\gamma}_0^\star h_0^{\star\prime}h_0^{\star\prime\prime}(1+h_0^{\star\prime 2})^{-3/2} - h_0^{\star\prime}\bar{\Phi}_0 = 0 \\ &\frac{d\tilde{\gamma}_0^\star}{dx_1^\star}(1+h_0^{\star\prime 2})^{-1/2}h_0^{\star\prime} + \tilde{\gamma}_0^\star h_0^{\star\prime\prime}(1+h_0^{\star\prime 2})^{-3/2} + \bar{\Phi}_0 + \sigma^\star = 0, \end{aligned} \tag{4.26}$$

where $\tilde{\gamma}_0^\star$ is the zero order approximation of $\tilde{\gamma}^\star$. Note that this expansion assumes that

$$(h^\star)''(y_1^\star) = (h_0^\star)''(y_1^\star) + \delta^\star(h_1^\star)''(y_1^\star) + ... \tag{4.27}$$

and in particular that $(h^\star)''(y_1^\star)$ is bounded on $[-1, 1]$.

Since $h_0^\star(x_1^\star)$ cannot satisfy both of these equations simultaneously, we need to"disregard" one of them. Recall that to zero order, the perturbation analysis reduces the differential momentum balance to a system of ordinary differential equations in $y_2^{\star\star}$, rather than partial differential equations. This makes the boundary conditions (4.26) overdetermined with the first of (4.26) extraneous. Notice also that it is the second of (4.26) that contains information about the far field loading. Thus, we determine the crack profile from $(4.26)_2$.

In a similar way, the ordinary differential equation from which one determines the

first order approximation of the crack profile $h_1^\star(x_1^\star)$ is the first order approximation of $(4.25)_2$, where one needs to use (4.21), namely

$$\begin{aligned}
&\frac{d\tilde{\gamma}_0^\star}{dx_1^\star}(1+h_0^{\star\prime 2})^{-1/2}h_1^{\star\prime}+\frac{d\tilde{\gamma}_1^\star}{dx_1^\star}(1+h_0^{\star\prime 2})^{-1/2}h_0^{\star\prime}-\frac{d\tilde{\gamma}_0^\star}{dx_1^\star}(1+h_0^{\star\prime 2})^{-3/2}h_0^{\star\prime}h_1^{\star\prime}\\
&-3\tilde{\gamma}_0^\star(1+h_0^{\star\prime 2})^{-5/2}h_0^{\star\prime\prime}h_0^{\star\prime}h_1^{\star\prime}+(\tilde{\gamma}_0^\star h_1^{\star\prime\prime}+\tilde{\gamma}_1^\star h_0^{\star\prime\prime})(1+h_0^{\star\prime 2})^{-3/2}\\
&+\bar{\Phi}_1-\int\bar{\tau}_{12,1}^{(0)}dy_2^{\star\star}+c=0.
\end{aligned}\tag{4.28}$$

From conducted numerical experiments it is evident that the contribution of the first order term $h_1^\star$ is insignificant, which guarantees that the zero order term $h_0^\star$ approximates the crack profile well enough.

4.3. Navier Equations in Terms of Displacements

The differential momentum balance in terms of the displacement vector $\mathbf{u}$ is given by the Navier equations:

$$\triangle\mathbf{u}+\frac{1}{1-2\nu}\mathrm{grad}\,\mathrm{div}\,\mathbf{u}-\frac{1}{\mu}\mathrm{grad}\Phi=0.\tag{4.29}$$

Thus (4.13) yields

$$\mathbf{b}=\mathrm{grad}_{\mathbf{x}^\star}\Phi^\star(\mathbf{x}^\star)=\begin{bmatrix}\bar{\Phi}_{,1}-\delta^{\star-1}h^{\star\prime}(x_1^\star)\bar{\Phi}_{,2}\\ \delta^{\star-1}\bar{\Phi}_{,2}\end{bmatrix}.\tag{4.30}$$

From here it is clear that $b_1^{(-2)}=b_2^{(-2)}=0$ and $b_1^{(-1)}=-h_0^{\star\prime}(x_1^\star)\bar{\Phi}_{,2}$, $\quad b_2^{(-1)}=\bar{\Phi}_{,2}$. One can easily show that the Navier equations in terms of the $(x_1^\star,x_2^\star)$ variables take the from

$$\begin{aligned}
&\frac{2(1-\nu)}{1-2\nu}\frac{\partial^2u_1^\star}{\partial x_1^{\star 2}}+\frac{1}{1-2\nu}\frac{\partial^2u_2^\star}{\partial x_1^\star\partial x_2^\star}+\frac{\partial^2u_1^\star}{\partial x_2^{\star 2}}-\frac{1}{\mu^\star}b_1=0\\
&\frac{\partial^2u_2^\star}{\partial x_1^{\star 2}}+\frac{1}{1-2\nu}\frac{\partial^2u_1^\star}{\partial x_1^\star\partial x_2^\star}+\frac{2(1-\nu)}{1-2\nu}\frac{\partial^2u_2^\star}{\partial x_2^{\star 2}}-\frac{1}{\mu^\star}b_2=0.
\end{aligned}\tag{4.31}$$

In terms of the scaled variables (4.4), using the expansions (4.15), equation (4.31) can be written in the from

$$\begin{aligned}
&\frac{2(1-\nu)}{1-2\nu}h_0^{\star\prime 2}\frac{\partial^2 u_1^{\star(0)}}{\partial y_2^{\star\star 2}} - \frac{1}{1-2\nu}h_0^{\star\prime}\frac{\partial^2 u_2^{\star(0)}}{\partial y_2^{\star\star 2}} + \frac{\partial^2 u_1^{\star(0)}}{\partial y_2^{\star\star 2}} - \frac{1}{\mu^\star}b_1^{(-2)} = 0\\
&h_0^{\star\prime\prime 2}\frac{\partial^2 u_2^{\star(0)}}{\partial y_2^{\star\star 2}} - \frac{1}{1-2\nu}h_0^{\star\prime}\frac{\partial^2 u_1^{\star(0)}}{\partial y_2^{\star\star 2}} + \frac{2(1-\nu)}{1-2\nu}\frac{\partial^2 u_2^{\star(0)}}{\partial y_2^{\star\star 2}} - \frac{1}{\mu^\star}b_2^{(-2)} = 0.
\end{aligned} \tag{4.32}$$

Equation $(4.15)_4$ implies that $u_2^{\star(0)} = h_0^\star(y_1^\star)$, and consequently, $\dfrac{\partial u_2^{\star(0)}}{\partial y_2^{\star\star}} = 0$. Since $b_1^{(-2)} = b_2^{(-2)} = 0$, we can conclude

$$\frac{\partial^2 u_1^{\star(0)}}{\partial y_2^{\star\star 2}} = 0 \quad \Rightarrow \quad u_1^{\star(0)} = a(y_1^\star)y_2^{\star\star} + b(y_1^\star). \tag{4.33}$$

We require that the inner solution approaches the outer as $y_2^{\star\star} \to \infty$. In view of equation (4.3), this yields

$$\begin{aligned}
&\lim_{y_2^{\star\star}\to\infty} u_1^{\star(0)} = \lim_{y_2^{\star\star}\to\infty}\big(a(y_1^\star)y_2^{\star\star} + b(y_1^\star)\big) = -\frac{\nu\sigma^\star}{2\mu^\star}y_1^\star\\
&\Rightarrow \quad a(y_1^\star) = 0, \quad b(y_1^\star) = -\frac{\nu\sigma^\star}{2\mu^\star}y_1^\star.
\end{aligned} \tag{4.34}$$

We proceed by equating the terms in front of $\delta^{\star-1}$ in (4.31), when written in terms of the inner variables $(y_1^\star, y_2^{\star\star})$:

$$\begin{aligned}
&\frac{2(1-\nu)}{1-2\nu}\left(-2h_0^{\star\prime}\frac{\partial^2 u_1^{\star(0)}}{\partial y_1^\star \partial y_2^{\star\star}} + h_0^{\star\prime 2}\frac{\partial^2 u_1^{\star(1)}}{\partial y_2^{\star\star 2}} + 2h_0^{\star\prime}h_1^{\star\prime}\frac{\partial^2 u_1^{\star(0)}}{\partial y_2^{\star\star 2}} - h_0^{\star\prime\prime}\frac{\partial u_1^{\star(0)}}{\partial y_2^{\star\star}}\right)\\
&+ \frac{1}{1-2\nu}\left(\frac{\partial^2 u_2^{\star(0)}}{\partial y_1^\star \partial y_2^{\star\star}} - h_0^{\star\prime}\frac{\partial^2 u_2^{\star(1)}}{\partial y_2^{\star\star 2}} - h_1^{\star\prime}\frac{\partial^2 u_2^{\star(0)}}{\partial y_2^{\star\star 2}}\right) + \frac{\partial^2 u_1^{\star(1)}}{\partial y_2^{\star\star 2}} - \frac{1}{\mu^\star}b_1^{(-1)} = 0,\\
&- 2h_0^{\star\prime}\frac{\partial^2 u_2^{\star(0)}}{\partial y_1^\star \partial y_2^{\star\star}} + h_0^{\star\prime 2}\frac{\partial^2 u_2^{\star(1)}}{\partial y_2^{\star\star 2}} + 2h_0^{\star\prime}h_1^{\star\prime}\frac{\partial^2 u_2^{\star(0)}}{\partial y_2^{\star\star 2}} - h_0^{\star\prime\prime}\frac{\partial u_2^{\star(0)}}{\partial y_2^{\star\star}}\\
&+ \frac{1}{1-2\nu}\left(\frac{\partial^2 u_1^{\star(0)}}{\partial y_1^\star \partial y_2^{\star\star}} - h_0^{\star\prime}\frac{\partial^2 u_1^{\star(1)}}{\partial y_2^{\star\star 2}} - h_1^{\star\prime}\frac{\partial^2 u_1^{\star(0)}}{\partial y_2^{\star\star 2}}\right)\\
&+ \frac{2(1-\nu)}{1-2\nu}\frac{\partial^2 u_2^{\star(1)}}{\partial y_2^{\star\star 2}} - \frac{1}{\mu^\star}b_2^{(-1)} = 0.
\end{aligned} \tag{4.35}$$

Taking into account the fact that

$$u_1^{\star(0)} = -\frac{\nu\sigma^\star}{2\mu^\star}y_1^\star, \quad u_2^{\star(0)} = h_0^\star(y_1^\star), \quad u_2^{\star(1)} = v_2^{\star(0)}(y_1^\star, y_2^{\star\star}) + h_0^\star(y_1^\star), \tag{4.36}$$

the above system simplifies to

$$\begin{aligned}
&\Big(\frac{2(1-\nu)}{1-2\nu}h_0^{\star\prime 2} + 1\Big)\frac{\partial^2 u_1^{\star(1)}}{\partial y_2^{\star\star 2}} - \frac{1}{1-2\nu}h_0^{\star\prime}\frac{\partial^2 v_2^{\star(0)}}{\partial y_2^{\star\star 2}} - \frac{1}{\mu^\star}b_1^{(-1)} = 0\\
&\Big(h_0^{\star\prime 2} + \frac{2(1-\nu)}{1-2\nu}\Big)\frac{\partial^2 v_2^{\star(0)}}{\partial y_2^{\star\star 2}} - \frac{1}{1-2\nu}h_0^{\star\prime}\frac{\partial^2 u_1^{\star(1)}}{\partial y_2^{\star\star 2}} - \frac{1}{\mu^\star}b_2^{(-1)} = 0.
\end{aligned} \tag{4.37}$$

After solving (4.37) for $\dfrac{\partial^2 u_1^{\star(1)}}{\partial y_2^{\star\star 2}}$ and $\dfrac{\partial^2 v_2^{\star(0)}}{\partial y_2^{\star\star 2}}$ and integrating with respect to $y_2^{\star\star}$, one obtains

$$\frac{\partial u_1^{\star(1)}}{\partial y_2^{\star\star}} = -\frac{(1-2\nu)\Phi_0^\star h_0^{\star\prime}}{2\mu^\star(1-\nu)(1+h_0^{\star\prime 2})} + c(y_1^\star) \tag{4.38}$$

and

$$\frac{\partial v_2^{\star(0)}}{\partial y_2^{\star\star}} = \frac{(1-2\nu)\Phi_0^\star}{2\mu^\star(1-\nu)(1+h_0^{\star\prime 2})} + d(y_1^\star). \tag{4.39}$$

From here it is easy to derive the zero order approximation of the stress components. For example, to find the shear stress $\tau_{12}^\star$ in a neighborhood of the crack surface we proceed as follows. Expanding (4.1) in terms of the inner variables one concludes that the zero order approximation of the shear stress is given by

$$\begin{aligned}
\bar{\tau}_{12}^{(0)} &= \mu^\star\left(\frac{\partial u_1^{\star(1)}}{\partial y_2^{\star\star}} + \frac{\partial u_2^{\star(0)}}{\partial y_1^\star} - h_0^{\star\prime}\frac{\partial u_2^{\star(1)}}{\partial y_2^{\star\star}} - h_1^{\star\prime}\frac{\partial u_2^{\star(0)}}{\partial y_2^{\star\star}}\right)\\
&= \mu^\star\left(\frac{\partial u_1^{\star(1)}}{\partial y_2^{\star\star}} + h_0^{\star\prime} - h_0^{\star\prime}\frac{\partial v_2^{\star(0)}}{\partial y_2^{\star\star}}\right).
\end{aligned} \tag{4.40}$$

Combining (4.38), (4.39) and (4.40) and matching the inner to the outer solution one readily shows

$$\bar{\tau}_{12}^{(0)} = -\frac{(1-2\nu)\Phi_0^\star h_0^{\star\prime}}{(1-\nu)(1+h_0^{\star\prime 2})}. \tag{4.41}$$

CHAPTER V

ENERGY BASED FRACTURE CRITERION

5.1. Introduction

Various approaches to the thermodynamic analysis of fracture have been studied in the literature, with or without consideration of temperature effects. These approaches have incorporated classical singular theories with singular stresses and singular power flux into the crack tip (Gurtin [19, 21], Gurtin and Yatomi [28]) or with cohesive zones designed to remove the singularities (Gurtin [20]). Others have included the notion of a *configurational force system*, with or without cohesive zone, (Gurtin and Shvartsman [27], Costanzo [8], Gurtin and Podio-Guidugli [25, 26]) or excess surface properties, with or without cohesive zone.

Separately, Gurtin and Murdoch ([24, 23]), Murdoch ([37]) and Fried and Gurtin ([17]) have developed a theory of elastic material surfaces, incorporating models with excess surface properties, not necessarily directed towards fracture.

The idea of ascribing excess properties to a dividing surface between two phases dates back to Gibbs. In the development of fracture theory, Griffith was the first one to introduce surface excess properties in the context of solids, but he did not build it into a model of fracture in any concrete way. To our knowledge, the first comprehensive attempt to develop a fracture theory including excess properties was offered by Eftis and Liebowitz in [10] (see also Zhang and Karihaloo [57], Van der Varst and De With [52]). Unfortunately, their development contains serious conceptual and technical flaws.

Our approach bears resemblance to several of the above modeling approaches in that it includes detailed description of the surface excess properties. What is new in

this approach is that, as shown in Chapter III, curvature-dependent excess properties together with the appropriate jump momentum balance, which defines the boundary condition on the fracture surface, lead to a theory with bounded stresses and strains. Further, even though the model in which the surface tension is taken to be constant exhibits a logarithmic crack tip stress singularity, this singularity does not lead to an influx of energy into the crack tip, and therefore the theory outlined below is applicable in this case as well.

An energy based fracture criterion is formulated, including terms similar to the classical notion of a critical energy release rate, defined in the setting of singular crack tip stresses and strains. Classically the energy release rate arises due to singular fields, whereas in the case of the modeling approach adopted here, a notion analogous to the energy release rate arises through a different mechanism, associated to the rate of working of the surface excess properties at the crack tip.

5.2. Fracture Kinematics

In our analysis of this problem, we will make the following assumptions.

1. Temperature is independent of position and time.

2. The rates of external and mutual energy transmission, and the rate of contact energy transmission are negligible.

3. Mass transfer is negligible at all phase interfaces.

4. Pressure in the gas phase between crack surfaces is the atmospheric pressure, considered negligible when compared to the stresses generated in the system by deformation.

Unlike in the previous chapters where the static problem is considered, in the current chapter we study dynamic crack propagation. Due to crack growth, in the modeling approach taken herein, we consider a continuous sequence of reference configurations (where the slit has different lengths). This approach avoids the need to consider mass transfer from the bulk material to the fracture surface and from the fracture surface to the crack tip.[1]

From here on, subscript κ denotes quantities defined relative to a natural reference (unloaded) configuration. The material body in the reference configuration is denoted by $\mathcal{B}_\kappa(t)$, where the time dependence is due to (possible) crack extension. $\mathcal{B}_\kappa(t)$ is viewed as an *evolving reference configuration*. The boundary of $\mathcal{B}_\kappa(t)$, denoted by $\partial\mathcal{B}_\kappa(t)$, has the decomposition

$$\partial\mathcal{B}_\kappa(t) = \mathcal{S}_\kappa \cup \Sigma_\kappa(t), \tag{5.1}$$

where $\mathcal{S}_\kappa$ denotes the boundary the body would have in the absence of the crack (which does not evolve with time) and $\Sigma_\kappa(t)$ denotes the crack. The location of the crack tip in the reference configuration is denoted by $\mathbf{c}(t)$ (Fig. 5.1). To that end, $\dot{\mathbf{c}}(t)$ is the *crack extension velocity*.

Let $\mathbf{X}$ denote the position of points in $\mathcal{B}_\kappa(t)$, and $\chi(\mathbf{X}, t)$, $\mathbf{X} \in \mathcal{B}_\kappa(t)$ - a motion of the cracked body which might be accompanied by crack extension. The body, its boundary sets and the crack tip in the current (deformed) configuration are denoted $\mathcal{B}_t$, $\mathcal{S}_t$, Σ_t and $\mathbf{c}_t$, respectively. Spatial points are denoted $\mathbf{x} \in \mathcal{B}_t$. The material and spatial descriptions of the displacement are denoted $\mathbf{u}_\kappa(\mathbf{X}, t)(:= \chi(\mathbf{X}, t) - \mathbf{X})$ and

[1] An alternative approach to modeling crack propagation takes the body to be the bulk material together with the gas phase. In this case no points are "added" to the boundary and thus one does not need to consider an evolving reference configuration. However in this approach one must account for the mass transfer between the bulk material, the dividing surface and the fracture tip. In essence, fracture propagation is viewed as a "chemical reaction" occurring at the crack edge.

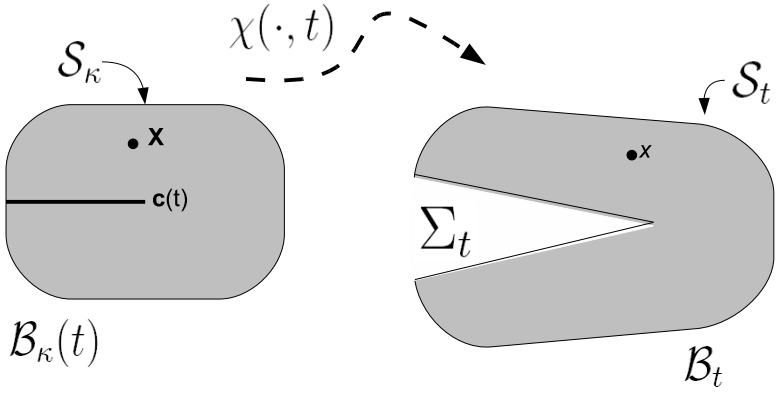

Fig. 5.1. Edge crack in the reference and current configurations.

$\mathbf{u}(\mathbf{x},t)$, respectively, and $\mathbf{v}(\mathbf{x},t)$ is the spatial description of the velocity. Let $\mathbf{F}(\mathbf{X},t)$ denote the deformation gradient. The gradient and divergence operators are denoted by grad and div in the spatial frame, and by ∇ and Div in the material frame.

5.3. Surface First Piola-Kirchhoff Stress Tensor

To simplify the discussion, the derivation of the fracture criterion given in Section 5.4 is in the context of a straight edge crack (in the reference configuration) in a bounded *two dimensional* body. However, for purposes of deriving an expression for the surface first Piola-Kirchhoff stress tensor, it is most natural to work in a three dimensional setting. Thus, within this section, we assume that $\mathcal{B}_t \subset \mathbb{R}^3$ and that Σ_t is a two dimensional surface. The results derived herein are valid in the two dimensional context as well, since the problem we consider can be viewed as a three dimensional problem, reduced to a two dimensional one.

We assume that there exists a surface (Cauchy) stress tensor $\mathbf{T}^{(\sigma)}$ which gives

contact forces in the fracture surface. In this section we derive an expression for the corresponding surface first Piola-Kirchhoff stress tensor $\mathbf{T}_\kappa^{(\sigma)}$.[2]

Let $\mathbf{s}_\kappa$ be an oriented curve in the fracture surface $\Sigma_\kappa(t)$, parameterized by arc length $S \in (0, L)$. Also, let $\boldsymbol{\nu}_\kappa$ denote the unit conormal vector to $\mathbf{s}_\kappa$, i.e., $\boldsymbol{\nu}_\kappa = \boldsymbol{\tau}_\kappa \times \mathbf{N}$, where $\mathbf{N}$ is the unit normal to $\Sigma_\kappa(t)$ and $\boldsymbol{\tau}_\kappa = \dfrac{d\mathbf{s}_\kappa}{dS}$ is the unit tangent to $\mathbf{s}_\kappa$. Let ds and dS be small length elements in the current and reference configuration respectively. Then

$$ds = \left|\left| \frac{d}{dS} \chi \circ \mathbf{s}_\kappa(S) \right|\right| dS = ||\mathbf{F}(\mathbf{s}_\kappa(S)) \boldsymbol{\tau}_\kappa(\mathbf{s}_\kappa(S))||\, dS = j\, dS. \tag{5.2}$$

$j = ||\mathbf{F}\boldsymbol{\tau}_\kappa||$ is sometimes called the Radon-Nikodym derivative of the arc length measure on $\mathbf{s} = \chi \circ \mathbf{s}_\kappa$ with respect to that on $\mathbf{s}_\kappa$ ([24]).

One can show that the unit conormal to the image $\mathbf{s}$ of the curve $\mathbf{s}_\kappa$ in the current configuration is given by the expression

$$\boldsymbol{\nu} = \frac{\mathbf{P}_t \mathbf{F}^{-T} \boldsymbol{\nu}_\kappa}{||\mathbf{P}_t \mathbf{F}^{-T} \boldsymbol{\nu}_\kappa||}, \tag{5.3}$$

where $\mathbf{P}_t$ is the perpendicular projection onto the tangent space $\mathcal{T}_\mathbf{x}$ to Σ_t at $\mathbf{x}$. Indeed, let $\mathbf{n}$ denote the unit normal to the surface Σ_t and $\boldsymbol{\tau}_t$ be the unit tangent to the curve $\mathbf{s}$. To show that $\boldsymbol{\nu}$, as given by (5.3), is conormal to $\mathbf{s}$ it suffices to prove that $\boldsymbol{\nu} \cdot \mathbf{n} = 0$ and $\boldsymbol{\nu} \cdot \boldsymbol{\tau}_t = 0$. The first one is clearly satisfied since $\boldsymbol{\nu} \in \mathcal{T}_\mathbf{x}$, while $\boldsymbol{n} \in \mathcal{T}_\mathbf{x}^\perp$. For the latter note that $\mathbf{P}_t = \mathbf{P}_t^T$ and $\mathbf{P}_t \mathbf{F} \boldsymbol{\tau}_\kappa = \mathbf{F} \boldsymbol{\tau}_\kappa$, consequently

$$\boldsymbol{\nu} \cdot \boldsymbol{\tau}_t = \frac{\mathbf{P}_t \mathbf{F}^{-T} \boldsymbol{\nu}_\kappa}{||\mathbf{P}_t \mathbf{F}^{-T} \boldsymbol{\nu}_\kappa||} \cdot \frac{\mathbf{F} \boldsymbol{\tau}_\kappa}{||\mathbf{F} \boldsymbol{\tau}_\kappa||} = \frac{\boldsymbol{\nu}_\kappa}{||\mathbf{P}_t \mathbf{F}^{-T} \boldsymbol{\nu}_\kappa||} \cdot \frac{\boldsymbol{\tau}_\kappa}{||\mathbf{F} \boldsymbol{\tau}_\kappa||} = 0.$$

The total force exerted by the material in $\mathbf{s}^+$ (the part of Σ_t into which $\boldsymbol{\nu}$ points)

[2]The derivation for $\mathbf{T}_\kappa^{(\sigma)}$ presented herein corrects a small mistake in [24] in the formula, corresponding to (5.3), relating the conormal in the current to the conormal in the reference configuration. For this reason, the expression for $\mathbf{T}_\kappa^{(\sigma)}$ derived here differs slightly from the formula given in [24].

on the material in $\mathbf{s}^-$ is

$$\int_{\mathbf{s}} \mathbf{T}^{(\sigma)}\boldsymbol{\nu} = \int_0^L \mathbf{T}^{(\sigma)}(\chi \circ \mathbf{s}_\kappa(S))\frac{\mathbf{P}_t\mathbf{F}^{-T}\boldsymbol{\nu}_\kappa}{||\mathbf{P}_t\mathbf{F}^{-T}\boldsymbol{\nu}_\kappa||} j\, dS = \int_{\mathbf{s}_\kappa} \mathbf{T}_\kappa^{(\sigma)}\boldsymbol{\nu}_\kappa$$

where

$$\mathbf{T}_\kappa^{(\sigma)} = \frac{||\mathbf{F}\boldsymbol{\tau}_\kappa||}{||\mathbf{P}_t\mathbf{F}^{-T}\boldsymbol{\nu}_\kappa||}\mathbf{T}^{(\sigma)}\mathbf{P}_t\mathbf{F}^{-T} \tag{5.4}$$

is the surface first Piola-Kirchhoff stress tensor.

Proposition 1. *Let $J = \det(\mathbf{F})$, then*

$$\frac{||\mathbf{F}\boldsymbol{\tau}_\kappa||}{||\mathbf{P}_t\mathbf{F}^{-T}\boldsymbol{\nu}_\kappa||} = J||\mathbf{F}^{-T}\mathbf{N}||, \tag{5.5}$$

in particular, (5.4) is independent of the conormal $\boldsymbol{\nu}_\kappa$. Furthermore, if $\mathbf{n} = \mathbf{F}^{-T}\mathbf{N}/||\mathbf{F}^{-T}\mathbf{N}||$ (i.e., $\mathbf{n}$ is the unit normal to Σ_t) and da_n and dA_N are area elements for surfaces in the current (respectively reference) configuration, normal to $\mathbf{n}$ and $\mathbf{N}$ respectively, then

$$da_n = J||\mathbf{F}^{-T}\mathbf{N}||dA_N = j_2\, dA_N,$$

i.e., $j_2 = J||\mathbf{F}^{-T}\mathbf{N}||$ is the Radon-Nikodym derivative of the area measure on Σ_t with respect to that on $\Sigma_\kappa(t)$.

Proof. By the Spectral Theorem ([22]), there exists a representation of $\mathbf{U}$ in the form

$$\mathbf{U} = \sum \alpha_i \mathbf{e}_i \otimes \mathbf{e}_i,$$

where $B = \{\mathbf{e}_i, i = 1, 2, 3\}$ is an orthonormal basis for the vector space $\mathcal{V}$, consisting of eigenvectors of $\mathbf{U}$, and α_i are the corresponding eigenvalues. Let $[\boldsymbol{\nu}_\kappa] = \langle a_\nu, b_\nu, c_\nu\rangle^T$ and $[\mathbf{N}] = \langle a_N, b_N, c_N\rangle^T$ be the representations of $\boldsymbol{\nu}_\kappa$ and $\mathbf{N}$, respectively, relative to

the basis B. Recall that $\boldsymbol{\tau}_\kappa = \mathbf{N} \times \boldsymbol{\nu}_\kappa$, therefore

$$j = ||\mathbf{F}\boldsymbol{\tau}_\kappa|| = \sqrt{\alpha_1^2(b_N c_\nu - b_\nu c_N)^2 + \alpha_2^2(c_N a_\nu - c_\nu a_N)^2 + \alpha_3^2(c_N a_\nu - c_\nu a_N)^2}. \quad (5.6)$$

Furthermore,

$$||\mathbf{P}_t\mathbf{F}^{-T}\boldsymbol{\nu}_\kappa|| = \left|\left|\left(\mathbf{I} - \frac{\mathbf{F}^{-T}\mathbf{N} \otimes \mathbf{F}^{-T}\mathbf{N}}{||\mathbf{F}^{-T}\mathbf{N}||^2}\right)\mathbf{F}^{-T}\boldsymbol{\nu}_\kappa\right|\right| = \left|\left|\mathbf{U}^{-1}\boldsymbol{\nu}_\kappa - \frac{\mathbf{U}^{-2}\mathbf{N}\cdot\boldsymbol{\nu}_\kappa}{||\mathbf{U}^{-1}\mathbf{N}||^2}\mathbf{U}^{-1}\mathbf{N}\right|\right|.$$

After some straightforward manipulations one concludes

$$\begin{aligned}\frac{||\mathbf{F}\boldsymbol{\tau}_\kappa||}{||\mathbf{P}_t\mathbf{F}^{-T}\boldsymbol{\nu}_\kappa||} &= \sqrt{\alpha_2^2\alpha_3^2 a_N^2 + \alpha_1^2\alpha_3^2 b_N^2 + \alpha_1^2\alpha_2^2 c_N^2} = \alpha_1\alpha_2\alpha_3\sqrt{\frac{a_N^2}{\alpha_1^2} + \frac{b_N^2}{\alpha_2^2} + \frac{c_N^2}{\alpha_3^2}} \\ &= J||\mathbf{F}^{-T}\mathbf{N}||.\end{aligned}$$

Now, by Nanson's formula,

$$\mathbf{n}da_n = J\mathbf{F}^{-T}\mathbf{N}dA_N.$$

Taking the inner product of the above equation with $\mathbf{n} = \mathbf{F}^{-T}\mathbf{N}/||\mathbf{F}^{-T}\mathbf{N}||$ yields

$$da_n = J||\mathbf{F}^{-T}\mathbf{N}||dA_N$$

which concludes the proof. □

5.4. Theoretical Derivation

From here on, $\mathcal{B}_t$ is assumed to be a bounded two dimensional body. Let $\mathcal{K}\{\mathcal{B}_t\}$ denote the kinetic energy of the body, expressed in terms of the current and the reference configuration:

$$\begin{aligned}\mathcal{K}\{\mathcal{B}_t\} &= \frac{1}{2}\int_{\mathcal{B}_t}\rho||\mathbf{v}||^2dv + \frac{1}{2}\int_{\partial\mathcal{B}_t}\rho^{(\sigma)}||\mathbf{v}||^2da + \frac{1}{2}\rho^{(c)}||\mathbf{v}(\mathbf{c}_t,t)||^2 \\ &= \frac{1}{2}\int_{\mathcal{B}_\kappa(t)}\rho_\kappa||\dot{\mathbf{x}}||^2dV + \frac{1}{2}\int_{\partial\mathcal{B}_\kappa(t)}\rho_\kappa^{(\sigma)}||\dot{\mathbf{x}}||^2dA + \frac{1}{2}\rho_\kappa^{(c)}||\dot{\mathbf{c}}_t||^2,\end{aligned} \quad (5.7)$$

where ρ is the mass density of $\mathcal{B}_t$, $\rho^{(\sigma)}$ is the surface mass density and $\rho^{(c)}$ is the mass density associated with the fracture tip $\mathbf{c}_t$. In a similar way, ρ_κ, $\rho_\kappa^{(\sigma)}$ and $\rho_\kappa^{(c)}$ are the mass density, surface mass density and mass density associated with the fracture tip in the reference configuration.[3]

Let $\mathcal{U}\{\mathcal{B}_t\}$ be the internal energy of $\mathcal{B}_t$ with $\mathcal{U}\{\mathcal{B}_t\} = \mathcal{A}\{\mathcal{B}_t\} + T\mathcal{S}\{\mathcal{B}_t\}$ where $\mathcal{A}\{\mathcal{B}_t\}$ denotes the stored energy, $\mathcal{S}\{\mathcal{B}_t\}$ - the entropy, and T - the constant absolute temperature. Let $\hat{A}$ and $\hat{A}^{(\sigma)}$ be respectively the free energy density and the surface free energy density per unit mass, then

$$\begin{aligned}\mathcal{A}\{\mathcal{B}_t\} &= \int_{\mathcal{B}_t} \rho\hat{A}dv + \int_{\partial\mathcal{B}_t} \rho^{(\sigma)}\hat{A}^{(\sigma)}da \\ &= \int_{\mathcal{B}_\kappa(t)} \rho_\kappa\hat{A}dV + \int_{\partial\mathcal{B}_\kappa(t)} \rho_\kappa^{(\sigma)}\hat{A}^{(\sigma)}dA.\end{aligned} \tag{5.8}$$

In the current model there is no free energy density associated with the crack tip, although it can easily be added, if needed. Further, let $\mathcal{P}\{\mathcal{B}_t\}$ be the power input to the body

$$\mathcal{P}\{\mathcal{B}_t\} = \int_{\mathcal{B}_\kappa(t)} \mathbf{b}_\kappa\cdot\dot{\mathbf{x}}\,dV + \mathbf{b}_\kappa^{(c)}\cdot\dot{\mathbf{c}}_t + \int_{\mathcal{S}_\kappa} \mathbf{s}_\kappa^e\cdot\dot{\mathbf{x}}\,dA + 2\mathbf{T}_\kappa^{(\sigma)}(\mathbf{c}(t))\boldsymbol{\nu}_\kappa(\mathbf{c}(t))\cdot\mathbf{F}(\mathbf{c}(t))\dot{\mathbf{c}}(t). \tag{5.9}$$

Here $\mathbf{s}_\kappa^e$ are the external tractions per unit area in the reference configuration acting on the body and $\mathbf{b}_\kappa^{(c)}$ is a mutual force acting at the crack tip, arising due to resistance of chemical bonds to opening of the fracture surfaces at the fracture tip. Note that $\mathcal{P}\{\mathcal{B}_t\}$ includes the power input not only through the external force system, but also from (possible) mutual body forces and surface tractions arising from the material response of the body (through the jump momentum balance). The last term in (5.9) represents the rate of working of the crack surface stresses at the crack tip and it is

[3]Due to the fact that the upper and lower fracture surfaces meet at an angle (strictly less than π), the fracture tip (in the case of 3D - fracture edge) is viewed as a "common point" (in the case of 3D - common line), endowed with mass density.

nonzero only when there is crack extension (only the part of the crack tip velocity which is due to crack extension (bond breaking) is taken into account - cf. (5.26)).

The fundamental power balance can be written in the form

$$\frac{d}{dt}\mathcal{K}\{\mathcal{B}_t\} + \frac{d}{dt}\mathcal{U}\{\mathcal{B}_t\} = \mathcal{P}\{\mathcal{B}_t\} - \mathcal{D}\{\mathcal{B}_t\}, \tag{5.10}$$

where $\mathcal{D}\{\mathcal{B}_t\}$ is the fracture energy dissipation rate.

The entropy inequality in the form of the Clausius-Duhem inequality ([46], p. 728, [30], p. 130) in the context of assumptions 1 and 2 reduces to

$$\frac{d}{dt}T\mathcal{S}\{\mathcal{B}_t\} \geq 0. \tag{5.11}$$

Next, following the analysis of Gurtin and Podio-Guidugli in [25], we derive the transport theorems appropriate for the current setting. It is important to keep in mind that in the setting of [25], the mechanical power flux into the crack tip is not zero due to the singular crack tip stress and strain fields, whereas here stresses and strains are bounded at the crack tip. For this reason, the transport relations needed here differ from the ones derived in [25, 26].

Lemma 2. Transport Relation for a "Bulk" Function in the Reference Configuration. *Let $\Phi(\mathbf{X}, t)$ be a field defined on $\mathcal{B}_\kappa(t) \times \mathbb{R}^+$ which is bounded and sufficiently smooth up to the crack from either side. Then*

$$\frac{d}{dt}\int_{\mathcal{B}_\kappa(t)} \Phi = \int_{\mathcal{B}_\kappa(t)} \dot{\Phi}, \tag{5.12}$$

where $\dot{\Phi}$ is the material time derivative of Φ.

Proof. Let $\mathcal{D}_\kappa^\delta(t)$ denote a disk of radius δ centered at the crack tip $\mathbf{c}(t)$ and moving

with it. Let $\mathcal{B}_\kappa^\delta(t) = \mathcal{B}_\kappa(t) \setminus \mathcal{D}_\kappa^\delta(t)$. Then

$$\frac{d}{dt}\int_{\mathcal{B}_\kappa^\delta(t)} \Phi = \int_{\mathcal{B}_\kappa^\delta(t)} \dot{\Phi} - \int_{\partial\mathcal{D}_\kappa^\delta(t)} \Phi\, \dot{\mathbf{c}}(t)\cdot\mathbf{N}.$$

Here $\mathbf{N}$ is the unit normal vector to $\partial\mathcal{D}_\kappa^\delta(t)$ pointing into the bulk material. Using the regularity and boundedness of Φ one concludes that

$$\frac{d}{dt}\int_{\mathcal{B}_\kappa(t)} \Phi = \lim_{\delta\to 0}\frac{d}{dt}\int_{\mathcal{B}_\kappa^\delta(t)} \Phi = \int_{\mathcal{B}_\kappa(t)} \dot{\Phi}.$$

□

Lemma 3. Transport Relation for a Function Defined on a Growing Surface in the Reference Configuration. *Consider $\mathcal{B}_\kappa(t) \subset \mathbb{R}^2$. Let $\Phi^{(\sigma)}(\mathbf{X}, t)$ be a field defined on the (possibly growing) crack surface $\Sigma_\kappa(t)\times\mathbb{R}^+$ which is bounded, and sufficiently smooth on $(\Sigma_\kappa(t)\times\mathbb{R}^+)\setminus(\{\mathbf{c}(t)\}\times\mathbb{R}^+)$. Then*

$$\frac{d}{dt}\int_{\partial\mathcal{B}_\kappa(t)} \Phi^{(\sigma)} = \int_{\partial\mathcal{B}_\kappa(t)} \dot{\Phi}^{(\sigma)} + 2\Phi^{(\sigma)}(\mathbf{c}(t))\,||\dot{\mathbf{c}}(t)||. \tag{5.13}$$

Proof. Let $l(t)$ be a curve in $\mathbb{R}^2$ parameterized by $\mathbf{l}(s,t)$, $0\le s\le 1$ with $\mathbf{a}(t) = \mathbf{l}(0,t)$ and $\mathbf{b}(t) = \mathbf{l}(1,t)$. Then the standard transport theorem yields

$$\frac{d}{dt}\int_{l(t)} \Phi = \int_{l(t)} \dot{\Phi} + \Phi(\mathbf{a}(t))\,\dot{\mathbf{a}}\cdot\mathbf{N}_a + \Phi(\mathbf{b}(t))\,\dot{\mathbf{b}}\cdot\mathbf{N}_b$$

where $\mathbf{N}_a$ and $\mathbf{N}_b$ are the unit tangent vectors to $l(t)$ at $\mathbf{a}(t)$ and $\mathbf{b}(t)$ respectively. Now let $l(t) = \mathcal{S}_\kappa \bigcup \Sigma_\kappa(t)$. Then $\mathbf{a}(t) = \mathbf{b}(t) = \mathbf{c}(t)$ and $\dot{\mathbf{a}}\cdot\mathbf{N}_a = \dot{\mathbf{b}}\cdot\mathbf{N}_b = ||\dot{\mathbf{c}}(t)||$, which concludes the proof. □

5.4.1. Momentum Balance Relations

Invoking the Transport Theorem (which has the usual form for a bulk control volume due to the fact that stresses and strains remain bounded) and standard localization

arguments, one derives the local form of the balance of linear momentum in the reference configuration

$$\rho_\kappa \ddot{\mathbf{x}} = \mathrm{Div}\mathbf{T}_\kappa + \mathbf{b}_\kappa, \qquad \mathbf{X} \in \mathcal{B}_\kappa(t) \tag{5.14}$$

and jump momentum balance

$$\begin{aligned} \rho_\kappa^{(\sigma)} \ddot{\mathbf{x}} &= \mathrm{Div}_{(\sigma)}\mathbf{T}_\kappa^{(\sigma)} - [\![\mathbf{T}_\kappa \mathbf{N}]\!], \qquad \mathbf{X} \in \Sigma_\kappa(t), \\ \rho_\kappa^{(\sigma)} \ddot{\mathbf{x}} &= \mathrm{Div}_{(\sigma)}\mathbf{T}_\kappa^{(\sigma)} - \mathbf{T}_\kappa \mathbf{N} + \mathbf{s}_\kappa^e, \qquad \mathbf{X} \in \mathcal{S}_\kappa. \end{aligned} \tag{5.15}$$

Here $[\![\cdot]\!]$ denotes the jump of the quantity across $\Sigma_\kappa(t)$ and $\mathbf{N}$ is the outward unit normal. For the problem considered herein, $\Sigma_\kappa(t) = \Sigma_\kappa(t)^+ \cup \Sigma_\kappa(t)^-$ is not just a dividing surface in the body, but rather a part of its boundary and $(5.15)_1$ could also be written in the form

$$\rho_\kappa^{(\sigma)} \ddot{\mathbf{x}} = \mathrm{Div}_{(\sigma)}\mathbf{T}_\kappa^{(\sigma)} - \mathbf{T}_\kappa^{\pm} \mathbf{N}^{\pm}, \qquad \mathbf{X} \in \Sigma_\kappa^{\pm}(t). \tag{5.16}$$

In addition to these, there is a momentum balance at the crack tip given by

$$\rho_\kappa^{(c)} \ddot{\mathbf{c}}_t = \mathbf{b}_\kappa^{(c)} + \big(\!\big(\rho_\kappa^{(c)}(\dot{\mathbf{c}}(t) \cdot \boldsymbol{\nu}_\kappa(\mathbf{c}(t)))\dot{\mathbf{c}}(t) - \mathbf{T}_\kappa^{(\sigma)}(\mathbf{c}(t))\boldsymbol{\nu}_\kappa(\mathbf{c}(t))\big)\!\big), \tag{5.17}$$

where $(\!(\cdot)\!)$ is the jump at the crack tip and $\boldsymbol{\nu}_\kappa(\mathbf{c}(t))$ is the conormal at $\mathbf{c}(t)$ (in two dimensional space this is the unit tangent to the fracture curve) pointing away from the fracture surface. Equation (5.17) is based on (2.1.9-15)/p. 129 in [47], stated with respect to the reference configuration and modified for the case of a propagating crack in a two dimensional body.

5.4.2. Necessary Condition for Crack Propagation

We now proceed with a derivation of a necessary condition for crack propagation, working in the reference configuration. Substitution of (5.7), (5.8) and (5.9) into

(5.10) yields

$$\begin{aligned}
&\frac{d}{dt}\left(\frac{1}{2}\int_{\mathcal{B}_\kappa(t)}\rho_\kappa||\dot{\mathbf{x}}||^2dV+\frac{1}{2}\int_{\partial\mathcal{B}_\kappa(t)}\rho_\kappa^{(\sigma)}||\dot{\mathbf{x}}||^2dA+\frac{1}{2}\rho_\kappa^{(c)}||\dot{\mathbf{c}}_t||^2\right.\\
&\left.+\int_{\mathcal{B}_\kappa(t)}\rho_\kappa\hat{A}dV+\int_{\partial\mathcal{B}_\kappa(t)}\rho_\kappa^{(\sigma)}\hat{A}^{(\sigma)}dA\right)\\
=&\int_{\mathcal{B}_\kappa(t)}\mathbf{b}_\kappa\cdot\dot{\mathbf{x}}\,dV+\mathbf{b}_\kappa^{(c)}\cdot\dot{\mathbf{c}}_t+\int_{\mathcal{S}_\kappa}\mathbf{s}_\kappa^e\cdot\dot{\mathbf{x}}\,dA+2\mathbf{T}_\kappa^{(\sigma)}(\mathbf{c}(t))\boldsymbol{\nu}_\kappa(\mathbf{c}(t))\cdot\mathbf{F}(\mathbf{c}(t))\dot{\mathbf{c}}(t)\\
&-\frac{d}{dt}T\mathcal{S}\{\mathcal{B}_t\}-\mathcal{D}\{\mathcal{B}_t\}.
\end{aligned}\tag{5.18}$$

Lemma 2 and Lemma 3 together with (5.14), (5.15) and (5.18) lead to

$$\begin{aligned}
&2\left(\frac{1}{2}\rho_\kappa^{(\sigma)}(\mathbf{c}(t))||\dot{\mathbf{c}}_t||^2+\rho_\kappa^{(\sigma)}(\mathbf{c}(t))\hat{A}^{(\sigma)}(\mathbf{c}(t))\right)\dot{\mathbf{c}}(t)\cdot\boldsymbol{\nu}_\kappa(\mathbf{c}(t))\\
&+\frac{1}{2}\frac{d\rho_\kappa^{(c)}}{dt}||\dot{\mathbf{c}}_t||^2+\rho_\kappa^{(c)}\ddot{\mathbf{c}}_t\cdot\dot{\mathbf{c}}_t+\int_{\mathcal{B}_\kappa(t)}\left(\mathrm{Div}\mathbf{T}_\kappa\cdot\dot{\mathbf{x}}+\rho_\kappa\dot{\hat{A}}\right)dV\\
&+\int_{\partial\mathcal{B}_\kappa(t)}\left(\mathrm{Div}_{(\sigma)}\mathbf{T}_\kappa^{(\sigma)}\cdot\dot{\mathbf{x}}-\mathbf{T}_\kappa\mathbf{N}\cdot\dot{\mathbf{x}}+\rho_\kappa^{(\sigma)}\dot{\hat{A}}^{(\sigma)}\right)dA\\
&=\ \mathbf{b}_\kappa^{(c)}\cdot\dot{\mathbf{c}}_t+2\mathbf{T}_\kappa^{(\sigma)}(\mathbf{c}(t))\boldsymbol{\nu}_\kappa(\mathbf{c}(t))\cdot\mathbf{F}(\mathbf{c}(t))\dot{\mathbf{c}}(t)-\frac{d}{dt}T\mathcal{S}\{\mathcal{B}_t\}-\mathcal{D}\{\mathcal{B}_t\}.
\end{aligned}\tag{5.19}$$

Use of the Divergence Theorem yields

$$\int_{\mathcal{B}_\kappa(t)}\mathrm{Div}\mathbf{T}_\kappa\cdot\dot{\mathbf{x}}\,dV=-\int_{\mathcal{B}_\kappa(t)}\mathbf{T}_\kappa\cdot\dot{\mathbf{F}}\,dV+\int_{\partial\mathcal{B}_\kappa(t)}\mathbf{T}_\kappa\mathbf{N}\cdot\dot{\mathbf{x}}\,dS\tag{5.20}$$

and similarly from the surface divergence theorem (cf. (A.6.3-7)/p. 670 and (2.1.9-3)/p. 126 in [47])

$$\begin{aligned}
\int_{\partial\mathcal{B}_\kappa(t)}\mathrm{Div}_{(\sigma)}\mathbf{T}_\kappa^{(\sigma)}\cdot\dot{\mathbf{x}}\,dS&=-\int_{\partial\mathcal{B}_\kappa(t)}\mathbf{T}_\kappa^{(\sigma)}\cdot\nabla_{(\sigma)}\dot{\mathbf{x}}\,dS+\left(\mathbf{T}_\kappa^{(\sigma)}(\mathbf{c}(t))\boldsymbol{\nu}_\kappa(\mathbf{c}(t))\cdot\dot{\mathbf{c}}_t\right)\\
&=-\int_{\partial\mathcal{B}_\kappa(t)}\mathbf{T}_\kappa^{(\sigma)}\cdot\dot{\mathbf{F}}\mathbf{P}_\kappa\,dS+2\mathbf{T}_\kappa^{(\sigma)}(\mathbf{c}(t))\boldsymbol{\nu}_\kappa(\mathbf{c}(t))\cdot\dot{\mathbf{c}}_t
\end{aligned}\tag{5.21}$$

with $\mathbf{P}_\kappa$ - the perpendicular projection operator onto $\partial\mathcal{B}_\kappa(t)$, where equation $\nabla_{(\sigma)}\mathbf{v}=\nabla\mathbf{v}\mathbf{P}_\kappa$ is used.

In virtue of (5.17), (5.20) and (5.21), equation (5.19) reduces to

$$\begin{aligned}
&\int_{\mathcal{B}_\kappa(t)} \left(\rho_\kappa \dot{\hat{A}} - \mathbf{T}_\kappa \cdot \dot{\mathbf{F}}\right) dV + \int_{\partial\mathcal{B}_\kappa(t)} \left(\rho_\kappa^{(\sigma)} \dot{\hat{A}}^{(\sigma)} - \mathbf{T}_\kappa^{(\sigma)} \cdot \dot{\mathbf{F}}\mathbf{P}_\kappa\right) dA \\
&+ 2\left(\frac{1}{2}\rho_\kappa^{(\sigma)}(\mathbf{c}(t))||\dot{\mathbf{c}}_t||^2 + \rho_\kappa^{(\sigma)}(\mathbf{c}(t))\hat{A}^{(\sigma)}(\mathbf{c}(t)) + \rho_\kappa^{(c)}\dot{\mathbf{c}}\cdot\dot{\mathbf{c}}_t\right)\dot{\mathbf{c}}(t)\cdot\boldsymbol{\nu}_\kappa(\mathbf{c}(t)) \qquad (5.22) \\
&+ \frac{1}{2}\frac{d\rho_\kappa^{(c)}}{dt}||\dot{\mathbf{c}}_t||^2 = 2\mathbf{T}_\kappa^{(\sigma)}(\mathbf{c}(t))\boldsymbol{\nu}_\kappa(\mathbf{c}(t))\cdot\mathbf{F}(\mathbf{c}(t))\dot{\mathbf{c}}(t) - \frac{d}{dt}T\mathcal{S}\{\mathcal{B}_t\} - \mathcal{D}\{\mathcal{B}_t\}.
\end{aligned}$$

Since in any isothermal process a thermoelastic material is hyperelastic ($\mathbf{T}_\kappa = \rho_\kappa \partial_{\mathbf{F}}\hat{A}$) with free energy function equal to the stored energy, ([30], p. 134), we have $\rho_\kappa\dot{\hat{A}} = \mathbf{T}_\kappa \cdot \dot{\mathbf{F}}$.

For simplicity and consistency with the literature ([47], p. 148) assume that the surface stress can be modeled as Eulerian, i.e., $\mathbf{T}^{(\sigma)} = \hat{\gamma}\mathbf{P}_t$. Let $\hat{A}^{(\sigma)}(\mathbf{X}) = \bar{A}^{(\sigma)}(\mathbf{F}(\mathbf{X})) = \tilde{A}^{(\sigma)}(j_2)$ where j_2 is as defined in Proposition 1. Then

$$\rho_\kappa^{(\sigma)}\dot{\hat{A}}^{(\sigma)} = \rho_\kappa^{(\sigma)}\frac{d}{dj_2}\tilde{A}^{(\sigma)}(j_2)\partial_{\mathbf{F}}j_2\cdot\dot{\mathbf{F}}.$$

Now,

$$\begin{aligned}
\partial_{\mathbf{F}}j_2 &= ||\mathbf{F}^{-T}\mathbf{N}||\partial_{\mathbf{F}}J + J\partial_{\mathbf{F}}||\mathbf{F}^{-T}\mathbf{N}|| \\
&= J||\mathbf{F}^{-T}\mathbf{N}||\mathbf{F}^{-T} - \frac{J}{||\mathbf{F}^{-T}\mathbf{N}||}(\mathbf{F}^{-T}\mathbf{N}\otimes\mathbf{F}^{-T}\mathbf{N})\mathbf{F}^{-T} \\
&= J||\mathbf{F}^{-T}\mathbf{N}||\mathbf{P}_t\mathbf{F}^{-T} = j_2\mathbf{P}_t\mathbf{F}^{-T}.
\end{aligned}$$

On the other hand, by Proposition 1,

$$\mathbf{T}_\kappa^{(\sigma)}\cdot\dot{\mathbf{F}}\mathbf{P}_\kappa = j_2\hat{\gamma}\mathbf{P}_t\mathbf{F}^{-T}\cdot\dot{\mathbf{F}}\mathbf{P}_\kappa = j_2\hat{\gamma}\mathbf{P}_t\mathbf{F}^{-T}\cdot\dot{\mathbf{F}}.$$

Since

$$\hat{\gamma} = \rho_\kappa^{(\sigma)}\frac{d}{dj_2}\tilde{A}^{(\sigma)}(j_2)$$

([47], p. 325), equation (5.22) reduces to

$$\begin{aligned} &2\left(\frac{1}{2}\rho_\kappa^{(\sigma)}(\mathbf{c}(t))||\dot{\mathbf{c}}_t||^2+\rho_\kappa^{(\sigma)}(\mathbf{c}(t))\hat{A}^{(\sigma)}(\mathbf{c}(t))+\rho_\kappa^{(c)}\dot{\mathbf{c}}\cdot\dot{\mathbf{c}}_t\right)\dot{\mathbf{c}}(t)\cdot\boldsymbol{\nu}_\kappa(\mathbf{c}(t)) \\ &+\frac{1}{2}\frac{d\rho_\kappa^{(c)}}{dt}||\dot{\mathbf{c}}_t||^2=\ 2\mathbf{T}_\kappa^{(\sigma)}(\mathbf{c}(t))\boldsymbol{\nu}_\kappa(\mathbf{c}(t))\cdot\mathbf{F}(\mathbf{c}(t))\dot{\mathbf{c}}(t)-\frac{d}{dt}T\mathcal{S}\{\mathcal{B}_t\}-\mathcal{D}\{\mathcal{B}_t\}. \end{aligned} \tag{5.23}$$

Notice that the terms remaining in (5.23) are non-zero only when the crack starts to propagate. Recall that $\mathbf{T}_\kappa^{(\sigma)}\boldsymbol{\nu}_\kappa=j\hat{\gamma}\boldsymbol{\nu}$. Assuming that the kinetic energy of the crack tip is negligible, (5.23) reduces to

$$\rho_\kappa^{(\sigma)}(\mathbf{c}(t))\hat{A}^{(\sigma)}(\mathbf{c}(t))\leq j\hat{\gamma}\frac{\dot{\mathbf{c}}(t)\cdot\mathbf{F}^T(\mathbf{c}(t))\boldsymbol{\nu}(\mathbf{c}_t)}{\dot{\mathbf{c}}(t)\cdot\boldsymbol{\nu}_\kappa(\mathbf{c}(t))}, \tag{5.24}$$

where we have used $\dot{\mathbf{c}}(t)\cdot\boldsymbol{\nu}_\kappa(\mathbf{c}(t))>0$, which holds true since $\boldsymbol{\nu}_\kappa(\mathbf{c}(t))$ is the unit tangent to the fracture surface pointing away from it and provided the crack can only change direction at a smaller than $\frac{\pi}{2}$ angle. Now, note that in the case of plane strain $j=||\mathbf{F}(\mathbf{c}(t))\boldsymbol{\tau}_\kappa(\mathbf{c}(t))||\equiv 1$.

Equation (5.24) gives a necessary condition for crack propagation. The left hand side of (5.24) depends only on the material properties at the crack tip, while the ratio at the right hand side is related to the deformation gradient and depends on the far-field loading.

Now, let $\hat{G}_c^{(\sigma)}$ be the critical value of the surface Gibbs free energy per unit mass, which depends only upon atomic bond strength, and γ be the surface energy. $\hat{G}_c^{(\sigma)}$ can be interpreted as the energy required to break the chemical bonds, while γ - as the energy required to overcome the long-range intermolecular forces. Then

$$\rho_\kappa^{(\sigma)}\hat{A}^{(\sigma)}=\rho_\kappa^{(\sigma)}\hat{G}_c^{(\sigma)}+\gamma.$$

Thus, if the crack does not change direction, i.e., if $\mathbf{P}_\kappa(\mathbf{c}(t))\dot{\mathbf{c}}(t)=\dot{\mathbf{c}}(t)$, using $\boldsymbol{\nu}_\kappa=\mathbf{P}_\kappa\mathbf{F}^T\boldsymbol{\nu}/||\mathbf{P}_\kappa\mathbf{F}^T\boldsymbol{\nu}||$, the necessary condition for crack propagation can be written in

the form

$$\rho_\kappa^{(\sigma)}(\mathbf{c}(t))\hat{G}_c^{(\sigma)}(\mathbf{c}(t)) + \gamma(\mathbf{c}(t)) \leq \hat{\gamma}||\mathbf{P}_\kappa(\mathbf{c}(t))\mathbf{F}^T(\mathbf{c}(t))\boldsymbol{\nu}(\mathbf{c}_t)||. \tag{5.25}$$

Note: The analysis in Section 5.4 can be performed in the current configuration, if needed, in a similar way, using the analogues of Lemmas 2 and 3 for the current configuration, as well as

$$\boldsymbol{\nu}_\kappa = \frac{\mathbf{P}_\kappa\mathbf{F}^T\boldsymbol{\nu}}{||\mathbf{P}_\kappa\mathbf{F}^T\boldsymbol{\nu}||}$$

and

$$\mathbf{T}^{(\sigma)} = \frac{1}{j_2}\mathbf{T}_\kappa^{(\sigma)}\mathbf{P}_\kappa\mathbf{F}^T.$$

In this case one has to be careful to distinguish motion of the crack tip due to crack extension (bond breaking) from motion of the crack tip due to deformation. A straightforward calculation gives

$$\dot{\mathbf{c}}_t = \mathbf{v}(\mathbf{c}_t, t) + \mathbf{F}(\mathbf{c}(t), t)\dot{\mathbf{c}}(t) \tag{5.26}$$

$$= \mathbf{v}(\mathbf{c}_t, t) + (\mathbf{I} - \operatorname{grad}\mathbf{u}(\mathbf{c}_t, t))^{-1}\dot{\mathbf{c}}(t) \tag{5.27}$$

in which $\mathbf{I}$ denotes the identity tensor. It follows that

$$\dot{\mathbf{c}}(t) = (\mathbf{I} - \operatorname{grad}\mathbf{u}(\mathbf{c}_t, t))(\dot{\mathbf{c}}_t - \mathbf{v}(\mathbf{c}_t, t)) \tag{5.28}$$

which gives the spatial description of the crack extension velocity. In the absence of crack extension (bond braking), $\dot{\mathbf{c}}(t) = \mathbf{0}$ while, in general, $\dot{\mathbf{c}}_t \neq \mathbf{0}$.

CHAPTER VI

FRACTURE CRITERION BASED UPON CRACK TIP STRESS

6.1. Classical Theory

The asymptotic solution (using LEFM) for stresses for the classical Griffith problem, valid both for plane stress and plane strain is ([51])

$$\begin{aligned}
\tau_{11} &= \frac{K_I}{\sqrt{2\pi r}} \cos\left(\frac{\theta}{2}\right)\left(1 - \sin\left(\frac{\theta}{2}\right)\sin\left(\frac{3\theta}{2}\right)\right) \\
\tau_{22} &= \frac{K_I}{\sqrt{2\pi r}} \cos\left(\frac{\theta}{2}\right)\left(1 + \sin\left(\frac{\theta}{2}\right)\sin\left(\frac{3\theta}{2}\right)\right) \\
\tau_{12} &= \frac{K_I}{\sqrt{2\pi r}} \cos\left(\frac{\theta}{2}\right)\sin\left(\frac{\theta}{2}\right)\sin\left(\frac{3\theta}{2}\right),
\end{aligned} \tag{6.1}$$

where (r, θ) are the coordinates of a polar coordinate system centered at the crack tip $x_1 = a, x_2 = 0$. K_I is the mode I stress intensity factor, which for an infinite plate with an internal crack of length $2a$, subject to a remotely applied uniform tensile traction σ_∞, is given by ([51])

$$K_I = \sigma_\infty \sqrt{\pi a}. \tag{6.2}$$

Combining (6.1) and (6.2) one concludes that the tensile stress ahead of the crack tip is

$$\tau_{22} = \frac{\sigma_\infty}{\sqrt{2}\sqrt{\frac{r}{a}}}. \tag{6.3}$$

In the case of plane strain, the *rate of release of stored elastic energy* $\mathcal{G}$ is related to the stress intensity factor by the following formula

$$K_I = \sqrt{\frac{\mathcal{G}E}{1-\nu^2}}, \tag{6.4}$$

where E is Young's modulus and ν is Poisson's ratio. In this sense, the concept of critical energy release rate is equivalent to the concept of critical stress intensity

factor.

6.2. Crack Tip Stress Criterion

Since the theory proposed herein predicts a finite crack tip stress (Section 3.4), there is an alternative fracture criterion, based on crack tip stress, apart from the energy based one, derived in Chapter V. This criterion is based on the assumption that the crack will start to propagate once the cleavage stress exceeds the stress required to overcome the short-range (chemical bonds) and long-range intermolecular forces. The required stress for a given material can be estimated through ab initio molecular dynamics calculations.

For example, for the model with curvature-dependent surface tension and no body force correction term, we estimate the tensile stress at the crack tip from (3.60):

$$\sigma_{22}(1,0) = -\gamma_0 u_{2,11}(1,0) + h.o.t. \ . \tag{6.5}$$

Since the considered model leads to finite stresses and strains, we conclude that the cleavage stress is well defined and can be calculated using the results from Section 3.4. Thus, the crack starts to propagate once the stress at the crack tip reaches the value of the critical stress[1], i.e.,

$$\sigma_{22}(1,0) \geq \frac{\sigma^{crit}}{E}.$$

This new approach to formulating a fracture criterion is very appealing with its straightforward physical interpretation and simple implementation.

[1]Here σ_{22} denotes the nondimensionalized tensile stress - cf. (2.7).

CHAPTER VII

SUMMARY

7.1. Conclusions

This dissertation focuses on the study of brittle fracture, using extension of continuum mechanics to the nanoscale, first proposed by Slattery ([46]) and later applied in the context of fractures by Oh et al ([39]). The main idea of the theory is to correct bulk material behavior in a neighborhood of the fracture surfaces for effects of long-range intermolecular forces from adjoining phases. This, however, leads to a nonlinear, nonlocal boundary value problem. Several techniques are used to resolve the behavior of the solution in a neighborhood of the crack surfaces.

In Chapter III integral transform methods, similar to the ones used to solve the classical Griffith problem, but modified to accommodate for different type of boundary conditions and a body force correction term, are applied to a class of models based on the modeling paradigm proposed in [39, 46]. First we consider a model of fracture including constant surface tension and using the jump momentum balance as a boundary condition at the crack surfaces and show that it leads to a sharp crack profile at the crack tip (as opposed to the blunt one predicted by the classical LEFM model) and stresses which exhibit a logarithmic singularity at the crack tip. The obtained linear integro-differential equation is solved using series expansion in terms of Chebyshev polynomials. Moreover, the sequence of solutions of the truncated systems of linear equations is shown to converge to the solution of the infinite system.

Further, a modified model is studied in which the surface excess property includes curvature dependence. We show that this model yields bounded stresses and strains. The resulting second order linear singular integro-differential equation is

solved numerically using spline collocation methods combined with product integration techniques.

Chapter IV provides an alternative approach, using asymptotic analysis, for deriving an approximation of the crack opening profile and cleavage stress. This approach is especially suitable to apply when the model includes a body force correction term, since the associated with it length scale is needed to rescale the variables and study the problem in a small region surrounding the crack surfaces. The fact that this model yields a well defined cleavage stress, allows for the construction of a fracture criterion based on crack tip stress, considered in Chapter VI.

Further, in Chapter V, using the global energy balance and the second law of Thermodynamics, in the spirit of [19, 21, 25, 26, 28], we derive an inequality, which involves the material properties at the crack tip and the rate of working of the crack surface stresses at the crack tip thereby giving rise to an energy based necessary condition for crack initiation. It should be emphasized that in the theory used herein there are no stress and strain crack tip singularities and hence there is no net flux of energy into a singular crack tip as occurs in classical elastic fracture mechanics. For this reason, a notion similar to that of the energy release rate arises in a very different way from the classical notion of ERR used in the papers cited above.

7.2. Future Work

An important step in continuing the analysis initiated in this dissertation is to find the domain in which the parameters of the curvature-dependent surface tension may vary, so that the model yields a physically reasonable solution for the crack profile. Furthermore, it is important to understand the physical meaning of the problem when these parameters are such that the resulting singular integro-differential operator has

a non-trivial kernel and hence is not invertible (Section 3.4).

We have shown that the incorporation of a mutual body force term leads to a compact perturbation of the singular integro-differential operator after linearization of the jump momentum balance boundary conditions under the assumption of small strains. Our conjecture is that this compact operator does not change the fundamental result, i.e., the model with non-zero curvature-dependent excess property and a mutual body force term, like the model with non-zero curvature-dependent excess property and no mutual body force term, yields bounded stresses and strains. In addition, we conjecture that if there are no surface excess properties at the crack surfaces, then no physically reasonable correction potential will be able to remove the crack tip stress singularities, that is, even with a mutual body force term the model will essentially behave like the classical LEFM model. We conjecture that it is the excess surface property, together with the correct boundary condition in the form of the jump momentum balance that is responsible for removing the stress and strain singularities at the crack tip.

There is a range of problems in interfacial mechanics that share the same essential modeling ingredient, namely the need of correction of the bulk material constitutive description near an interface due to the close proximity of one or more neighboring phases of dissimilar material. Once the theory for fracture in a single phase material is developed and tested against experimental data, the techniques used for this simpler problem could easily be extended and applied to other interfacial mechanics problem areas such as interfacial fracture, as well as the growth and stability of ultra-thin solid films on a solid substrate (e.g. metal/metallic oxide composite or diamond coatings on metallic substrates).

In the case of interfacial fracture, an important goal of the analysis will be to study whether the incorporation of excess properties of the dividing surfaces removes

the interpenetration of the two fracture surfaces in front of the crack tip, characteristic of the LEFM approach.

Another direction in which the analysis developed in this dissertation could be extended to is the case of three dimensional cracks. In particular, a first step in this direction would be the important canonical case of a "penny shaped" crack.

Furthermore, following [26], while accounting for the important differences in the two theories, the framework used herein could be extended to a fracture theory which allows kinking and curving in the crack propagation. An important problem related to this is to study how the crack front (in the case of a three dimensional crack) evolves with crack propagation.

And finally, in this dissertation mode I fracture was considered as a first step. Similar techniques to the ones applied here could be used to consider shear mode (mode II), tear mode (mode III) and mixed mode fracture which are of interest in many cases.

REFERENCES

[1] M. A. Abdou, *Fredholm-Volterra integral equation with singular kernel*, Appl. Math. Comput., 137 (2003), pp. 231–243.

[2] F. F. Abraham, *The atomic dynamics of fracture*, J. Mech. Phys. Solids, 49 (2001), pp. 2095–2111.

[3] F. F. Abraham, D. Brodbeck, W. E. Rudge, and X. Xu, *A molecular dynamics investigation of rapid fracture mechanics*, J. Mech. Phys. Solids, 45 (1997), pp. 1595–1619.

[4] F. F. Abraham and H. Gao, *How fast can cracks propagate?*, Phys. Rev. Lett., 84 (2000), pp. 3113–3116.

[5] K. E. Atkinson, *The numerical solution of integral equations of the second kind*, volume 4 of Cambridge Monographs on Applied and Computational Mathematics, Cambridge University Press, Cambridge, 1997.

[6] A. A. Badr, *Integro-differential equation with Cauchy kernel*, J. Comput. Appl. Math., 134 (2001), pp. 191–199.

[7] R. L. Burden, J. D. Faires, and A. C. Reynolds, *Numerical analysis*, Prindle, Weber & Schmidt, Boston, MA, 1978.

[8] F. Costanzo, *An analysis of 3d crack propagation using cohesive zone models and the theory of configurational forces*, Math. Mech. Solids, 6 (2001), pp. 149–173.

[9] F. de Hoog and R. Weiss, *Asymptotic expansions for product integration*, Math. Comp., 27 (1973), pp. 295–306.

[10] J. Eftis and H. Liebowitz, *On surface energy and the continuum thermodynamics of brittle fracture*, Engrg. Fracture Mech., 8 (1976), pp. 459–485.

[11] F. O. Farid, *Spectral properties of perturbed linear operators and their application to infinite matrices*, Proc. Amer. Math. Soc., 112 (1991), pp. 1013–1022.

[12] F. O. Farid and P. Lancaster, *Spectral properties of diagonally dominant infinite matrices I*, Proc. Roy. Soc. Edinburgh Sect. A, 111 (1989), pp. 301–314.

[13] J. Fineberg, S. P. Gross, M. Marder, and H. L. Swinney, *Instability in dynamic fracture*, Phys. Rev. Lett., 67 (1991), pp. 457–460.

[14] G. B. Folland, *Fourier analysis and its applications*, The Wadsworth & Brooks/Cole Mathematics Series, Wadsworth & Brooks/Cole Advanced Books & Software, Pacific Grove, CA, 1992.

[15] A. Fomethe and G. A. Maugin, *On the crack mechanics of hard ferromagnets*, Internat. J. Non-Linear Mech., 33 (1998), pp. 85–95.

[16] J. I. Frankel, *A Galerkin solution to a regularized Cauchy singular integro-differential equation*, Quart. Appl. Math., 53 (1995), pp. 245–258.

[17] E. Fried and M. E. Gurtin, *Thermomechanics of the interface between a body and its environment*, Contin. Mech. Thermodyn., 19 (2007), pp. 253–271.

[18] J. W. Gibbs, *Collected works*, volume 1, Longmans, New York, 1928.

[19] M. E. Gurtin, *On the energy release rate in quasi-static elastic crack propagation*, J. Elasticity, 9 (1979), pp. 187–195.

[20] M. E. Gurtin, *Thermodynamics and the cohesive zone in fracture*, Z. Angew. Math. Phys., 30 (1979), pp. 991–1003.

[21] M. E. Gurtin, *Thermodynamics and the Griffith criterion for brittle fracture*, Internat. J. Solids Structures, 15 (1979), pp. 552–560.

[22] M. E. Gurtin, *An introduction to continuum mechanics*, Academic Press, New York, 1981.

[23] M. E. Gurtin and A. I. Murdoch, *Addenda to our paper "A continuum theory of elastic material surfaces" (Arch. Rational Mech. Anal.* **57** *(1975), 291–323)*, Arch. Rational Mech. Anal., 59 (1975), pp. 389–390.

[24] M. E. Gurtin and A. I. Murdoch, *A continuum theory of elastic material surfaces*, Arch. Rational Mech. Anal., 57 (1975), pp. 291–323.

[25] M. E. Gurtin and P. Podio-Guidugli, *Configurational forces and the basic laws for crack propagation*, J. Mech. Phys. Solids, 44 (1996), pp. 905–927.

[26] M. E. Gurtin and P. Podio-Guidugli, *Configurational forces and a constitutive theory for crack propagation that allows for kinking and curving*, J. Mech. Phys. Solids, 46 (1998), pp. 1343–1378.

[27] M. E. Gurtin and M. M. Shvartsman, *Configurational forces and the dynamics of planar cracks in three-dimensional bodies*, J. Elasticity, 48 (1997), pp. 167–191.

[28] M. E. Gurtin and C. Yatomi, *On the energy release rate in elastodynamic crack propagation*, Arch. Rational Mech. Anal., 74 (1980), pp. 231–247.

[29] D. Holland and M. P. Marder, *Ideal brittle fracture of silicon studied with molecular dynamics*, Phys. Rev. Lett., 80 (1998), pp. 746–749.

[30] I.-S. Liu, *Continuum mechanics*, Springer-Verlag, Berlin, 2002.

[31] M. Marder and S. Gross, *Origin of crack tip instabilities*, J. Mech. Phys. Solids, 43 (1995), pp. 1–48.

[32] J. C. Mason and D. C. Handscomb, *Chebyshev polynomials*, Chapman & Hall/CRC, Boca Raton, FL, 2003.

[33] G. A. Maugin and C. Trimarco, *Dissipation of configurational forces in defective elastic solids*, Arch. Mech. (Arch. Mech. Stos.), 47 (1995), pp. 81–99.

[34] S. G. Mikhlin and S. Prössdorf, *Singular integral operators*, Springer-Verlag, Berlin, 1986. Translated from German by Albrecht Böttcher and Reinhard Lehmann.

[35] M. Moody and P. Attard, *Curvature dependent surface tension from a simulation of a cavity in a Lennard-Jones liquid close to coexistence*, J. Chem. Phys., 115 (2001), pp. 8967–8977.

[36] M. Moody and P. Attard, *Curvature-dependent surface tension of a growing droplet*, Phys. Rev. Lett., 91 (2003), pp. 56104-1–56104-4.

[37] A. I. Murdoch, *A thermodynamical theory of elastic material interfaces*, Quart. J. Mech. Appl. Math., 29 (1976), pp. 245–275.

[38] N. I. Muskhelishvili, *Singular integral equations*, Noordhoff International Publishing, Leyden, 1977. Boundary problems of function theory and their application to mathematical physics. Revised translation from Russian, edited by J. R. M. Radok, reprint of the 1958 edition.

[39] E. S. Oh, J. R. Walton, and J. C. Slattery, *A theory of fracture based upon an extension of continuum mechanics to the nanoscale*, J. Appl. Mechanics, 73 (2006), pp. 792–798.

[40] È. N. Samoĭlova, *Spline approximations of the solution of a singular integro-differential equation*, Izv. Vyssh. Uchebn. Zaved. Mat., 11 (2001), pp. 35–45.

[41] J. Saranen and G. Vainikko, *Periodic integral and pseudodifferential equations with numerical approximation*, Springer Monographs in Mathematics. Springer-Verlag, Berlin, 2002.

[42] J. Schmelzer, I. Gutzow, and J. Schmelzer, Jr., *Curvature-dependent surface tension and nucleation theory*, J. Colloid Interface Sci., 178 (1996), pp. 657–665.

[43] G. Schmidt, *Spline collocation for singular integro-differential equations over* $(0, 1)$, Numer. Math., 50 (1987), pp. 337–352.

[44] S. A. Silling, *Reformulation of elasticity theory for discontinuities and long-range forces*, J. Mech. Phys. Solids, 48 (2000), pp. 175–209.

[45] J. Sivaloganathan and S. J. Spector, *On cavitation, configurational forces and implications for fracture in a nonlinearly elastic material*, J. Elasticity, 67 (2002), pp. 25–49.

[46] J. C. Slattery, *Interfacial transport phenomena*, Springer-Verlag, New York, 1990.

[47] J. C. Slattery, L. Sagis, and E.-S. Oh, *Interfacial transport phenomena*, Springer-Verlag, New York, 2 edition, 2007.

[48] L. I. Slepyan, M. V. Ayzenberg-Stepanenko, and J. P. Dempsey, *A lattice model for viscoelastic fracture*, Mech. Time-Dep. Mater., 3 (1999), pp. 159–203.

[49] J. G. Swadener, M. I. Baskes, and M. Nastasi, *Molecular dynamics simulation of brittle fracture in silicon*, Phys. Rev. Lett., 89 (2002).

[50] E. B. Tadmor, R. Philips, and M. Ortiz, *Mixed atomistic and continuum models of deformation in solids*, Langmuir, 12 (1996), pp. 4529–4534.

[51] D. J. Unger, *Analytical fracture mechanics*, Dover Publications, Mineola, NY, 2001.

[52] P. G. T. Van der Varst and G. De With, *Notes on the paper - a thermodynamic framework of fracture mechanics*, Engrg. Fracture Mech., 51 (1995), pp. 333–334.

[53] J. R. Walton, *Lecture notes on method of intergal transfroms*, Lecture notes for Math 603, Fall 1996, Texas A&M University.

[54] P. Wesseling, *An asymptotic expansion for product integration applied to Cauchy principal value integrals*, Numer. Math., 24 (1975), pp. 435–442.

[55] S. P. Xiao and T. Belytschko, *A bridging domain method for coupling continua with molecular dynamics*, Comp. Meth. Appl. Mech. & Engr., 193 (2004), pp. 1645–1669.

[56] E. Zeidler, *Nonlinear functional analysis and its applications I*, Springer-Verlag, New York, 1986. Fixed-point theorems, Translated from German by Peter R. Wadsack.

[57] C. Y. Zhang and B. L. Karihaloo, *A thermodynamic framework of fracture mechanics*, Natur. Sci. J. Xiangtan Univ., 14 (1992), pp. 148–159.

VITA

Tsvetanka Bozhidarova Sendova was born in Sofia, Bulgaria. She studied at Sofia University St. Kliment Ohridski beginning September 1998 and graduated in July 2002 with a Bachelor of Science degree in mathematics. In the fall of 2002 she enrolled in the doctoral program in the Department of Mathematics, Texas A&M University. Tsvetanka can be contacted at:

Department of Mathematics

Texas A&M University

College Station, TX 77843-3368

U. S. A.

E-mail address: sendova@math.tamu.edu